5-2009

Controlling Nonspecific Adsorption of Proteins at Bio-Interfaces for Biosensor and Biomedical Applications

Harshil D. Dhruv
Utah State University

CONTROLLING NONSPECIFIC ADSORPTION OF PROTEINS AT BIO-INTERFACES FOR BIOSENSOR AND BIOMEDICAL APPLICATIONS

by

Harshil D. Dhruv

A dissertation submitted in partial fulfillment
of the requirements for the degree

of

DOCTOR OF PHILOSOPHY

in

Biological Engineering

Approved:

David W. Britt Committee Chairman	Anhong Zhou Committee Member
Soonjo Kwon Committee Member	Marie K. Walsh Committee Member
Silvana Martini Committee Member	Byron R. Burnham Dean of Graduate Studies

UTAH STATE UNVERSITY
Logan, Utah

2009

ABSTRACT

Controlling Nonspecific Adsorption of Proteins at Bio-interfaces for Biosensor and Biomedical Applications

by

Harshil D. Dhruv, Doctor of Philosophy

Utah State University, 2009

Major Professor: Dr. David W. Britt
Department: Biological and Irrigation Engineering

Partitioning of poly(ethyleneglycol) (PEG) molecules in 2-D and 3-D systems is presented as a self-assembly approach for controlling non-specific adsorption of proteins at interfaces.

Lateral restructuring of multi-component Langmuir monolayers to accommodate adsorbing proteins was investigated as a model 2-D system. Ferritin adsorption to monolayers containing cationic, nonionic, and PEG bearing phospholipids induced protein sized binding pockets surrounded by PEG rich regions. The number, size, and distribution of protein imprint sites were controlled by the molar ratios, miscibility, and lateral mobility of the lipids.

The influence of PEG chain length on the ternary monolayer restructuring and protein distribution was also investigated using DSPE-PEG_x (x= 7, 16, 22). Monolayer miscibility analysis demonstrated that longer PEG chains diminished the condensed phase formation for a fixed ratio of lipids. Thus, incorporation of longer PEG chains,

intended to diminish protein adsorption outside of the imprint sites of cationic / non-ionic lipids, leads to dramatic changes in monolayer phase behavior and protein distribution in this 2-D system.

The assembly of PEG-amphiphiles at elastomer surfaces and subsequent protein adsorption was investigated as a model 3-D system. Polydimethylsiloxane (PDMS) substrates were modified with block copolymers comprised of PEG and PDMS segments by two methods: (1) the block copolymer was mixed with PDMS during polymerization; (2) the block copolymer diffused into solvent swollen PDMS monoliths. Hydrophilic surfaces resulted for both approaches that, for 600 D block copolymer, exhibited up to 85% reduction in fibrinogen adsorption as compared to native PDMS. Higher MW block copolymers (up to 3000 D) resulted in less hydrophilic surfaces and greater protein adsorption, presumably due to diffusion limitations of copolymer in the PDMS monolith. All modified PDMS surfaces were dynamic and restructured when cycled between air and water. PDMS transparency also decreased with increase in block copolymer concentration for both methods, limiting this modification protocol for applications requiring high polymer transparency.

The 2-D system presents a bottom-up approach, where adsorbing protein constructs the binding site, while the 3-D system presents a top down approach, where protein-binding elements may be introduced into the PEG-bearing polymer for fabrication of surfaces with controlled protein adsorption.

(220 pages)

To my parents

Dinesh B. Dhruv and Poornima D. Dhruv

and

my loving wife

Nikita Zaveri

ACKNOWLEDGMENTS

I would like to express my deepest gratitude to my professor and mentor, Dr. David W. Britt, for giving me the opportunity to dream, create, and discover in his laboratory during my PhD work. I would also like to thank other professors on my committee, including Dr. Marie K. Walsh, Dr. Anhong Zhou, Dr. Silvana Martini, and Dr. Soonjo Kwon, for their valuable support and advice during the course of my work. I am heartily thankful to the late Dr. Lyman S. Willardson for giving me the opportunity to study at Utah State University.

I am thankful to all my colleagues at Dr. Britt's lab for their help and discussion in improving my dissertation. I gratefully acknowledge the help given by Mr. Bradley Tuft for collecting stability study data for PDMS samples. I am also thankful to all my friends at Utah State University for giving me a friendly environment during the course of my studies.

Finally, I would like to thank my parents, my sister, and my wife for their continuous support and encouragement they have provided me during these years, without which this journey would not have been possible for me.

Harshil Dhruv

CONTENTS

Page

LIST OF TABLES

LIST OF FIGURES

LIST OF SCHEMES

LIST OF SYMBOLS, NOTATIONS, AND DEFINITIONS

Symbol Key

π	surface pressure
A	area per molecule
ΔV	surface potential
ε_0	permittivity of the vacuum
μ	normal component of the effective dipole moment
ε_0	effective dielectric constant
ψ_0	electric double layer potential

Abbreviation Key

PEG	poly(ethylene glycol)
PEO	poly(ethylene oxide)
PDMS	poly(dimethylsiloxane)
PC	phosphorylcholine
PU	polyurethanes
PET	poly(ethyleneterephthalate)
PE	polyethylene
PHEMA	poly(2-hydroxyethylmetylacrylate)
PMEA	poly(2-methoxyethylacrylate)
OEG	oligo(ethyleneglycol)
SAMs	self-assembled monolayers
LCST	lower critical solution temperature

PEGMA	poly(ethylene glycol) monomethacrylate
ATRP	atom transfer radical polymerization
SI-ATRP	surface initiated-atom transfer radical polymerization
OEGMA	oligo(ethylene glycol) methyl methacrylate
PPO	poly(propylene oxide)
VDW	van der Waals
LB	Langmuir-Blodgett
PLL	poly(L-lysine)
G	gaseous phase
LE	liquid expanded phase
LC	liquid condensed phase
S	solid phase
C	collapse phase
A_L	limiting area
DPPC	dipalmitoylphosphatidylcholine
DPPE	dipalmitoylphosphatidylethanolamine
DSPE	distearoyloylphosphatidylethanolamine
PS	poly(styrene)
OTS	*n*-octadecyltrichlorosilane
FTS	1*H*1*H*2*H*2*H*-perfluorodecyltrichlorosilane
IDA	iminodiacetate
NTA	nitrilotriaceiticacid
DMPC	dimyristoylphosphatidylcholine

UVO	ultraviolet ozone
Bio-DOPE	1,2-dioleyol-sn-glycero-3-phosphoethanolamine-N-(biotinyl)
EOF	electro osmotic flow
PLA	poly(lactic acid)
SME	methyl stearate
DOMA	dioctadecyldimethylammonium bromide
MIPs	molecular imprinting polymers
PEG_{350}	1,2-disteaoyl-*sn*-glycero-3-phosphoethanolamine-N-[methoxy(polyethyleneglycol)-350]
PEG_{750}	1,2-disteaoyl-*sn*-glycero-3-phosphoethanolamine-N-[methoxy(polyethyleneglycol)-750]
PEG_{1000}	1,2-disteaoyl-*sn*-glycero-3-phosphoethanolamine-N-[methoxy(polyethyleneglycol)-1000]
SD	SME:DOMA (2:1)
AFM	atomic force microscopy
NBD-PE	1-oleoyl-2-[12-[(7-nitro-2-1,3-benzoxadiazol-4-yl)amino]dodecanoyl]-*sn*-glycero-3-phosphoethanolamine
IRAS	infrared reflection-absorption spectroscopy
XPS	X-ray photoelectron spectroscopy
BSA	bovine serum albumin
PS-g-SPEO	poly(styrene)-graft-stearyl-poly(ethylene oxide)
PDMS-b-PEO	poly(dimethylsiloxane)-bis- poly(ethylene oxide)
RT	room temperature
PBS	phosphate buffered saline
SDS	sodium dodecyl sulfate

CHAPTER 1

INTRODUCTION

1.1 Background

A number of artificial materials are used in direct contact with biological systems, and these materials play an important role in human life. Examples include extracorporeal devices, bioreactors, bioseparation systems, diagnostic devices, drug delivery systems, and a variety of biomedical implants. Use of these devices reduces the cost and time of many processes, which simplifies disease diagnosis and improves patient quality of life.

There are a number of problems associated with the use of materials that come in contact with biological systems.[1-8] One significant problem associated with all material surfaces exposed to solutions containing biological samples, is unwanted adsorption of protein or biofouling. Biofouling is a common term used to describe the non-specific adsorption of proteins on artificial surfaces. Biofouling is a major problem affecting advances in biological science including traditional fields, such as protein separation chromatography,[9] food processing,[10] biomedical devices,[11-13] as well as the emerging field of microfluidic devices/bioMEMS,[7, 8, 14, 15] high throughput bioassays,[16-18] biosensors,[19-23] and tissue engineening.[1, 3, 6, 24] The potential effect implicated by the broad involvement of non-specific protein adsorption has inspired multidisciplinary studies focused on understanding the mechanism of non-specific protein adsorption at surfaces and developing strategies of surface modification aimed at minimizing non-

specific protein adsorption. However, despite these multidisciplinary efforts, the performance of modern biomaterials for various applications is far from satisfactory.[25]

The development of these protein repellent or “antifouling” coatings, forms an active area of research within a broader field of biointerface science – the science of controlling biomolecular interactions at interfaces.[26] This area also has implications for the development of novel biomaterials for various applications, because protein adsorption is often the first step in a cascade of adsorption events that occurs when an artificial material is placed in a biological medium. Further, inhibition of non-specific adsorption to a surface also improves the biocompatibility of biomedical implants.

A variety of approaches has been developed to render the biologically relevant surfaces protein repellent, out of which coating or modification of surfaces with neutral hydrophilic polymers, is a widely accepted method as a means to reduce non-specific adsorption of proteins. Further, there are only a limited number of materials that are suitable for surface modification aimed at preventing non-specific protein adsorption. In this small arsenal, poly(ethylene glycol) (PEG) ,also referred as poly(ethylene oxide) (PEO), is widely explored as a “nonfouling” (protein resistant) material.[27, 28] Based on research over the past three decades, a PEG coating of high density must be achieved to obtain the optimal protein repellency and hence the biocompatibility of PEG modified surfaces.[28]

The goal of this work is to explore specific methods to control non-specific adsorption of proteins at surfaces, and to evaluate an approach for creating patterns of proteins that can be applied to the development of novel biosensors and biomedical devices.

1.2 Hypotheses and Objectives

This research is driven by the following **hypotheses**:

"Immobilization of poly(ethylene glycol) (PEG) molecules on surfaces reduces non-specific adsorption of the proteins at surfaces when they come in contact with biological environment."

To test these hypotheses, a series of controlled experiments have been designed based on preliminary studies and reviews of the scientific literature.

The main objective of this research is to develop novel methods to control non-specific adsorption of proteins at surfaces, and to evaluate an approach for creating patterns of proteins that can be applied to the development of biosensors and biomedical devices. To achieve this objective, the experimental work of this research will be divided into three specific aims:

1. *Construction of multicomponent lipid monolayer films containing PEG bearing phospholipids.* Langmuir monolayers of a mixture of lipids containing poly(ethylene glycol) (PEG) bearing phospholipids will be investigated as a model system to create protein specific binding pockets with reduced non-specific protein adsorption.
2. *Incorporation of PEG bearing phospholipids with different PEG chain lengths in multicomponent lipid monolayer films.* Different molecular weight PEG bearing phospholipids will be incorporated in Langmuir monolayers of a mixture of lipids to investigate the effectiveness of higher molecular weight PEG chains in reducing non-specific protein adsorption.
3. *Immobilization of PEO molecules on the surface of a Poly(dimethylsiloxane) (PDMS) elastomer.* PDMS substrates will be modified with AB and ABA type block

copolymers comprised of PEO and PDMS segments by the physical entanglement method to increase its hydrophilicity and biocompatibility.

1.3 Dissertation Outline

Chapter 2 of this dissertation gives comprehensive background information on the causes and consequences of the non-specific protein adsorption to the bio-interfaces, and methods to reduce the non-specific protein adsorption. Further, detailed description of poly(ethyleneglycol) (PEG), the most widely used protein repellent polymer, and theories behind its effectiveness in reducing the non-specific adsorption of proteins are also presented. A comprehensive review of the literature on techniques to immobilize PEG molecules on surfaces with specific advantages and disadvantages of each technique is also discussed. At the end of Chapter 2 a brief overview on poly(dimethylsiloxane) (PDMS), a widely used biomedical polymer, and methods to immobilize PEG molecules on its surface is given.

In Chapter 3 a unique approach for molecular imprinting of proteins in Langmuir monolayers is presented, where PEG bearing lipids have been used in order to reduce non-specific adsorption of proteins, and define single protein binding pockets. In Chapter 4 the Langmuir monolayers approach has been extended to investigate the influence of PEG chain length on protein adsorption by using PEG bearing lipids with varying PEG chain lengths. Further, it is also demonstrated that PEG bearing lipids with longer chain lengths, introduced in mixed lipid monolayers in order to provide better steric barrier against protein adsorption, also leads to dramatic differences in the size and distribution of domains within the mixed monolayers.

In Chapter 5 a novel method for surface modification of poly(dimethylsiloxane) (PDMS), a widely used medical grade polymer with poly(ethyleneoxide) (PEO), is discussed. This simple, rapid, and cost effective method is compared to presently available techniques. Low molecular weight functional block copolymers with a PDMS anchor chain has been shown to modify the surface properties of PDMS when mixed in with a PDMS prepolymer, before the polymerization process. In Chapter 6, the outcome of this dissertation work is summarized and future directions are discussed.

1.4 References

1. Marchant, R. E. *J. Adhes.* **1986,** 20, (3), 211-225.
2. Helmus, M. N.; Hubbell, J. A. *Cardiovasc. Pathol.* **1993,** 2, (3), S53-S71.
3. Langer, R.; Vacanti, J. P. *Science* **1993,** 260, (5110), 920-926.
4. Leonard, E. F. *Cardiovasc. Pathol.* **1993,** 2, (3), S3-S10.
5. Kunzler, J. F. *Trends Polym. Sci.* **1996,** 4, (2), 52-59.
6. El-Ali, J.; Sorger, P. K.; Jensen, K. F. *Nature* **2006,** 442, (7101), 403-411 .
7. Psaltis, D.; Quake, S. R.; Yang, C. H. *Nature* **2006,** 442, (7101), 381-386.
8. Whitesides, G. M. *Nature* **2006,** 442, (7101), 368-373.
9. Hanson, M.; Unger, K. K. *Trac-Trends Anal. Chem.* **1992,** 11, (10), 368-373.
10. Horbett, T. A.; Brash, J. L. *ACS Symp. Ser.* **1987,** 343, 1-33.
11. Hench, L. L. *J. Biomed. Mater. Res.* **1980,** 14, (6), 803-811.

12. Hench, L. L. *Science* **1980,** 208, (4446), 826-831.

13. Hench, L. L.; Wilson, J. *Science* **1984,** 226, (4675), 630-636.

14. Quake, S. R.; Scherer, A. *Science* **2000,** 290, (5496), 1536-1540.

15. Grayson, A. C. R.; Shawgo, R. S.; Johnson, A. M.; Flynn, N. T.; Li, Y. W.; Cima, M. J.; Langer, R. *Proc. IEEE* **2004,** 92, (1), 6-21.

16. Groth, T.; Renil, M.; Meinjohanns, E. *Comb. Chem. High Throughput Screen* **2003,** 6, (7), 589-610.

17. Zhu, H.; Snyder, M. *Curr. Opin. Chem. Biol.* **2003,** 7, (1), 55-63.

18. Harbers, G. M.; Emoto, K.; Greef, C.; Metzger, S. W.; Woodward, H. N.; Mascali, J. J.; Grainger, D. W.; Lochhead, M. J. *Chem. Mat.* **2007,** 19, (18), 4405-4414.

19. Collings, A. F.; Caruso, F. *Rep. Prog. Phys.* **1997,** 60, (11), 1397-1445.

20. Mar, M. N.; Ratner, B. D.; Yee, S. S. *Sens. Actuator B-Chem.* **1999,** 54, (1-2), 125-131.

21. Metzger, S. W.; Natesan, M.; Yanavich, C.; Schneider, J.; Lee, G. U. *J. Vac. Sci. Technol. A-Vac. Surf. Films* **1999,** 17, (5), 2623-2628.

22. Masson, J. F.; Battaglia, T. M.; Cramer, J.; Beaudoin, S.; Sierks, M.; Booksh, K. S. *Anal. Bioanal. Chem.* **2006,** 386, (7-8), 1951-1959.

23. Strehlitz, B.; Nikolaus, N.; Stoltenburg, R. *Sensors* **2008,** 8, (7), 4296-4307.

24. Griffith, L. G.; Naughton, G. *Science* **2002,** 295, (5557), 1009-+.

25. Hench, L. L.; Boccaccini, A. R.; Day, R. M.; Gabe, S. M. Third-generation gene-activating biomaterials. In *Thermec'2003, Pts 1-5*, Chandra, T. T. J. M. S. T., Ed. 2003; Vol. 426-4, pp 179-184.

26. Chilkoti, A.; Hubbell, J. A. *MRS Bull.* **2005,** 30, (3), 175-176.

27. Harris, J. M. ed. *Poly(Ethylene Glycol) Chemistry: Biotechnical and Biomedical Applications.* Plenum Press: New York, 1992; p 485.

28. Sheth, S. R.; Leckband, D. *Proc. Natl. Acad. Sci. U. S. A.* **1997,** 94, (16), 8399-8404.

CHAPTER 2

LITERATURE REVIEW

2.1 Protein Adsorption to Biologically Relevant Surfaces

A number of synthetic materials are used in contact with biological systems, which are commonly referred to as biomaterials. A biomaterial is defined as a nonviable material that is intended to be exposed to a biological environment.[1] And these biomaterials play a very important role in our life. Examples include extracorporeal devices, bioreactors, bioseparation systems, diagnostic devices, drug delivery systems, and a variety of biomedical implants. Understanding the mechanism and dynamics of interactions involved in biological systems is essential in predicting and controlling these systems. Modern biotechnology and bioengineering techniques have enhanced our ability to manipulate these interactions so as to create novel biomaterials for a wide variety of applications. Development of a fundamental understanding of the interactions taking place between bio-molecules and biomaterial surfaces at the molecular level is needed to develop novel biosensors and biomedical devices.

Proteins, linear copolymers of 20 different L-amino acids, are at the center of life. They assert their importance through different types of interaction such as, protein-protein interactions, protein-nucleic acid interactions, and protein surface interactions. Interaction of proteins in a biological system to the biomaterial surface plays a major role in dictating the performance of that particular system.

2.1.1 Specific Protein Adsorption. Specific molecular interactions are the

fundamental processes governing control of both biological form and function.[2] This impressive and ubiquitous biological phenomenon is mediated in the main, by proteins. These specific interactions are generally found to be non-covalent interactions between bio-molecules, and molecules present at the cell surface. A strong but non-covalent bond can occur between two macromolecules with a unique combination of interactions, such as steric, ionic and directional bonds. Such specific interactions are also referred to as "complementary", "lock-and-key", "ligand-receptor (LR)" or "recognition" interactions, and also form the foundation of a molecular imprinting technology.

The binding energy of specific interactions depends strongly on the local geometry and chemistry.[3] The affinity and uniqueness of the binding sites are the two major characters for specific interactions. If the interactions are highly selective, small differences in the chemistries can generate large differences in binding affinities, while poor selectivity can be used to inhibit the binding of one ligand by an inhibitor which has a similar structure and composition as the receptor.

Specific adsorption of proteins to the artificial biomaterial surfaces are mainly utilized in the development of protein sensors for the detection of proteins, chromatographic protein separations, and most recently, in the development of protein microarrays. By developing an understanding of the interactions taking place between bio-molecules and biomaterial surfaces, and with the use of novel technologies, a biomaterial surface can be engineered to increase its specificity towards a particular biomolecule for a desired application.

However, it is important to note that the specific interactions between biomaterial surfaces and proteins are a much more complicated process. Many different forces may

act at different locations and/or at different times, which can affect the specific molecular interaction event. Rearrangement of the molecules can happen both normally and laterally, i.e., different events can occur at different locations on the surface or away from the surface (at or away from the center of action), either simultaneously or sequentially.[4] In most cases, the molecular interactions taking place in a biological environment are not the only interaction of energy or force happening between two entities, but the overall effect on the whole system.[5]

2.1.2 Non-specific Protein Adsorption. The non-specific adsorption of proteins, a key event when biomaterial surfaces come in contact with a biological environment, is a complex event that is difficult to illustrate, and often leads to the failure or loss of activity of biomaterial. The process of non-specific adsorption of protein is governed by: the properties of protein (structure, size, and distribution of charge and polarity); the properties of a tested biomaterial surface (charge, roughness, and state of surface energy); environmental conditions (pH, ionic strength, and temperature); and the kinetics of the adsorption process.[6] Despite the apparent complexity of the adsorption process, many physiological responses are clearly linked to the adsorbed protein layers.[7]

2.1.2.1 Causes of Non-specific Protein Adsorption. The causes of non-specific protein adsorption at the solid-liquid interface (biomaterial surface-biological environment interface) are mainly attributed to two key components: (1) the surface properties of tested biomaterial and (2) the nature of proteins present in the biological medium. Comprehensive reviews are available in the literature for hypotheses based on experimental measurements[6, 8, 9] and theoretical calculations[10] describing the molecular events taking place during non-specific protein adsorption. A concise overview of key

factors contributing towards non-specific protein adsorption is presented here.

Based on widespread research, some general correlations have also been developed between protein properties and their adsorption to surfaces.[6, 8, 9, 11, 12] (1) Larger proteins are more likely to interact with surfaces because they can contact the surface at more sites and hence adsorption is more likely for larger proteins. (2) Protein adsorption is greatly influenced by the charge and distribution of charges on the surface of the protein molecule. (3) Adsorption also depends on the stability of the protein structure, because an unfolding of a protein structure can lead to increased conformational freedom of the peptide chain and also make more sites available for protein-surface contacts.

The adsorption process of proteins in general can be divided into three stages: the initial stage, the intermediate stage or reversibly bound stage, and the final stage yielding an irreversibly adsorbed protein layer.[13, 14] Different molecular forces exerted during the adsorption process (hydrophobic interactions, electrostatic forces, and hydrogen bonding) (Figure 2.1) depend on the nature of the biomaterial surface and protein, the particular orientation of the protein by which it approaches the biomaterial surface, and the overall binding energetics.[6, 8, 9, 12]

Initial adsorption is determined by the tertiary or quaternary structure of a protein, followed by an energetically driven unfolding process.[8, 9, 15, 16] Proteins in an aqueous environment are generally folded in such a way that their hydrophobic components are engulfed by their hydrophilic components in order to minimize the energetically unfavored polar-nonpolar interactions between surrounding water molecules and the hydrophobic protein components. However, there is no single protein that has a

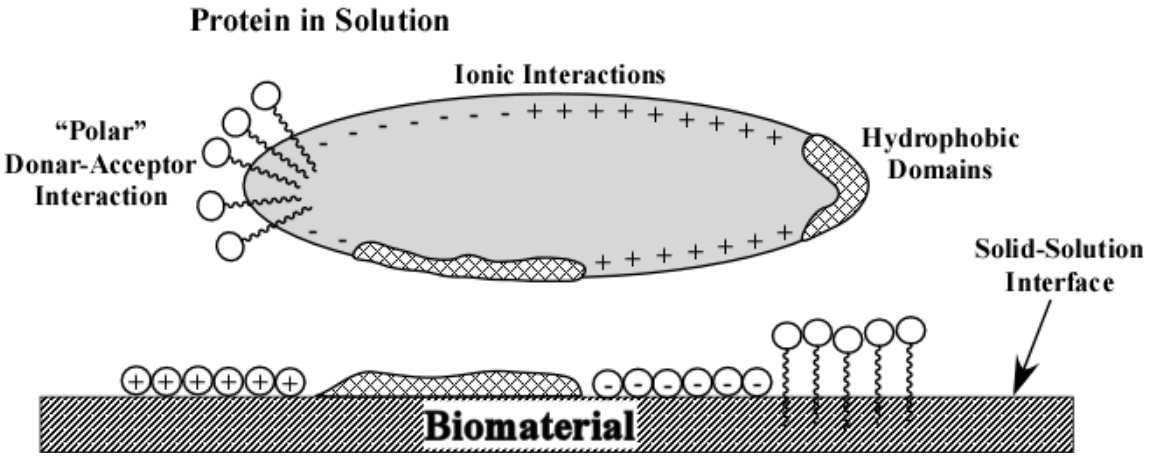

Figure 2.1. Illustration of non-specific adsorption of proteins on a well characterized surface through various driving forces (such as H-bonding, hydrophobic interactions, and electrostatic interactions). Figure adapted from Ref. 6.

completely hydrophilic surface, and as a consequence, hydrophobic interactions are unavoidable. Protein adsorption through hydrophobic interactions can be generalized as the interfacial free energy driven adsorption as proposed by Andrade, Norde, Lyklema and others.[6, 11, 17, 18] Alternatively, the electrostatic attraction theory was also investigated, but only with limited success for two reasons: (1) the force is too small under the physiological condition and too short ranged to exert any major effect on the binding event and (2) the heterogeneous charge distribution on the protein surface makes the analysis complex, if at all possible.[6, 12]

When a biomaterial surface is exposed to a complex biological environment such as blood or a body fluid, the surface is instantaneously contaminated by adsorption of small molecules, e.g. water and ions, resulting in the formation of a water layer as well as an electrical double layer, followed by adsorption of larger molecules, i.e. proteins.[6] Due to the limited ability of surface modification techniques, early studies focused on the adsorption of proteins to bio-interfaces, utilized different types of off-the-shelf substrates,

e.g. plastic, glass, and metal surfaces.[8, 19-21] Due to the low control of surface physiochemical properties for these materials, a number of model systems have been developed that are amenable for investigating protein adsorption processes. In particular, self-assembled monolayers (SAMs) of alkyl-silanes on glass and alkyl-thiols on gold are widely employed model systems. Furthermore, mixed SAMs have been applied to vary the composition of surface chemistry in a predictable and reproducible fashion.[22] Consequently, in a series of research efforts, Whitesides et. al. used SAMs[23] and a mixed SAMs[24] system to conduct a systematic study of the relationship between surface wettability and the extent of protein adsorption. These studies confirmed the previous hypotheses that proteins tend to adsorb more readily onto a more hydrophobic surface.[6, 11, 17, 18, 25] In addition, SAMs can also be easily produced on sensor surfaces such as QCM, SPR, and AFM for investigating molecular level behavior of protein on surfaces.[24, 26] However, one disadvantage of using SAMs is that they are highly ordered and therefore they do not represent the surface of "real world" materials, which are heterogeneous, less ordered, and responsive to changes in the environment.[6, 26]

Other factors that affect the adsorption process include solution conditions and the kinetics of adsorption. The pH value of liquid will affect charges on the biomaterial surface and overall protein charges, and thus affect the adsorption process. A two-fold increase in the adsorption density of ^{125}I-labeled human plasma albumin was observed on a negatively charged polystyrene surface when the pH of solution was decreased from 7.4 to 4.0.[27] The effect of pH on adsorption is also considered to be related with the isoelectric point of proteins. The well-known "Vroman effect" describes the competitive adsorption of plasma proteins, that are dependent on concentration and contact time.[28]

This phenomenon was later re-examined and confirmed by means of the Surface Plasmon Resonance (SPR) technique (using protein specific antibody).[29, 30] Additionally, given the ability of *in situ* measurement of SPR and its high sensitivity, authors were able to relate the tendency of adsorption of proteins to its properties such as, molecular weight, surface affinity, and bulk concentration, which is believed to affect the rate of mass transportation. Thus, the kinetics of adsorption also affects the final composition of an adsorbed protein layer.[8, 9, 31]

2.1.2.2 Consequences of Non-specific Protein Adsorption The consequences of non-specific protein adsorption depend on the nature of study. For *in vitro* applications, the direct impact is frequently encountered. For example, in the chromatographic separation of proteins, the target protein could be lost if there is a high level of irreversible, non-specific protein adsorption.[32, 33] Protein storage also requires minimum non-specific adsorption in order to minimize loss and activity of proteins. In extracorporeal devices where *in vitro* handling of blood and other body fluids is necessary, non-specific adsorption of proteins can lead to a loss or even absence of essential blood components.

The non-specific protein adsorption can also limit the effectiveness of the surface that provides the active component for biosensors. A typical biosensor consists of probe molecules immobilized on a substrate and the probe molecules generate a signal upon binding with the target molecules (Figure 2.2a). The non-specific adsorption of proteins on these substrates lowers the signal from the sensor and often causes high background (noise) signal (Figure 2.2b).[34] The inhibition of protein adsorption is even more critical for applications involving substrates with nano or micron sized features, such as

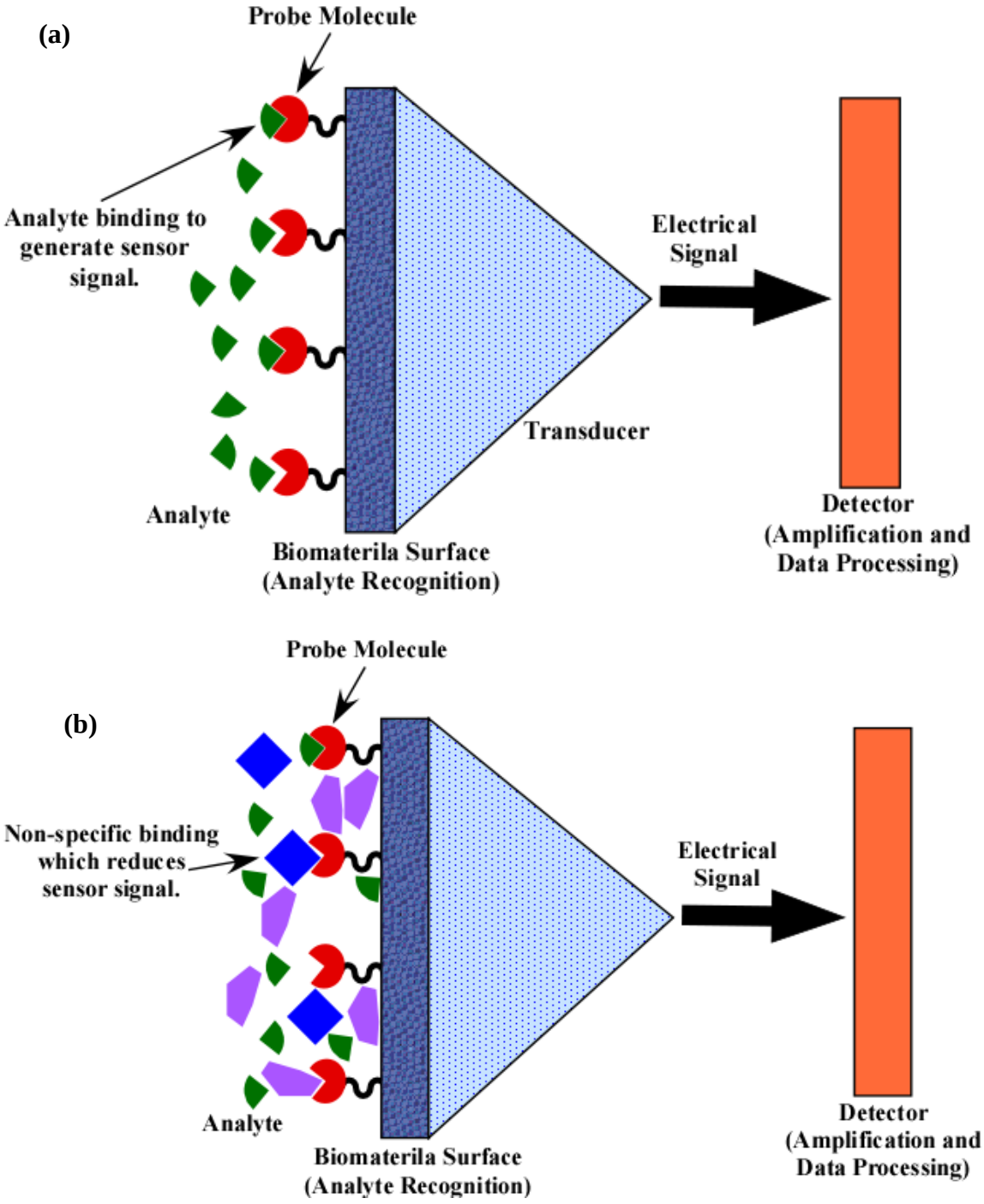

Figure 2.2. Schematic representing components of a typical biosensor. (a) Illustration of analyte binding to probe molecule. (b) Illustration of non-specific binding events.

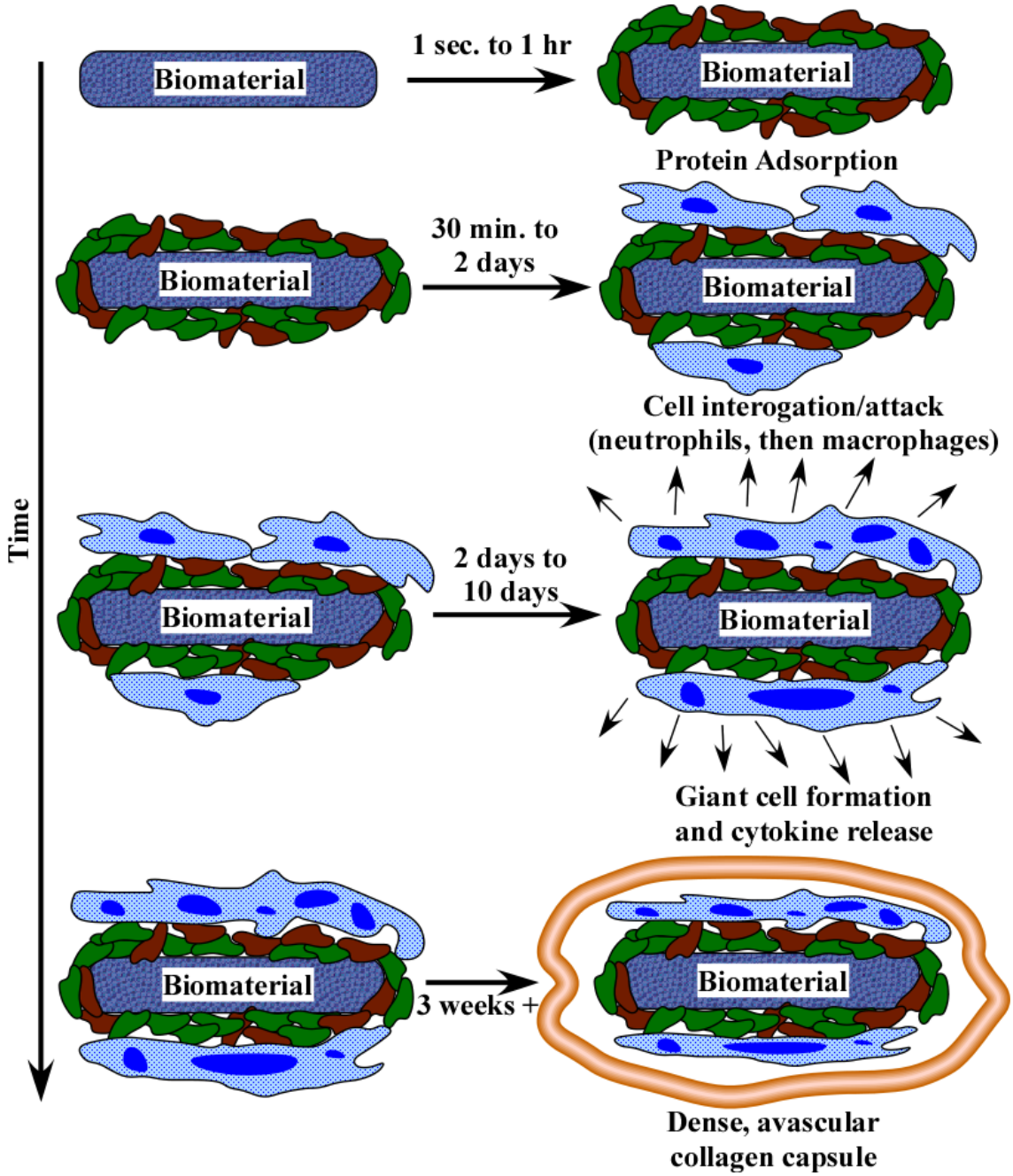

Figure 2.3. Illustration of the foreign body reaction by higher organisms to an implanted synthetic material/biomaterial. Figure adapted from Ref. 7.

nanoparticles, microchannels, and thin porous membranes, due to the large surface area they present for interaction.

For *in vivo* applications indirect impact of non-specific adsorption is normally observed. In clinical applications, adsorption of the protein and other components of the biological fluid to the surface of the biomedical device are believed to be a first occurrence event, and is often referred to as conditioning,[35, 36] which directly lead to the different physiological responses (Figure 2.3). For example, the adsorption of plasma proteins onto cardiovascular implants causes thrombus development.[18, 37] Similar effects are observed in the fouling of contact lenses with tear proteins.[38] Often, the adsorbed protein layer interacts with other biomolecules and cells, leading to their adsorption on the surface. An example is the formation of a biofilm to yield a colony of immobilized bacteria on a surface of a biomedical implant, which then shows enhanced resistance to antibiotics due to their robust sutructure.[9, 35] There is also evidence showing that a kinetically governed adsorption process elicits different cell adhesion behavior. Thus, prevention of non-specific adsorption of protein will alter the wound healing response that leads to the attraction of giant foreign body cells and the fibrous capsule formation via cellular mechanism.[35]

2.2 Surface Modification to Prevent Non-specific Protein Adsorption

There are two main aspects of biomaterial properties which are important for its applications in different fields: bulk properties and surface properties. Bulk properties include mechanical, thermal, magnetic properties and many others.[7] Surface roughness, surface chemistry, surface charge distribution, and interfacial free energy are typical

indices of surface properties of a material.[35] A match between the bulk properties of a material and demands of a specific application must be done on a case by case basis. However, the match of the bulk properties for a specific application is just a first, necessary step for creation of an ideal biomaterial. But, as discussed earlier, when a biomaterial surface is exposed to a biological environment, implanted biomedical devices elicit a host response mechanism and biosensors tends to lose their signal, which can lead to failure of the specific device. Thus, it is necessary to have a certain type of surface modification for a biomaterial which will improve biocompatibility of that material, while retaining the desired bulk properties.

Among the many surface properties, in this work, we will focus on surface modification aimed at preventing non-specific protein adsorption. A variety of approaches have been developed to render the biologically relevant surfaces protein repellent, which are discussed in detail in the following sections.

2.3 Protein Repellent/Nonfouling Coating Materials

Surface fouling is recognized as a major factor determining the biocompatibility of any biomedical device. The search for nonfouling materials to increase biocompatibility of implantable devices has never stopped. Yet, there are only a limited number of such materials available, which efficiently restrict non-specific protein adsorption. Nearly three decades ago, Merill[39] proposed a set of molecular level characteristics which explained the lowest level of protein adsorption observed experimentally. More recently, Whitesides and co-workers have thoroughly evaluated the four molecular level characteristics, which surface bound functional groups or polymers

Table 2.1. Summary of Molecular Level Characteristics of Nonfouling coating Materials.

	Hydrophilic	H-bond Acceptor	Not H-bond Donor	Neutral Charge
Phosphorylcholine	+	+	+	+
Oligo/Polysaccharides	+	+	-	±
Polyacrylates				
PHEMA	+	+	-	+
PMEA	+	+	+	+
OEGs/PEGs	+	+	+	+

*Table adapted from Ref 42.

must possess to inhibit protein adsorption: (1) they should be hydrophilic, (2) they should contain hydrogen bond acceptors, (3) they should not contain hydrogen bond donors, and (4) their overall electrical charge should be neutral.[40, 41]

To date a number of nonfouling coating materials have been explored for increasing the biocompatibility of biomaterials which can be generally divided into two major categories: (1) biomimetic materials including phosphorylcholine (PC), oligo/polysaccharides (dextran/heparin), bovine serum albumin (BSA), and other proteins; (2) synthetic polymers such as oligo/poly(ethylene glycol) (OEG/PEG), acrylates, and other hydrophilic synthetic polymers. Some of these nonfouling materials are summarized in Table 2.1 from the stand point of its molecular level characteristics,[42] described in the four "rules" above, required for efficient inhibition of protein adsorption.

2.3.1 Biomimetic Materials. Biomimetic materials such as PC and oligo/polysaccharides (dextran/heparin) occur naturally and prevent non-specific protein

adsorption in biological systems.[43-46]

2.3.1.1 Phosphorylcholines (PC). Use of PC as nonfouling material is a biomimetic approach inspired by cell surfaces, which exploits the apparent nonfouling characteristics of phospholipids.[43, 45-49] For example, the red blood cell plasma membrane is naturally nonfouling, attributed to the phospholipid bilayer structure. A number of studies have shown that lipids containing PC derived head groups, such as phosphatidylcholine, offer a significant reduction in protein adsorption on a substrate surface.[43, 47-54] The protein resistance of these lipid films is believed to be caused by a combination of zwitterionic nature of the PC headgroup (Figure 2.4) and the large amount of water that adsorb on the headgroup in aqueous solution.[47-49] The neutral net charge on PC helps to reduce long range electrostatic attraction between the surface and proteins in solution, while the water adsorbed on the headgroup produces a low energy interface in aqueous media and a decreased driving force for protein adsorption. Several studies testing protein adsorption on PC phospholipids films, prepared through Langmuir-Blodgett (LB) technique[43, 47, 53] or vesicle fusion,[50-52, 54] have shown them to be highly protein resistant surfaces. Rejection of albumin has been shown to reach as high as 90% on PC coated surfaces.[50, 52] PC lipid films have also been shown to reduce the

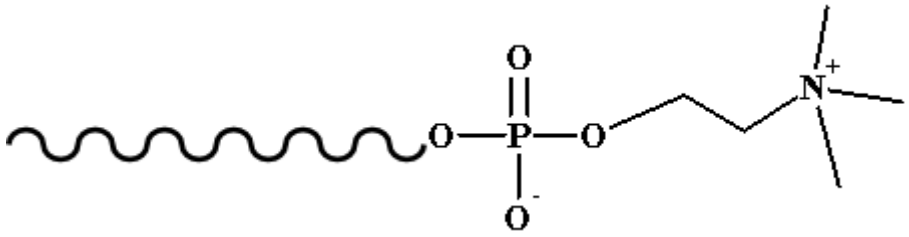

Figure 2.4. Molecular structure of phosphorylcholine headgroup.

adsorption of fibronectin by 90-99%.[43, 51] Further, studies have also been done to synthesize PC-terminated thiols, that can be used to prepare pure SAMs and mixed SAMs on gold surfaces and have been shown to reduce protein adsorption.[55-57] SAMs prepared from PC terminated thiols have shown to reduce adsorption of fibrinogen by 80-85%.[57]

Studies have also been performed to incorporate PC groups into polymers, which could then be immobilized to a surface. Copolymers that contain PC as pendant chains have been coated to biopolymers including: (1) polyurethanes (PU)[58] and poly(ethyleneterephthalate) (PET)[46] by physisorption, (2) polysulfone by blending,[59] (3) polyethylene (PE) by photoinduced graft polymerization,[60] (4) poly(dimethylsiloxane) (PDMS) by physical entanglement through swelling-deswelling.[61] Surfaces that incorporated more than 0.25 mole fraction of PC were reported to reduce protein adsorption and platelet adhesion.

2.3.1.2 Oligo/Polysaccharides. Use of oligo/polysaccharides presents another biomimetic approach that has been explored by researchers to prepare protein non-fouling surfaces. For example, while cell-cell interactions are extremely complex, there is little or no non-specific interaction of extra cellular matrix components with the cell surface.[62] *In vivo* biomolecular interactions are strongly influenced by pendent oligosaccharide chains which are present on many plasma proteins and cell surface glycolipids.[63] In an effort to mimic the non-adhesive glycocalyx, several researchers have synthesized copolymers containing oligosaccharide moieties for the modification of hydrophobic surfaces.[62]

Dextran is the most widely used oligo/polysaccharide as a hydrophilic segment in these copolymers which possesses high chain flexibility resulting from α(1→6) linkage

between the glucose subunits (Figure 2.5), and high mobility of sugar side chains provides a steric barrier against non-specific protein adsorption similar to the natural glycocalyx.[64] A variety of studies have been performed by Merchant and coworkers to incorporate dextran into copolymers as a segment in linear polymers[64-66] or as pendant chain in comb polymers.[44, 67] These linear and comb copolymers have been used as surfactants, where the hydrophobic segments provide the adhesion sites via hydrophobic interaction for surface modification of biomaterials. In protein adsorption studies, up to 90% of albumin and 70% of plasma adsorption were suppressed under dynamic conditions.[62] On the other hand, thiol substituted dextrans have also been synthesized and immobilized through S-metal interaction onto metal (gold and silver) surfaces to create protein repellent biomaterials.[68]

Heparin is another example of a polysaccharide, which acts as a nonfouling coating material.[69-71] Heparin is a highly-sulfated glycosaminoglycan (Figure 2.6) and has

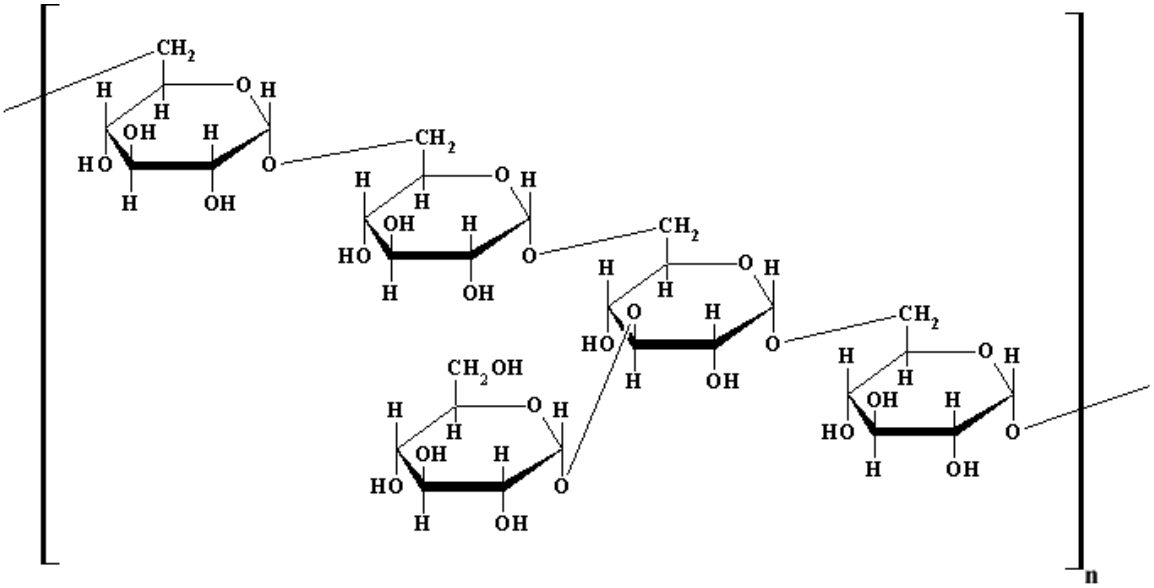

Figure 2.5. Molecular structure of dextran.

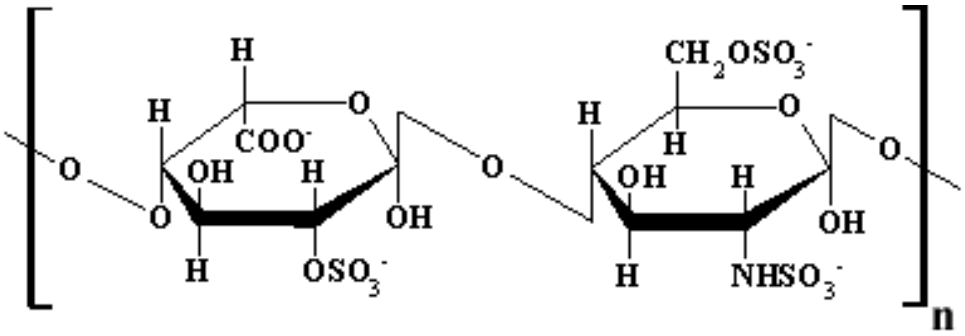

Figure 2.6. Molecular structure of heparin.

the highest negative charge density of any known biological molecule. Its activity is compromised for longer dwell time when immobilized on a surface, because heparin is most effective in a solution. A heparin grafted PE surface showed a 75% reduction in thrombus mass when compared with an untreated PE surface after a contact time of 60 min.[71]

2.3.2. Synthetic Polymers. Another major category of materials are the synthetic polymers. Inspired by the interfacial free energy theory and hydrophobic rule, acrylate based polymers were one of the first polymers explored.[72] Further, some early work with PEG containing block copolymers indicated that a surface enriched with PEG would render the surface protein resistant.[73] This finding has directed many researchers to explore PEG as a nonfouling surface coating material.

2.3.2.1 Polyacrylates. For a number of years, a significant amount of attention has been given to acrylate based polymers (Figure 2.7) as nonfouling materials.[74] In general, these polymers are utilized in hydrogel form, rather than as a surface modifying chemical functionality. Nevertheless, these polymers deserve mention in a broad discussion of nonfouling materials. Use of hydrophilic gels as an alternative to solid

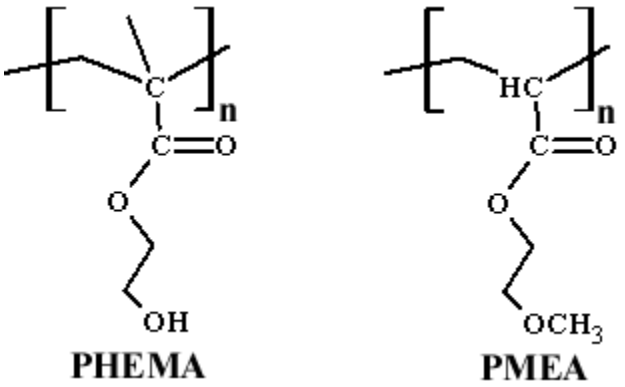

Figure 2.7. Molecular structures of acrylate based polymers poly(2-hydroxyethylmetylacrylate) (PHEMA) and poly(2-methoxyethylacrylate) (PMEA)

plastics in biomaterials was first proposed in 1960 by Wichterle and Lim[72] and poly(2-hydroxyethylmetylacrylate) (PHEMA) was found to be a viable candidate due to its high water content, bioinert character, resistance to hydrolysis, and its mechanical and optical properties. PHEMA has been used widely as a biomaterial hydrogel since the seminal work of Wichterle and Lim, and a variety of properties have been studied and adjusted through copolymerization with other monomers.[74] Beyond its use in ophthalmic lenses,[75, 76] PHEMA has found application in drug delivery vehicles,[77, 78] neural tissue templating,[79, 80] and hemocompatible films.[81-83] For example, copolymers of HEMA/styrene and HEMA/dimethylsiloxane were found to suppress platelet adhesion and aggregation, and thus reduce thrombus formation.[82]

Further, the nonfouling performance of related acrylate polymer, poly(2-methoxyethylacrylate) (PMEA), has been investigated.[84-87] In a preliminary investigation, PMEA was shown to display excellent blood compatibility in terms of platelet and leukocyte adhesion, complement activation, and coagulation.[84] Further investigation of protein adsorption on PMEA using circular dichroism (CD) spectroscopy, suggested that

while the mass of adsorbed albumin and fibrinogen on PMEA and PHEMA were similar, the conformation of adsorbed proteins was closer to that of protein in a solution on PMEA.[85] Because of this conformational difference, platelet adhesion was more suppressed on PMEA as compared to PHEMA, which may be the result of a lack of hydrogen bond donors[41] in PMEA.

2.3.2.2 Oligo- and Poly(ethyleneglycol)s. Deposition of oligo/poly(ethyleneglycol) (OEG/PEG) chains on a surface has readily been demonstrated to decrease the biological fouling that occurs at biomaterial surfaces.[88] PEG is generally accepted as one of the most biocompatible polymers, and has been subject of immense interest in the preparation of nonfouling surfaces.[89] The following section will focus mainly on the PEG and its chemical and physical properties, which contribute to its ability to resist proteins. Further, several strategies for immobilization of PEG on surfaces will also be discussed in detail.

2.4 Poly(ethyleneglycol) (PEG).

PEG, often referred to as poly(ethyleneoxide) (PEO) is a linear or branched neutral polyether (Figure 2.8) available in variety of molecular weights, and soluble in water and most organic solvents. Despite its apparent simplicity, PEG has been found to be highly effective synthetic polymer in reducing non-specific protein adsorption. There

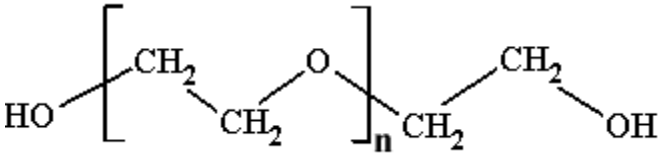

Figure 2.8. Molecular structure of poly(ethyleneglycol) (PEG).

are five key early works that established the basis for the application of PEG as nonfouling material, which are:[88] (1) the observation that PEG can be used to drive proteins and nucleic acid from a solution for purification and crystal growth,[90-92] (2) Albertsson's discovery that PEG and dextran, when mixed with a buffer, form an aqueous polymer two-phase system, which are hospitable to biological materials and are extremely useful for the purification of these biological materials,[93] (3) the discovery that PEG interacts with cell membranes to give cell fusion,[94-96] (4) Davis and Abuchowski's observation that covalent attachment of PEG to protein gives active conjugates that are non-immunogenic and non-antigenic, and have greatly increased serum lifetime,[97] and (5) Nagaoka's finding that covalent attachment of PEG to surfaces greatly retards protein adsorption to these surfaces.[73] This early research has led to several active areas of investigation, and with progress in the field of biotechnology and biomedical science, use of PEG has increased greatly over the years in diverse applications.

2.4.1 PEG Properties. PEGs possess a variety of properties pertinent to biological applications and an enormous amount of work has been done to explore these properties for different applications, which can be found in literature.[88] However, in this section PEG properties pertaining to its ability to impart nonfouling character to the biomaterial surfaces will be discussed briefly. There is currently an enormous amount of literature present concerning the nature and mechanism of nonfouling PEG surfaces. The present view and theories on mechanism of fouling resistance by PEG and similar types of hydrophilic polymers is divided into two opposing schools of thought: the physical view (physical interactions) and the chemical view (chemico-molecular interactions) of fouling resistance.[98]

2.4.1.1 The Physical View of Fouling Resistance. The description of the behavior and properties of PEG at surfaces has been the subject of many studies and some of the key models are discussed here briefly. The physical view of the fouling resistance is mainly based on the steric effect and one of the most successful theories in recent history of polymer physics, i.e. Alexander-De Gennes theory of polymer brushes.[99-102] Andrade and Jeon[103, 104] were the first to attempt and model protein resistant properties of PEO-coated surfaces based on Alexander-De Gennes theory. This model explains the inertness of PEG chains in terms of steric repulsion generated by compression of a tethered PEO layer as the protein approaches the surface. Steric repulsion is caused by the dehydration and confinement of the highly flexible and hydrated PEO chains. Further, according to their model, a high surface density and long chain length of PEO is necessary of optimal protein resistance. A limitation of this model is that it is only valid for very long PEO chains (n>200), and only brush regime of the polymer conformation was considered.

While the model of Andrade and Jeon may be supported by some experimental evidence, it cannot explain the non-fouling behavior of OEG-terminated SAMs (OEG SAMs) prepared by Prime and Whitesides,[24, 105] which have a significantly short chain length and fewer degrees of freedom then long chain PEOs. Further, Szleifer and coworkers[106-109] proposed a modified model by applying a single chain mean field theory (SCMF), and showed that the fouling resistance of the OEG SAMs can be explained. The SCMF theory fully accounts for the chain configuration, temperature, surface density of the polymer, and composition of the sample in case of the mixture. The theory produces a probability distribution function which has shown good agreement with experimental

observation of Prime and Whitesides' work. Further, this model also established that the surface grafting density of the polymer is a more important parameter while the polymer chain length has a weak effect.

The latest milestone in the physical view of fouling resistance was presented by Halperin,[110] which extends the analysis of Andarde et. al. and Szleifer. Briefly, according to Halperin's model, the effective potential experienced by a protein approaching a polymer (in brush conformation) coated surface results from the sum of: (1) a purely attractive interaction between the bare surface and the protein and (2) a purely repulsive interaction between the protein and the swollen polymer brush. And sum of the two potentials gives rise to the effective interaction which can be tuned. This model nicely describes the interplay of the thickness of the brush layer, of the surface grafting density of the polymer chains, and the size of the incoming protein.

All models described above make up the physical view of fouling resistance and depict steric repulsion as the key phenomenon behind protein repellency of PEG grafted surfaces. It also establishes that entropic contribution bears more weight than any enthalpic contribution in the system.[98] However, these models do not account for interfacial chemistry and molecular structure, and fail to take into account the role of water in the system. At best, these models portray water molecules as spherical, neutral particles.[98]

2.4.1.2 The Chemical View of Fouling Resistance. It is clear from the previous discussion that protein adsorption resistance models based on theories of a tethered polymer chain consider water as medium or as a spherical non-interacting molecule. But in reality, water plays an important role in imparting protein resistance to PEG tethered

surfaces. It is through hydrogen bonding that the PEG molecule interacts with the surrounding condensed phase, and it is the basis of high solubility of PEG in water.

A significant step forward in the chemical view of fouling resistance was proposed by Besseling et al.[111-114] They proposed a theory of hydration forces between surfaces and recognized the orientation dependent properties of the fluids and its application to water at interfaces, which can be easily applied to PEG tethered surfaces in relation to PEG solubility. Because a water molecule has electron donor (oxygen) and electron acceptor (hydrogen) regions,[115] to maximize hydration, the model predicts that surfaces too, should have a prevalence of either an electron donor or acceptor site. The ether linkage in PEG bears a strong Lewis base character due to the lone electron pairs on the oxygen atoms. The resulting interaction between PEG and water is one of the strongest of water soluble polymers, and it is this strong interaction that provides the orientation to water molecules in hydrated polymer. Because of this strong interaction, the enthalpic penalty of stripping water molecules from the PEG cannot be easily overcome by proteins, which form the basis of the chemical view of fouling resistance.

Another aspect of chemico-molecular view suggests that the three dimensional structure of the tethered polymer layer plays a role in fouling resistance. This phenomenon was established by Grunze and coworkers[116, 117] through their experimental work on nonfouling behavior of OEG SAMs. Experimental work on OEG SAMs showed that helical and amorphous conformations of tethered OEG chains were found to be resistant to fibrinogen adsorption. On the other hand, where OEG chains were packed very tightly with high surface grafting density, the OEG chains essentially solvate each other and attain *'all-trans'* conformation, which adsorbs fibrinogen due to a weak

interfacial water layer. This observation was recently re-examined and confirmed by Li et. al. that when OEG SAMs are packed above optimal surface density, they adsorb more protein due to the presence of a weak interfacial water layer.[118]

Despite the numerous investigations into underlying mechanisms by which surface bound PEG restricts adsorption, it is not fully understood or agreed upon. Empirically, however, there is agreement that PEG surface coatings, when of sufficient packing density and chain length, impart a broad non-fouling character to the surface. But it still is not clear, if it is PEG that imparts and controls fouling resistance to the biomaterial surface or if it is the water associated with PEG. It is necessary to determine and what the thermodynamic mechanism behind fouling resistance is.[98]

Another unique property of PEG which plays a role in its adsorption to surfaces is the polymers temperature dependent aqueous solubility. To be more precise, PEGs possess a lower critical solution temperature (LCST) above which PEG becomes insoluble and forms two different phases.[89] The LCST varies with molecular weight, concentration, pH, and the addition of salts. The LCST phenomenon has also been utilized to achieve higher PEG surface grafting densities.[119] Further, this LCST grafting method was also shown to promote the formation of a polymer brush structure on the surface as the solution temperature is reduced.

2.5 Traditional PEG Surface Immobilization Methods.

A variety of different methods for immobilizing PEG on biomaterial surfaces have been proposed in the literature. Traditional methods of PEGylating biomaterial surfaces can be divided into three different categories: (1) non-covalent immobilization,

(2) chemical coupling or chemisorptions, and (3) graft copolymerization. Modification of biomaterial surfaces with polymers can be realized through two general approaches: "grafting-to" or "grafting-from" (Figure 2.9).[42] The first two categories, i.e. non-covalent immobilization and chemical coupling are generally classified as "grafting-to" approaches (Figure 2.9 (b)), while plasma or radiation graft copolymerization comes under "grafting-form" approach (Figure 2.9 (a)). Normally in "grafting-to" processes, a polymer end-functionalized with a chemical moiety which has an affinity to the surface of interest is adsorbed from a solution onto that surface. In grafting from approach monomer units of a particular polymer (e.g. PEG) are polymerized at the surface of interest or to a reactive initiator present at the surface of interest. The following discussion will give a brief overview of all three different categories of techniques for PEGylation of surfaces with the main focus on non-covalent immobilization approaches (subject of this dissertation). Further, specific approaches for the protein patterning with reduced non-specific adsorption will also be discussed.

2.5.1 Graft Copolymerization. Graft copolymerization presents a strategy to immobilize PEGs directly to the surface, where polymerization with PEG containing macromonomer is carried out at the surface of interest. In these types of approaches, usually a low molecular weight moiety capable of initiating polymerization (or initiator) is adsorbed to the surface. Then, the monomer of interest is introduced to the system in the presence of catalyst to initiate the polymerization reaction at the surface of the biomaterial. The main advantage of using these types of "grafting-from" approaches is that, steric hindrance effects and diffussional limitations are minimized due to the much smaller size of monomeric units used for the polymerization purpose.[120] Thus, it is

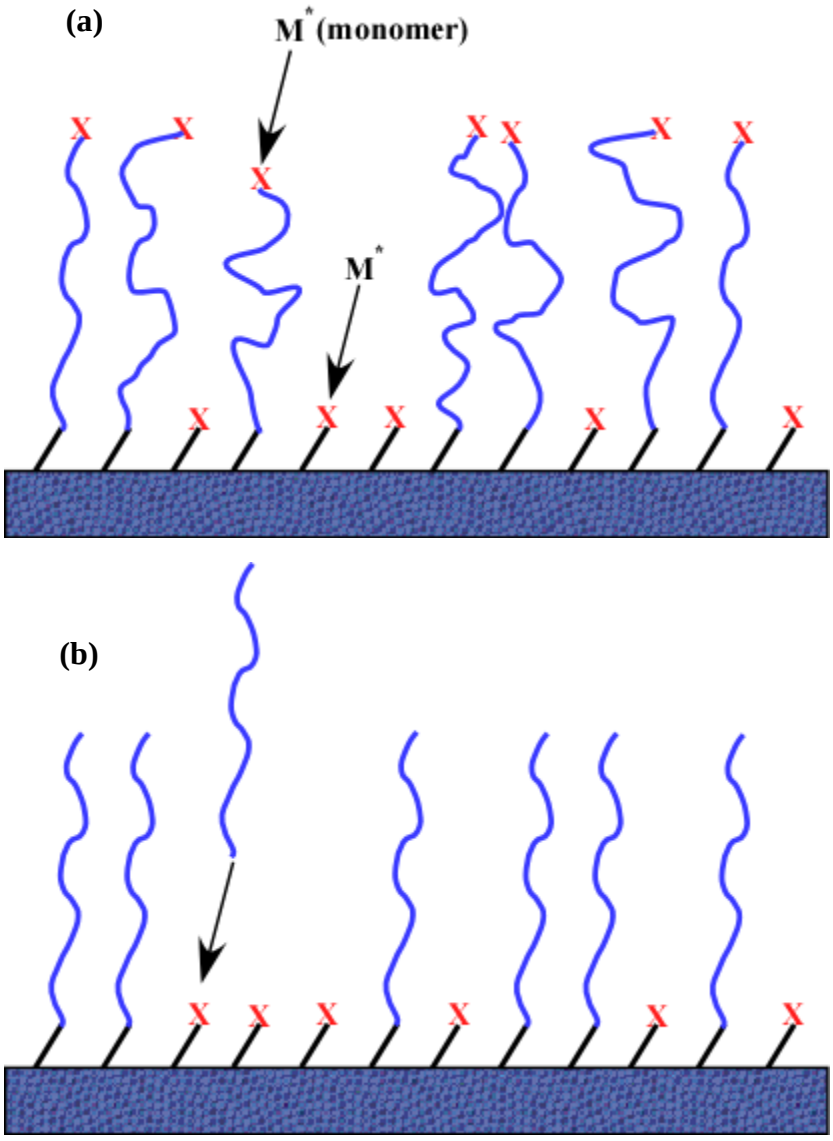

Figure 2.9. Schematic illustration of (a) "grafting-from" and (b) "grafting-to" approaches. In (a) monomers attached to the growing polymer chain vs. in (b) preformed polymer chain is attached to the surface.

possible to produce a very thick polymer layer with high surface grafting density using graft polymerization, which can be very efficient in repelling protein to the surfaces.

Various studies have been reported in the literature to immobilize PEG on material surfaces using graft polymerization approaches.[121-124] For example, Zhang et.al[123] utilized a three step approach for modification of stainless steel surfaces. Initially they modified a stainless steel surface with a mercaptopropyl silane, followed by exposure to argon (Ar) plasma and air plasma to form peroxides and hydroperoxides on the surface. Consequently, a solution of PEG monomethacrylate (PEGMA) was spread on the surface and allowed to dry, followed by polymerization with exposure to UV light. Their results indicated that they were able to achieve a polymer layer that efficiently resists the non-specific adsorption of proteins. Further studies have been carried out by investigators using plasma to initiate polymerization of PEGMA to modify the surface properties of poly(tetrafluorothylene)[122] and Si(100).[124] However, the methods described above present approaches to modify the surfaces with a specific material (e.g. PEG), and require a unique coupling chemistry specific to the surface of interest.

Surface initiated-atom transfer radical polymerization (SI-ATRP) is one more approach that is gaining increasing attention of researchers to achieve the graft polymerization of desired molecules to the surface of interest.[125-128] It is similar to the simple ATRP, and produces polymer chains with well defined structures (Figure 2.10).[125] SI-ATRP presents a powerful approach to modify the surface of a material not only with the PEG but with a variety of different materials, which do not require surface specific coupling chemistry, because simple graft polymerization and can be utilized in the development of protein selective surfaces and biosensors. Briefly, SI-ATRP utilizes

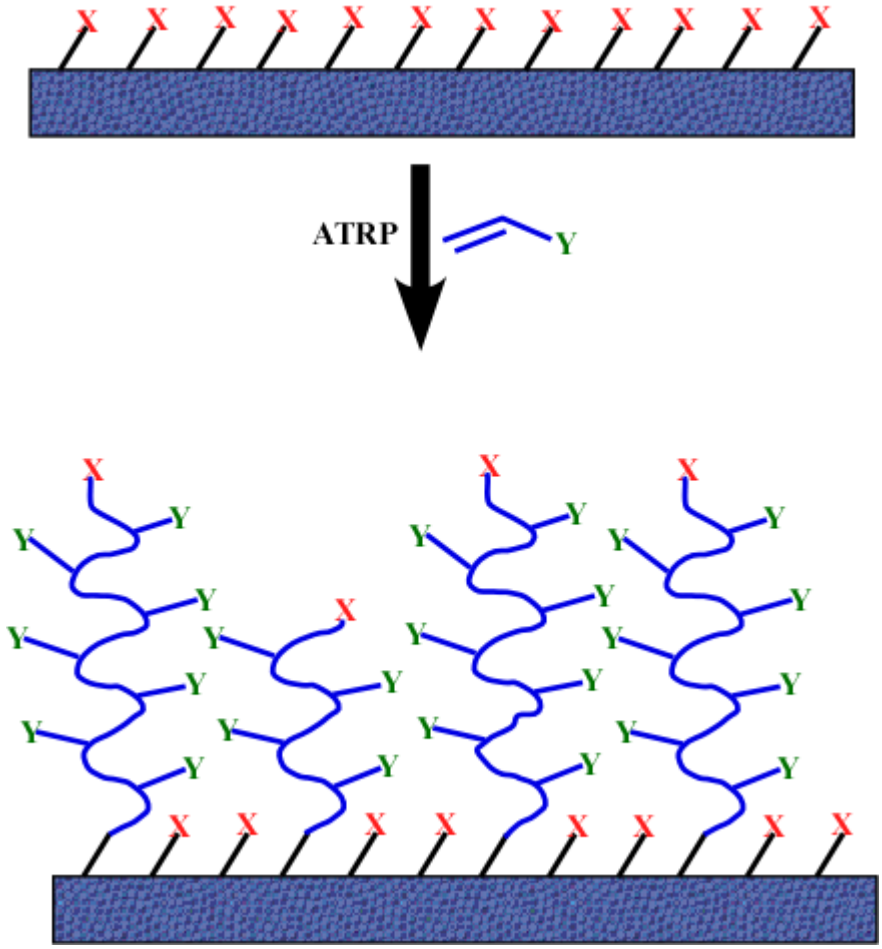

Figure 2.10. Schematic illustration of "grafting-from" approach through SI-ATRP.

immobilization of the reactive initiator to the surface either by chemisorptions or by addition to the original material in small quantities before its formation, which can later be utilized to polymerize a different material of interest. For example, Ma and coworkers[127] utilized SI-ATRP by first chemisorbing alkanethiol with pendant bromoisobutyrate on a gold surface to prepare reactive SAMs, followed by polymerization of oligo(ethylene glycol) methyl methacrylate (OEGMA) to achieve a nonfouling PEG coating on a gold surface. Recently, a novel method for the functional surface modification of a widely used organic polymer poly(dimethylsiloxane) (PDMS) was described by Wu et al.[128] using SI-ATRP, where a vinyl terminated initiator was mixed in with base polymer and a curing agent that actually forms the PDMS, resulting in an initiator integrated PDMS surface which can be later utilized for desirable functionalization of PDMS surfaces (PDMS will be discussed in greater detail in the last section of this Chapter). However, a challenge for SI-ATRP is that polymer chains grow in very close proximity, and probability of reaction termination is considerably higher than in a normal solution phase ATRP, which makes control over the polymerization reaction difficult.[120]

2.5.2 Chemical Coupling. Chemical coupling presents a simpler approach as compared to graft polymerization, where small molecules attach directly to the surface through a chemical bond without involving any heterogeneous synthesis steps. This method has been widely used to covalently couple molecules to substrates through a variety of different chemistries such as thiol and silane chemistry (Figure 2.11).

Molecules with terminal thiol functionalities have been employed for surface modification of metals, because sulfur coordinates very strongly with metals and forms a

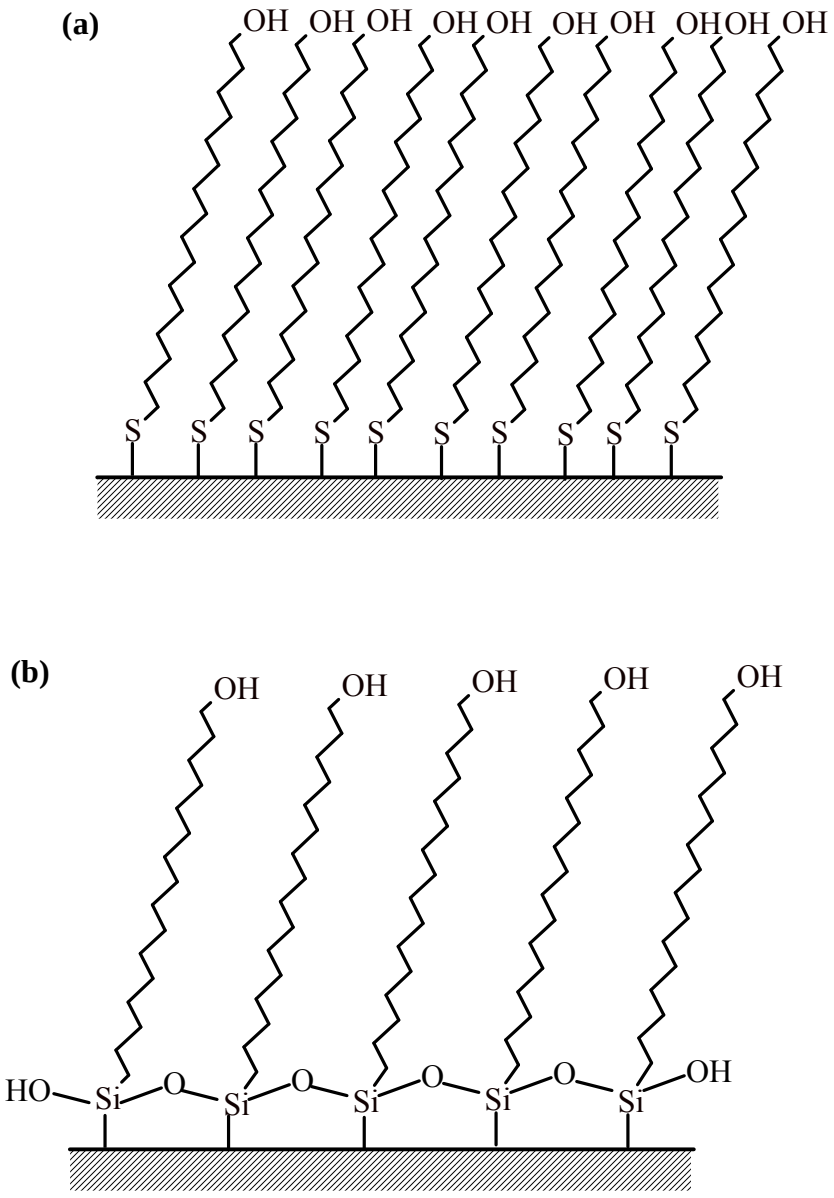

Figure 2.11. Schematic illustration of chemical coupling through (a) thiol chemistry (chemical coupling through thiol terminated molecules) and (b) silane chemistry (chemical coupling through silanol terminated molecules).

covalent bond. Prime and Whitesides[24] first reported the SAMs of OEG as a model system to study protein adsorption at interfaces. Further, they also demonstrated that SAMs of $(EG)_6$-thiol significantly reduces non-specific protein adsorption to the gold surface using elipsometric measurements. Mrksich et al.[129] expanded on Prime and Whitesides's work and demonstrated that $(EG)_6$-thiol SAMs adsorb ~2% of the protein as compared to methyl terminated SAMs, using the more sensitive Surface Plasmon Resonance (SPR) technique. Further, Wuelfing et.al[130] demonstrated that thiol terminated PEG can also be employed for surface modification of gold to obtain a thicker polymer layer. However, major drawbacks of thiol terminated SAMs is, that they are susceptible to oxidative instability and their utility is generally restricted to noble metal surfaces.[4]

To circumvent the problems associated with thiol terminated SAMs, several investigators have studied the ability of PEG-silane to modify surfaces with an oxide layer to prepare nonfouling surfaces.[131-133] This approach presents an opportunity to modify the range of biomaterials by generating an oxide layer through oxygen plasma on the surface of interest. Generally, first a PEG molecule is functionalized with trichlorosilane or trimethoxysilane group to form PEG-$OSiCl_3$ or PEG-$OSi(OCH_3)3$ (also available commercially), followed by the condensation reaction between hydrolyzed silanol groups of PEG and oxide layer on the surface, renders the surface modified with PEG chains. Jo et al.[131] investigated fibrinogen adsorption on a PEG-silane modified glass surface and demonstrated ~95-98% reduction in non-specific adsorption as compared to the control surface. Further, the silane based chemical coupling approach is also advantageous for development of PDMS based micro-devices and its various applications.[134] However, the major drawback of this technique is that it is difficult to

control the silanization process. It is also sometimes difficult to generate oxide layers on certain inert materials.

A variety of studies have reported on controlled protein adsorption using thiol terminated SAMs[24, 135-137] to develop regularly spaced protein patterns displaying high density and natural protein conformations. However, this method has some key limitations due to (1) the limited lateral mobility of the functional molecules (functional molecules provide specific adsorption site for proteins within inert PEG coated surface) and subsequently depressed multivalent interactions between the proteins and functional molecules, (2) the molar ratios and spatial arrangement of different matrix and functional molecules cannot be precisely controlled on the substrate surface and (3) the protein adsorption in the regions with functional molecules is mostly non-selective, i.e. orientation and interaction of protein with functional molecules cannot be controlled.

2.5.3 Non-covalent Immobilization. Non-covalent immobilization is one of the simplest and most straightforward approaches to achieve surface coating to reduce non-specific protein adsorption without involving any chemical coupling steps. There are a variety of different techniques that fall in the category of non-covalent immobilization. These include physisorption, Langmuir-Blodgett film deposition, and vapor deposition. In general, all non-covalent immobilization techniques are based on the immobilization of specific molecules or polymers on the surface of interest based on the non-covalent interactions, such as hydrophobic interactions, van der Waals (VDW) interactions, electrostatic interactions, etc.[138]

Physisorption and Langmuir-Blodgett film deposition techniques for creating protein non-fouling surfaces will be discussed briefly in the following sections. Further,

Langmuir monolayer and Langmuir-Blodgett techniques have also been discussed in detail with their applications in creating protein selective surfaces.

2.5.3.1 Physisorption. Several groups have explored the use of ABA type amphiphilic block copolymer, Pluronics® (commercially available), through physisorption to PEGylate the surface to create a nonfouling coating on biomaterials.[139-141] These copolymers are composed of poly(propyleneoxide) (PPO) flanked by PEO blocks, an arrangement that yields a copolymer with a relatively hydrophobic middle portion, and hydrophilic ends. It is believed that the PPO segment promotes the physisorption (serves as an anchor) of the molecule from an aqueous solution onto a hydrophobic surface, while PEO segments orient away from the surface, transforming formerly hydrophobic surfaces into hydrophilic and protein repellent surfaces. Green et al.[142] demonstrated a PPO segment length dependent adsorption behavior of Pluronics® in a SPR study, providing direct evidence for hydrophobic interaction driven adsorption processes. Using this type of strategy, Neff and coworkers[143] have used PEO-PPO-PEO end functionalized with RGD containing peptides to control the surface peptide density, while limiting the non-specific adsorption of protein on a polystyrene surface. Further, Lee et al.[140] also suggested that physisorbed films of comb-shaped block copolymers (multiple PEO blocks present on an anchor polymer chain, as opposed to just two PEO blocks on ends of an anchor chain in ABA type block copolymer) will be more suitable when compared to ABA type block copolymers. This is because comb block copolymers present more hydrophobic interaction sites and have less tendency of self-aggregation.

A more robust physisorption process involves electrostatic interaction, where charged molecules adsorb to the surface of opposite charge. For example, poly(L-lysine)

(PLL) has been demonstrated to adsorb to negatively charged surfaces.[144-146] Taking these electrostatic interactions into account, several researchers have synthesized copolymers of PEG with PLL back bone (PLL-g-PEG), and demonstrated that these graft copolymers are capable of conferring protein resistance to negatively charged surfaces.[144-146] However, as no covalent bonds are present between the coating material and the surface of interest, they tend to desorb very readily and thus physisorption has not been explored as much as other covalent coupling methods for PEGylating the surfaces.

2.5.3.2 Langmuir and Langmuir-Blodgett (LB) Technique. Langmuir and LB monolayer represents a very elegant two-dimensional technique to precisely control the packing of water insoluble amphiphilic molecules such as lipids or polymer surfactants at interfaces. Even though Langmuir and LB monolayers present relatively similar type of interfaces, they possess a characteristic difference in their location, i.e. air/water interface vs. solid substrate, respectively. Further, a thorough understanding of Langmuir monolayer behavior is crucial for utilizing the LB technique, which basically involves the formation of a monolayer film on the air/water interface with subsequent transfer onto a solid substrate as a viable route for making active thin films with controllable thicknesses, and architecture to be applied in various applications.[147]

2.5.3.2.1 Langmuir Monolayers. Langmuir monolayers are constructed via the Langmuir trough that allows for the production of well-organized monolayers. The Langmuir technique involves the spreading of amphiphilic water insoluble molecules onto an aqueous subphase, and then compressing them as shown in Figure 2.12. The amphiphilic molecules are generally lipids or polymeric surfactants with hydrophilic and hydrophobic moieties. These amphiphilic molecules are introduced onto the aqueous

surface via a non-aqueous volatile solvent that rapidly evaporates to leave them oriented at the air/water interface. Further, they orient themselves at the air/water interface in such a way that their hydrophilic moiety penetrates the aqueous subphase and their hydrophobic moiety orient towards the air.[148] As a result, amphiphilic molecules at the air/water interface form a two-dimensional system, which can be described by a plot of surface pressure as a function of the area of the water surface available to each molecule, known as surface pressure-area (π-A) isotherm. The shape of π-A isotherm can provide valuable information on phase behavior and stability of the monolayer and molecular dimension of molecules at the air/water interface.

A π-A isotherm of a phospholipid monolayer is presented in Figure 2.13 demonstrating number of distinct regions. These regions correspond to different phases experienced by the monolayer when compressed at the air/water interface. Terminology for these different phases was first proposed by W.D. Harkins.[149] Prior to compression, the surfactant molecules are known to be in the "gaseous phase," where they

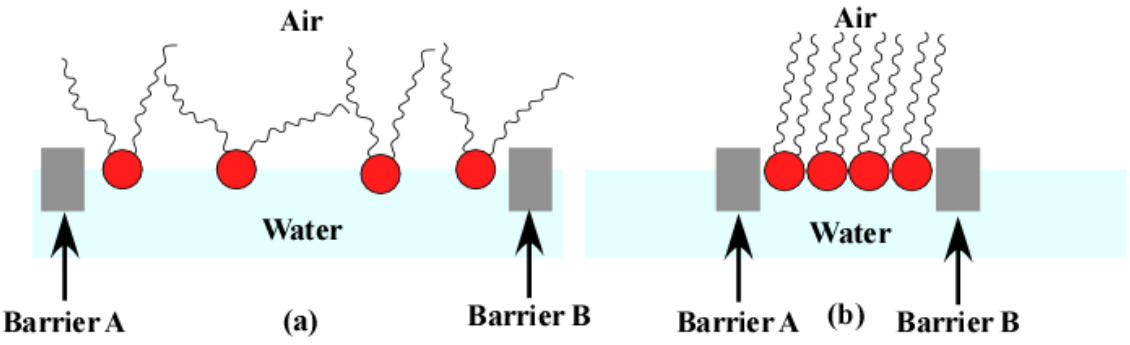

Figure 2.12. Schematic illustration of amphiphilic molecules on water subphase of a Langmuir trough. Prior to compression of barriers (A & B), molecules are in the (a) expanded phase (disordered). Upon compression of barriers, molecules come together and form (b) the compressed phase (ordered).

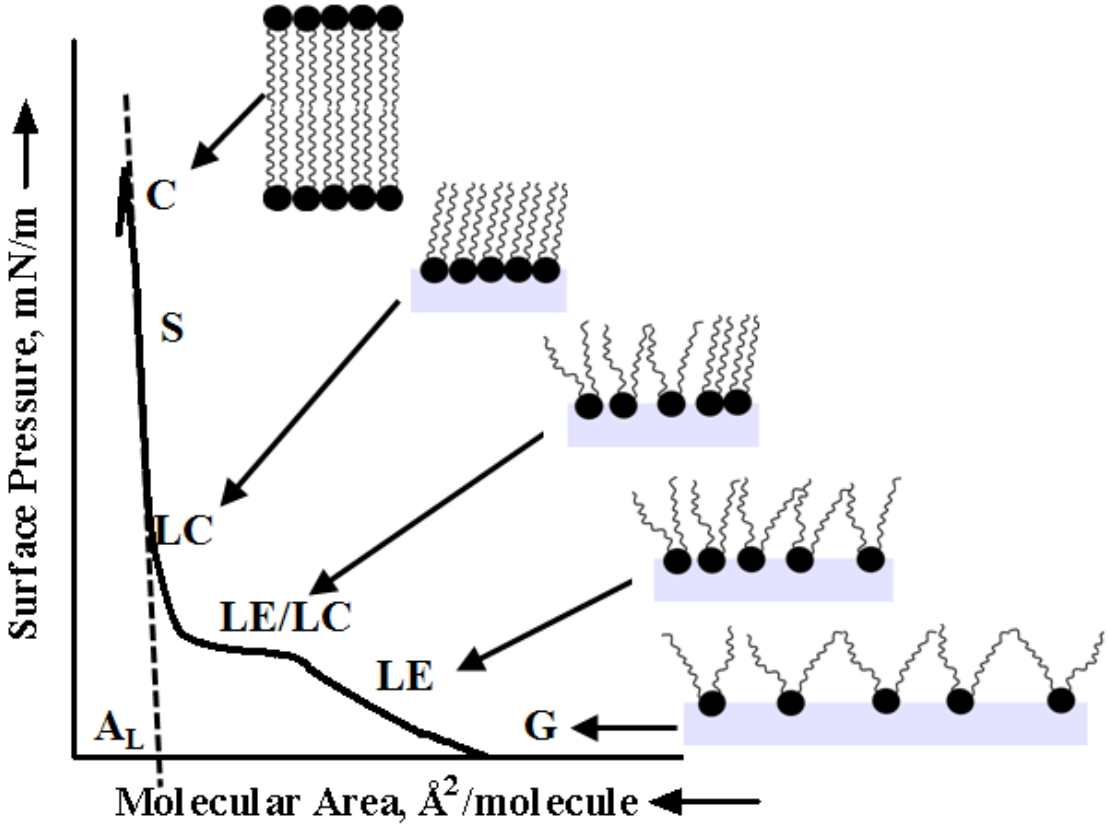

Figure 2.13. A typical π-A isotherm of a phospholipid with two hydrocarbon chains undergoing a phase transition on air/water interface. A phospholipid tends to reveal six distinct regions: 1. Gaseous (G), 2. Liquid Expanded (LE), 3. Coexistence of Liquid Expanded/Liquid Condensed (LE/LC), 4. Liquid Condensed (LC), 5. Solid (S), and 6. Collapse (C). The dotted line intersecting the X-axis correspond to the limiting area (A_L). Figure is adapted from the Reference 147.

are disordered and experience no interaction with each other. Upon compression, phase transition takes place from the "gaseous phase" to the "liquid expanded (LE) phase" where contact between headgroups takes place, but high mobility of the hydrophobic chain is maintained. Upon further compression, the "LE phase" undergoes a transition to the "liquid condensed (LC) phase", where the headgroups and hydrophobic chains are now aligned in nearly their closest packing. At even higher compression, the lipids reach their highest packing known as the "solid phase." If the monolayer is compressed further, it will collapse into a three-dimensional structure.

Further, mainly for phospholipid monolayers, the π-A isotherm reveals a two phase coexistence (first order phase transition) between the liquid expanded/liquid condensed (LE/LC) phases. The transition region is extremely temperature dependent, where if the temperature increases π value at which transition occurs, also increases and vice versa.[148] As mentioned above, the π-A isotherm can also provide quantitative information corresponding to the molecular dimension of the amphiphilic molecule at the air/water interface. By extrapolating the slope of solid phase to zero pressure, the point at which this line intersects X-axis is called the limiting molecular area (A_L): this point represents the hypothetical area occupied by one amphiphilic molecule in the condensed phase.[148]

2.5.3.2.2 Langmuir-Blodgett (LB) Films. LB technique is a useful method that allows researchers to further investigate the properties of monolayers and multilayers. The LB technique involves the deposition of monolayers from the air/water interface onto a solid substrate. The solid substrate can be either hydrophilic (glass, SiO_2, etc.) or hydrophobic (silanized glass, highly ordered pyrolytic graphite, etc.). There are various

parameters that affect the type of LB films formed. These parameters include the nature of the monolayer, nature of the substrate, deposition speed, and π at which deposition takes place.[150]

2.5.3.2.3 Langmuir and LB Films for Protein Repellent Coatings. Combination of water insoluble, PEG containing molecules and Langmuir technique present an opportunity to create dense PEG brushes: water insoluble, PEG containing molecules residing on the air/water interface can be compressed by Langmuir trough barriers to control the surface PEG density.[151] Further, this highly compressed PEG containing monolayer can be transferred to the different surfaces to reduce non-specific protein adsorption. Given the delicacy of this technique and the nature of information it provides, a variety of fundamental studies have been performed with the PEG containing water insoluble molecules to better understand the conformational behavior of PEG with varying surface densities.[152-158] These fundamental studies have been performed using a novel class of compound, i.e. PEG-lipid conjugates, also known as lipopolymers.

Very few investigations can be found in the literature utilizing the Langmuir and LB monolayer technique to create protein non-fouling surfaces. Byun et al.[159] investigated the behavior of mixed lipids monolayers of dipalmitoylphosphatidylcholine(DPPC), which is naturally protein repellent owing to its PC headgroup, and dipalmitoylphosphatidylethanolamine-PEG (DPPE-PEG, PEG lipid) (PEG MW 5000) at the air/water interface, and demonstrated that transferred LB films on a glass surface with just 3 mol% PEG lipid concentration was greatly effective in reducing platelet adhesion as compared to pure DPPC films. Further, Hui et al.[160] investigated the mixed monolayers of DPPE and distearoylphosphatidylethanolamine-

PEG (DSPE-PEG) with different molecular weights of PEG chains (PEG MW 750-5000), which were transferred to DPPE coated glass surfaces. Their results demonstrated that the concentration of PEG lipids required to reduce the protein adsorption on LB films decreases as MW of grafted PEG chain increases. Further, Jogikalmath and Hlady[151] investigated Langmuir monolayers of poly(styrene)-b-poly(ethylene oxide) (PS-b-PEO) (MW of PS segment 12,200 and PEO segment 23,900) on air/water interface using SPR and demonstrated that more than 0.1 PEO chain/nm^2 was required to inhibit albumin or ferritin adsorption. Further, they also suggested that half-reduction of albumin adsorption required approximately three fold higher PEO surface density than the half-reduction of ferritin adsorption. This finding suggests that size of the protein of interest plays an important role in designing the surfaces to control non-specific protein adsorption.

2.6 Langmuir and LB Films for Protein Patterning.

Controlling immobilization of proteins and other biomolecules on surfaces while preventing non-specific adsorption of unwanted species, is crucial to fundamental biological research[161, 162] as well as to the development of biologically integrated devices with micron to nano scale resolution having a variety of applications including high-throughput proteomic arrays and combinatorial library screening.[163-168]

Langmuir and LB monolayers prepared from amphiphilic molecules such as lipids provide prominent type of interface which organize by self-assembly, and their fundamental two dimensional properties that offer several advantages:[169] (1) Sophisticated tools in Lipid technology facilitate the coating of almost every surface with different techniques. (2) Due to the two-dimensional physical properties, the phase

behavior of these lipid films (LE to LC transition, Figure 2.13) permit lateral organization and pattern formation. (3) Lipid interfaces present an opportunity to create customized and programmable surfaces with the large number of possible membrane components. (4) Use of natural membrane components in lipid assemblies suppresses phenomena of denaturation or non-specific adsorption which would otherwise mask specific binding effects.

Even though Langmuir and LB monolayers present relatively similar types of molecular recognition platforms, it is essential to illustrate a characteristic difference between these two interfaces from a protein patterning standpoint. As discussed earlier, the primary distinction between these two types of monolayers is location (i.e., air/water interface vs. solid substrate, respectively), however the lipid behavior in the two films can vary greatly, which in turn may influence the interaction of other molecules such as proteins, with the films and subsequently protein patterning.[170] Thus, Langmuir and LB monolayers essentially present two different types of, but closely associated, protein patterning platforms: (1) In Langmuir monolayers, lipid mobility and subsequent patterning is guided by a template molecule such as a protein. (2) In LB films, lipid mobility is leveraged to realize the pattern formation, which is then needed to bind a template molecule such as protein.

Various studies[169-184] have been reported on Langmuir monolayer coated surfaces exhibiting controlled protein adsorption, where molar ratios of matrix and functional lipids can be precisely controlled with high lateral mobility of the functional lipids at the air/water interface. Fang et al.[176, 178] reported an approach for selective protein immobilization where they combined Langmuir monolayers with SAMs to create phase

separated OTS/FTS (*n*-Octadecyltrichlorosilane/1*H*1*H*2*H*2*H*-perfluorodecyltrichlorosilane) monolayers and demonstrated that protein preferentially binds to the *–CH₃* terminated regions of the patterned monolayers. However, protein selectivity of the patterned monolayers was lost at higher protein concentrations on the surfaces. Arnold and co-workers[171, 172, 174, 175, 177, 179-182] presented a versatile and convenient method for targeting proteins with surface-accessible histidine residues to lipid assemblies, bearing iminodiacetate (IDA) lipids as functional lipids loaded with divalent metal ions (Cu^{2+} or Ni^{2+}), using metal ion coordination chemistry. Further, they investigated a variety of matrix lipids having structures similar to the functional IDA lipids to optimize the miscibility, in order to prepare metal chelating lipid monolayers and bilayers patterned at the nano-meter scale. Dietrich and co-workers[169, 173] reported a very novel approach of specific immobilization as well as a two-dimensional organization of histidine-tagged biomolecules via coordinative binding to nitrilotriaceiticacid (NTA) chelator complexes linked to the lipid interface. However, in their approach they deliberately mismatched the alkyl tails of matrix lipids (DMPC, C_{14}) and functional lipids (NTA-DODA, C_{18}) to induce immiscibility and generate patterning at the micro-scale, derived from the phase behavior of the binary lipid systems. Most recently, Britt et al.[170] and Du et al.[183, 184] demonstrated a novel bottom-up approach for protein patterning in the Langmuir monolayers based on protein directed binding to the mixture of cationic/nonionic lipids in the fluid monolayers to generate protein induced patterns on micro-meter scale. However, the success was limited by a large fraction of irreversibly bound protein on the patterned monolayers, attributed in part to strong protein-protein interactions (aggregation) during the patterning process.

These above discussed approaches facilitate an opportunity of generating protein patterns at micro-meter and nano-meter scales (Figure 2.14) based on the selection of component lipids, i.e. functional lipids which serve as binding site for proteins and matrix lipids, and their fundamental two-dimensional physical properties (e.g. phase behavior, diffusion) in Langmuir monolayers. Thus, Langmuir monolayers of mixture of lipids containing poly(ethylene glycol) (PEG) bearing phospholipids as matrix lipid can serve as a generic platform for synthesis of protein patterns with reduced non-specific adsorption, which will be investigated in this dissertation. Further, applications of this PEG bearing Langmuir monolayers as platforms for two-dimensional molecular imprinting of proteins will also be tested.

Over the years, Langmuir and LB film techniques have been utilized by scientist primarily to investigate the fundamental science and to study model systems. Even so, these techniques are slowly finding their niche in the field of applications (e.g.

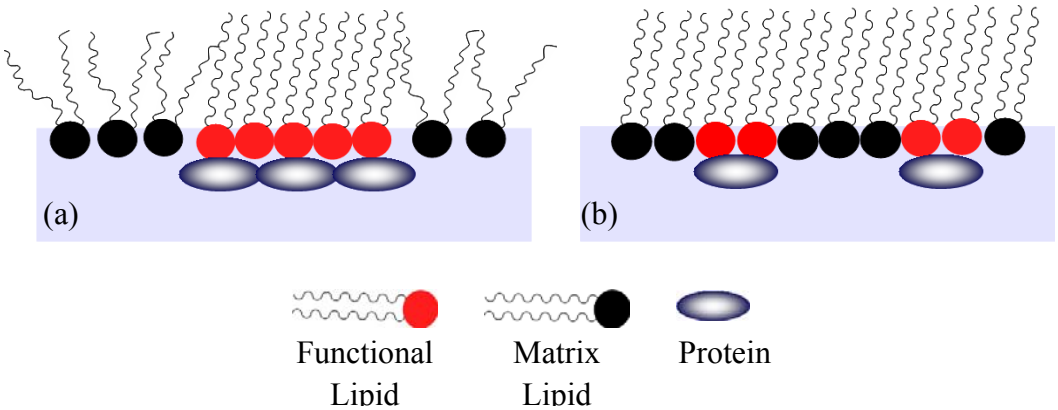

Figure 2.14. Patten formation and specific binding of proteins to functional lipids (a) Model illustrating the lateral organization and pattern formation at micro-meter scale based on phase behavior induced through intentional alkyl tail mismatch between functional lipids and matrix lipids. (b) Model illustrating the lateral organization and pattern formation at the nano-meter scale based on the miscibility of functional lipids and matrix lipids.

development of sensors surfaces for QCM and SPR), practice of Langmuir and LB techniques in industry is far from satisfactory in today's date because of problems associated with its scale up. Thus, a more applied system of PEG-partitioning and assembly at elastomer, poly(dimethylsiloxane) (PDMS), surfaces will be investigated as a final element of these dissertation, compared to the two dimensional assembly of PEG-layers at the air/water interface.

2.7 Poly(Dimethylsiloxane) (PDMS).

Poly(dimethylsiloxane) (PDMS) is commercially available medical grade polymer. PDMS normally comes in convenient two part kit of base polymer and curing agent. The PDMS polymer is synthesized by mixing base polymer and curing agent in suitable mass ratio followed by curing (cross-linking reaction), either at moderate temperatures (65-70 ºC) for short periods of time or at room temperature for 24-48 hrs. (Figure 2.15). The base polymer consists of dimethylsiloxane oligomers terminated with vinyl end groups, platinum catalyst, and silica filler while the curing agent is composed of cross-linking agent (dimethylhydrogensiloxane) and an inhibitor. The cross-linking occurs by hydrosilylation to create silicone-carbon bonds between the vinyl groups in the base polymer and the silicone hydride of the curing agent in the presence of platinum catalyst to create CH_2–CH_2 links between the chains.

PDMS is widely used in soft lithography applications,[40, 185-188] microfluidic devices,[189-195] and biological systems[134, 196-198] including blood contacting surfaces.[199-202] PDMS is a choice material given a range of favorable properties, including:[190] (1) low temperature polymerization conditions and low viscosity allowing PDMS to flow into

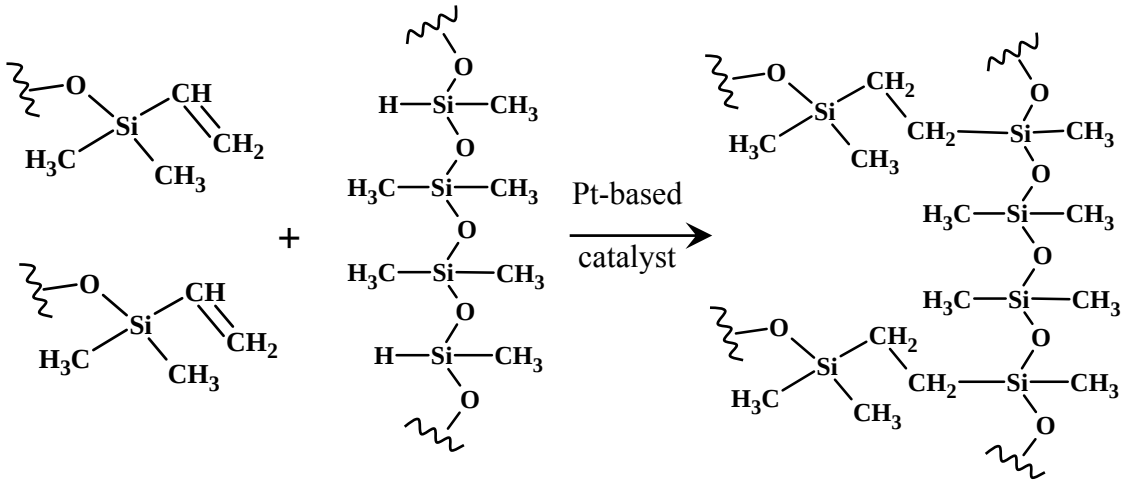

Figure 2.15. Synthesis of poly(dimethylsiloxane) polymer. The reaction proceeds by cross-linking of dimethylsiloxane oligomers terminated with vinyl groups with dimethylhydrogensiloxane in the presence of a platinum catalyst. The reaction proceeds via hydrosilylation to create silicone-carbon bonds resulting in CH_2–CH_2 links between chains.

micro-scale patterns on template surfaces; (2) good mechanical properties and tunable elasticity, favoring preservation of micro-scale features imprinted in the PDMS from a master template, allowing applications in microfluidic chips and even facilitated mechanical pumping of fluids within microchannels;[40, 203] (3) high optical transparency down to 280 nm, allowing for applications in bio-analyte detection over a wide range of wavelengths;[192] (4) low biological activity and toxicity, which favors applications in medicine and novel methods such as cell patterning;[193] (5) high gas permeability, necessary for oxygen delivery to growing cells in a closed systems such as bioreactors.[204]

While the mechanical, optical, and gas transport properties of PDMS are very favorable, the high hydrophobicity of the polymer (static water contact angle of 115º) often limits applications. Complications include: (1) significant non-specific protein adsorption limiting its application in biomedical and biosensor devices;[196] (2) resistance to flow of polar liquids in the microchannels of a microfluidic device;[190] and (3) swelling

in presence of organic solvents.[205] These disadvantages limit the use of PDMS in some applications. In consequence, a facile and cost-effective method for surface modification of PDMS needs to be developed which imparts hydrophilic properties to the PDMS surface and retains the desired bulk properties.

2.7.1 PDMS Surface Modification Strategies. A variety of surface modification strategies have been developed to render the PDMS surface hydrophilic and protein repellent using hydrophilic polymers, such as poly(ethyleneglycol) (PEG) to increase the applicability of PDMS. Further, these PDMS surface modification strategies can be divided into three broad categories, namely physisorption, covalent modification, and physical entanglement. Surface modification of PDMS with physisorption mainly involves the use of charged surfactants[206, 207] and polyelectrolyte multilayers (PEMs),[208-210] and is driven by hydrophobic interaction and electrostatic force respectively. However, this simple method yields modified PDMS surfaces exhibiting low stability and can only withstand lower shear stress.[190]

Covalent coupling of hydrophilic polymers to the PDMS surface generates stable and desirable surface properties, but it is difficult to achieve, because PDMS is chemically inert. Chemical coupling and graft copolymerization strategies for surface modification with PEG, which has been employed by different researchers, is similar to the methods discussed in previous sections of PEG immobilization techniques. Briefly, covalent coupling methods for surface modification of PDMS can be generally divided into two classifications known as grafting-from and grafting-to approaches.[211] The grafting-from approach employs active species existing on the PDMS surface to initiate the polymerization of monomers from the surface, while in the case of the grafting-to

approach, performed polymer chains carrying reactive groups at the end or side chains are covalently coupled to the surface. In the grafting-to approach, generally the first step is to render the surface reactive through exposure to oxygen plasma[185] or ultraviolet ozone (UVO)[212, 213] etching, resulting in a glass-like silicate layer with chemically reactive groups (–OH) on the surface. Additional surface modification is achieved via chemical coupling of target molecules to the –OH following standard protocols. However, the underlying glass-like layer remains brittle, limiting its applications where elasticity is required, and has also been found to be unstable when stored in air.[214] In the grafting-from approach of covalent coupling, UV energy has been widely applied for surface graft polymerization of polymers with the aid of a photoinitiator or photosensitizer.[215-219] Additionally, graft polymerization through exposure to radiation has also been investigated for surface modification of PDMS with hydrophilic polymers.[80, 220] Recently, a novel chemical cross-linking method for functional surface modification of PDMS was described by Wu et al.,[128] where a vinyl terminated initiator was mixed with a liquid PDMS prepolymer prior to curing, resulting in an initiator integrated PDMS surface which can be utilized later for desirable functionalization of PDMS surface using surface initiated–atom transfer radical polymerization (SI–ATRP). However, these covalent coupling methods require multiple reaction steps and are time consuming, which can be costly and inefficient.

2.7.2 Physical Entanglement Method. The physical entanglement technique presents a very elegant approach for modification of PDMS surfaces. This method takes advantage of PDMS swelling in the presence of certain organic solvents. In this approach, the first step is swelling of a cross-linked PDMS monolith in an amphiphilic

copolymer (usually with PDMS segment as anchor group) solution, followed by deswelling to embed / anchor the amphiphilic copolymers on the surface of the cross-linked PDMS. When amphiphilic copolymer molecules are tethered, van der Waals force and hydrophobic interactions between the PDMS monolith and PDMS segments in block copolymers lead to a hydrophilic surface (Figure 2.16). To our knowledge only two such studies have been reported in the literature utilizing physical entanglement through swelling-deswelling for surface functionalization of PDMS. Han et al.[221] first reported the use of this method to immobilize PDMS-b-PEO molecules on PDMS surface and demonstrated increased hydrophilicity of PDMS surface. Further, Seo et al.[61] used ABA type block copolymer of poly(2-methacryloyloxyethylphosphorylcholine) (MPC) and PDMS (MPC-PDMS-MPC) to synthesize phosphorylcholine terminated PDMS surfaces via swelling-deswelling protocol, and demonstrated significant reduction in protein adsorption as compared to native PDMS surface. They also demonstrated increased hydrophilicity of PDMS surfaces. However, this method is very time consuming and requires an organic solvent such as chloroform to sufficiently swell the PDMS.

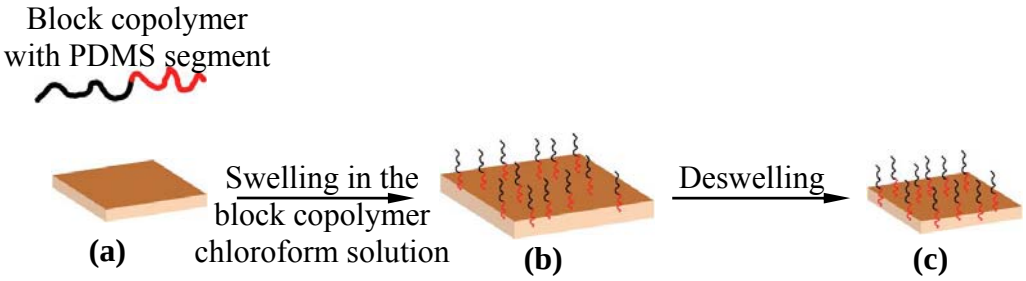

Figure 2.16. Modification of PDMS surface with physical entanglement through swelling-deswelling method. (a) Pristine PDMS, (b) PDMS swelling in the block copolymer chloroform solution, (c) Modified PDMS surface after deswelling. Figure adapted from Ref. 221.

Further, a few studies[222-225] have also been reported in the literature, where functionalization of the PDMS surface was achieved by bulk modification of PDMS through a premixing method, i.e., addition of the functional molecules to the liquid PDMS prepolymer prior to curing. This premixing method was first utilized by Neys et al.[222] to create catalytic PDMS films with porphyrin doping of PDMS prepolymer. Further, Zare and coworkers[223] investigated bulk modification of PDMS for protein immobilization on PDMS surface through addition of biotinylated phospholipids (1,2-dioleoyl-sn-glycero-3-phosphoethanolamine-N-(biotinyl) (Bio–DOPE)) to PDMS prepolymer. In one more study, Zare and coworkers[224] fabricated bulk-modified PDMS microchips by adding a carboxylic acid (undecylenic acid) to the prepolymer prior to curing. This study mainly focused on introducing charged groups to increase the electro osmotic flow (EOF) in PDMS microchannels, which ultimately results in improvement of the separation efficiency and reduction of peak broadening in PDMS microfluidic devices. However, in both studies by Zare et. al. additive doped PDMS showed similar hydrophobicity behavior as native PDMS. Further, a recent study by Xiao et al.[225] investigated bulk modification of PDMS microchips by addition of amphiphilic copolymer poly(lactic acid)-poly(ethyleneglycol) (PLA-PEG) for reducing hydrophobicity as well as the non-specific protein adsorption to PDMS microchannels. They demonstrated that due to the non-ionic nature of the PEG EOF within bulk modified PDMS microchannels was decreased and non-specific protein (myoglobin) adsorption was also reduced drastically owing to excellent protein repellent properties of PEG.

Further, a very facile approach for nonfouling and hydrophilic surface modification of PDMS based on commercially available materials through the physical

entanglement method will be investigated as a part of this dissertation work. In this approach, a variety of amphiphilic block copolymers will be mixed in with the viscous base and curing agent of Sylgard® 184, to yield an amphiphilic block copolymer integrated PDMS.

2.8 References

1. Williams, D. F. ed. *Definitions in Biomaterials*. Elsvier: Amsterdam, 1987; p 72.

2. Turner, N. W.; Jeans, C. W.; Brain, K. R.; Allender, C. J.; Hlady, V.; Britt, D. W. *Biotechnol. Prog.* **2006,** 22, (6), 1474-1489.

3. Hench, L. L.; Wilson, J. *Science* **1984,** 226, (4675), 630-636.

4. Xu, Z. Ph.D. Thesis, Case Western Reserve University, Cleveland, OH, 2000.

5. Kauzmann, W. *Adv. Protein Chem.* **1959,** 14, 1-63.

6. Andrade, J. D.; Hlady, V. *Adv. Poly. Sci.* **1986,** 79, 1-63.

7. Ratner, B. D.; Bryant, S. J. *Annu. Rev. Biomed. Eng.* **2004,** 6, 41-75.

8. Horbett, T. A.; Brash, J. L. *ACS Symp. Ser.* **1987,** 343, 1-33.

9. Horbett, T. A. Proteins at interfaces - An overview. In *Proteins at Interfaces Ii - Fundamentals and Applications*, Horbett, T. A.; Brash, J. L., Eds. 1995; Vol. 602, pp 1-23.

10. Talbot, J.; Tarjus, G.; Van Tassel, P. R.; Viot, P. *Colloid Surf. A* **2000,** 165, (1-3), 287-324.

11. Lyklema, J. *Colloids Surf.* **1984,** 10, (AUG), 33-42.

12. Leckband, D.; Israelachvili, J. *Q. Rev. Biophys.* **2001,** 34, (2), 105-267.

13. Krisdhasima, V.; McGuire, J.; Sproull, R. *J. Colloid Interface Sci.* **1992,** 154, (2), 337-350.

14. Rabe, M.; Verdes, D.; Rankl, M.; Artus, G. R. J.; Seeger, S. *Chemphyschem* **2007,** 8, (6), 862-872.

15. Soderquist, M. E.; Walton, A. G. *J. Colloid Interface Sci.* **1980,** 75, (2), 386-397.

16. Ivarsson, B.; Lundstrom, I. *CRC Crit. Rev. Biocomp.* **1986,** 2, (1), 1-96.

17. Koutsoukos, P. G.; Mummeyoung, C. A.; Norde, W.; Lyklema, J. *Colloids Surf.* **1982,** 5, (2), 93-104.

18. Norde, W. *Adv. Colloid Interface Sci.* **1986,** 25, (4), 267-340.

19. Hench, L. L. *J. Biomed. Mater. Res.* **1980,** 14, (6), 803-811.

20. Hench, L. L. *Science* **1980,** 208, (4446), 826-831.

21. Cheng, Y. L.; Darst, S. A.; Robertson, C. R. *J. Colloid Interface Sci.* **1987,** 118, (1), 212-223.

22. Bain, C. D.; Whitesides, G. M. *J. Am. Chem. Soc.* **1988,** 110, (19), 6560-6561.

23. Sigal, G. B.; Mrksich, M.; Whitesides, G. M. *J. Am. Chem. Soc.* **1998,** 120, (14), 3464-3473.

24. Prime, K. L.; Whitesides, G. M. *Science* **1991,** 252, (5009), 1164-1167.

25. Coleman, D. L.; Gregonis, D. E.; Andrade, J. D. *J. Biomed. Mater. Res.* **1982,** 16, (4), 381-398.

26. Bain, C. D.; Whitesides, G. M. *Angew. Chem., Int. Ed. Engl.* **1989,** 28, (4), 506-512.

27. Vandulm, P.; Norde, W. *J. Colloid Interface Sci.* **1983,** 91, (1), 248-255.

28. Vroman, L. *Nature* **1962,** 196, (4853), 476-&.

29. Green, R. J.; Davies, J.; Davies, M. C.; Roberts, C. J.; Tendler, S. J. B. *Biomaterials* **1997,** 18, (5), 405-413.

30. Green, R. J.; Davies, M. C.; Roberts, C. J.; Tendler, S. J. B. *Biomaterials* **1999,** 20, (4), 385-391.

31. Elbert, D. L.; Hubbell, J. A. *Annu. Rev. Mater. Sci.* **1996,** 26, 365-394.

32. Hiatt, C. W.; Shelokov, A.; Rosentha.Ej; Galimore, J. M. *J. Chromatogr.* **1971,** 56, (2), 362-&.

33. Hanson, M.; Unger, K. K. *Trac-Trends Anal. Chem.* **1992,** 11, (10), 368-373.

34. Masson, J. F.; Battaglia, T. M.; Cramer, J.; Beaudoin, S.; Sierks, M.; Booksh, K. S. *Anal. Bioanal. Chem.* **2006,** 386, (7-8), 1951-1959.

35. Gristina, A. G. *Science* **1987,** 237, (4822), 1588-1595.

36. Gristina, A. G.; Hobgood, C. D.; Webb, L. X.; Myrvik, Q. N. *Biomaterials* **1987,** 8, (6), 423-426.

37. Kottkemarchant, K.; Anderson, J. M.; Rabinovitch, A. *Biomaterials* **1986,** 7, (6), 441-448.

38. Kunzler, J. F. *Trends Polym. Sci.* **1996,** 4, (2), 52-59.

39. Merrill, E. W., Distinctions and Correspondences among Surfaces Contacting Blood. In *Ann. N. Y. Acad. Sci.*, 1987; Vol. 516, pp 196-203.

40. Quake, S. R.; Scherer, A. *Science* **2000,** 290, (5496), 1536-1540.

41. Ostuni, E.; Chapman, R. G.; Liang, M. N.; Meluleni, G.; Pier, G.; Ingber, D. E.; Whitesides, G. M. *Langmuir* **2001,** 17, (20), 6336-6343.

42. Dalsin, J. L. Ph.D. Thesis, Northwestern University, Chicago, IL, 2004.

43. Malmsten, M. *J. Colloid Interface Sci.* **1995,** 172, (1), 106-115.

44. Holland, N. B.; Qiu, Y. X.; Ruegsegger, M.; Marchant, R. E. *Nature* **1998,** 392, (6678), 799-801.

45. Lewis, A. L. *Colloid Surf. B-Biointerfaces* **2000,** 18, (3-4), 261-275.

46. Lewis, A. L.; Cumming, Z. L.; Goreish, H. H.; Kirkwood, L. C.; Tolhurst, L. A.; Stratford, P. W. *Biomaterials* **2001,** 22, (2), 99-111.

47. Chapman, D. *Langmuir* **1993,** 9, (1), 39-45.

48. Ueda, T.; Watanabe, A.; Ishihara, K.; Nakabayashi, N. *J. Biomater. Sci.-Polym. Ed.* **1991,** 3, (2), 185-194.

49. Ishihara, K.; Oshida, H.; Endo, Y.; Ueda, T.; Watanabe, A.; Nakabayashi, N. *J. Biomed. Mater. Res.* **1992,** 26, (12), 1543-1552.

50. Ross, E. E.; Bondurant, B.; Spratt, T.; Conboy, J. C.; O'Brien, D. F.; Saavedra, S. S. *Langmuir* **2001,** 17, (8), 2305-2307.

51. Glasmastar, K.; Larsson, C.; Hook, F.; Kasemo, B. *J. Colloid Interface Sci.* **2002,** 246, (1), 40-47.

52. Ross, E. E.; Spratt, T.; Liu, S. C.; Rozanski, L. J.; O'Brien, D. F.; Saavedra, S. S. *Langmuir* **2003,** 19, (5), 1766-1774.

53. Vermette, P.; Gauvreau, V.; Pezolet, M.; Laroche, G. *Colloid Surf. B-Biointerfaces* **2003,** 29, (4), 285-295.

54. Kim, K.; Kim, C.; Byun, Y. *Biomaterials* **2004,** 25, (1), 33-41.

55. Diem, T.; Czajka, B.; Weber, B.; Regen, S. L. *J. Am. Chem. Soc.* **1986,** 108, (19), 6094-6095.

56. Fabianowski, W.; Coyle, L. C.; Weber, B. A.; Granata, R. D.; Castner, D. G.; Sadownik, A.; Regen, S. L. *Langmuir* **1989,** 5, (1), 35-41.

57. Tegoulia, V. A.; Rao, W. S.; Kalambur, A. T.; Rabolt, J. R.; Cooper, S. L. *Langmuir* **2001,** 17, (14), 4396-4404.

58. Ishihara, K.; Hanyuda, H.; Nakabayashi, N. *Biomaterials* **1995,** 16, (11), 873-879.

59. Ishihara, K.; Fukumoto, K.; Iwasaki, Y.; Nakabayashi, N. *Biomaterials* **1999,** 20, (17), 1553-1559.

60. Ishihara, K.; Iwasaki, Y.; Ebihara, S.; Shindo, Y.; Nakabayashi, N. *Colloid Surf. B-Biointerfaces* **2000,** 18, (3-4), 325-335.

61. Seo, J. H.; Matsuno, R.; Konno, T.; Takai, M.; Ishihara, K. *Biomaterials* **2008,** 29, (10), 1367-1376.

62. Marchant, R. E.; Yuan, S.; Szakalasgratzl, G. *J. Biomater. Sci.-Polym. Ed.* **1994,** 6, (6), 549-564.

63. Bongrand, P. ed. *Physical Basis of Cell-Cell Adhesion.* CRC Press: Boca Raton, FL, 1988.

64. Zhang, T. H.; Marchant, R. E. *Macromolecules* **1994,** 27, (25), 7302-7308.

65. Zhang, T. H.; Marchant, R. E. *J. Colloid Interface Sci.* **1996,** 177, (2), 419-426.

66. Ruegsegger, M.; Zhang, T. H.; Marchant, R. E. *J. Colloid Interface Sci.* **1997,** 190, (1), 152-160.

67. Qiu, Y. X.; Zhang, T. H.; Ruegsegger, M.; Marchant, R. E. *Macromolecules* **1998,** 31, (1), 165-171.

68. Frazier, R. A.; Matthijs, G.; Davies, M. C.; Roberts, C. J.; Schacht, E.; Tendler, S. J. B. *Biomaterials* **2000,** 21, (9), 957-966.

69. Anderson, J. M.; Kottkemarchant, K. *Crit. Rev. Biocomp.* **1985,** 1, 111-204.

70. Kim, S. W.; Feijen, J. *Crit. Rev. Biocomp.* **1985,** 1, 229-260.

71. Allmer, K.; Hilborn, J.; Larsson, P. H.; Hult, A.; Ranby, B. *J. Polym. Sci. Pol. Chem.* **1990,** 28, (1), 173-183.

72. Wichterle, O.; Lim, D. *Nature* **1960,** 185, (4706), 117-118.

73. Mori, Y.; Nagaoka, S.; Takiuchi, H.; Kikuchi, T.; Noguchi, N.; Tanzawa, H.; Noishiki, Y. *Trans. Am. Soc. Artificial Internal Organs* **1982,** 28, 459-463.

74. Montheard, J. P.; Chatzopoulos, M.; Chappard, D. *J. Macromol. Sci.-Rev. Macromol. Chem. Phys.* **1992,** C32, (1), 1-34.

75. Menapace, R.; Skorpik, C.; Juchem, M.; Scheidel, W.; Schranz, R. *J. Cataract. Refract. Surg.* **1989,** 15, (3), 264-271.

76. Khan, A. J.; Percival, S. P. B. *J. Cataract. Refract. Surg.* **1999,** 25, (10), 1404-+.

77. Sefton, M. V.; Nishimura, E. *J. Pharm. Sci.* **1980,** 69, (2), 208-209.

78. Seki, T.; Kawaguchi, T.; Sugibayashi, K.; Juni, K.; Morimoto, Y. *Int. J. Pharm.* **1989,** 57, (1), 73-75.

79. Dalton, P. D.; Flynn, L.; Shoichet, M. S. *Biomaterials* **2002,** 23, (18), 3843-3851.

80. Flynn, L.; Dalton, P. D.; Shoichet, M. S. *Biomaterials* **2003,** 24, (23), 4265-4272.

81. Nojiri, C.; Okano, T.; Koyanagi, H.; Nakahama, S.; Park, K. D.; Kim, S. W. *J. Biomater. Sci.-Polym. Ed.* **1992,** 4, (2), 75-88.

82. Terada, S.; Suzuki, K.; Nozaki, M.; Okano, T.; Takemura, N. *J. Reconstr. Microsurg.* **1997,** 13, (1), 9-16.

83. Ito, E.; Suzuki, K.; Yamato, M.; Yokoyama, M.; Sakurai, Y.; Okano, T. *J. Biomed. Mater. Res.* **1998,** 42, (1), 148-155.

84. Onishi, M.; Shimura, K.; Seita, Y.; Yamashita, S. *Radiat. Phys. Chem.* **1995,** 46, (2), 219-223.

85. Tanaka, M.; Motomura, T.; Kawada, M.; Anzai, T.; Kasori, Y.; Shiroya, T.; Shimura, K.; Onishi, M.; Mochizuki, A. *Biomaterials* **2000,** 21, (14), 1471-1481.

86. Tanaka, M.; Mochizuki, A.; Motomura, T.; Shimura, K.; Onishi, M.; Okahata, Y. *Colloid Surf. A* **2001,** 193, (1-3), 145-152.

87. Tanaka, M.; Mochizuki, A.; Shiroya, T.; Motomura, T.; Shimura, K.; Onishi, M.; Okahata, Y. *Colloid Surf. A* **2002,** 203, (1-3), 195-204.

88. Harris, J. M. ed. *Poly(Ethylene Glycol) Chemistry: Biotechnical and Biomedical Applications.* Plenum Press: New York, 1992; p 485.

89. Bailey, F. E.; Koleske, J. V. *Alkylene Oxides and Their Polymers*. Marcel Dekker Inc: New York, 1991; Vol. 35, p 272.

90. Polson, A.; Potgieter, G. M.; Largier, J. F.; Joubert, F. J.; Mears, G. E. F. *Biochim. Biophys. Acta* **1964,** 82, (3), 463-&.

91. Zeppezau.M; Brishamm.S *Biochim. Biophys. Acta* **1965,** 94, (2), 581-&.

92. Chun, P. W.; Fried, M.; Ellis, E. F. *Anal. Biochem.* **1967,** 19, (3), 481-&.

93. Albertsson, P. A. *Partition of cell particles and macromolecules.* 3rd ed.; Wiley: New York, 1986; p 324.

94. Kao, K. N.; Constabe.F; Michaylu.Mr; Gamborg, O. L. *Planta* **1974,** 120, (3), 215-227.

95. Ahkong, Q. F.; Fisher, D.; Tampion, W.; Lucy, J. A. *Nature* **1975,** 253, (5488), 194-195.

96. Pontecorvo, G. *Somatic Cell Genetics* **1975,** 1, (4), 397-400.

97. Abuchowski, A.; Vanes, T.; Palczuk, N. C.; Davis, F. F. *J. Biol. Chem.* **1977,** 252, (11), 3578-3581.

98. Morra, M. *J. Biomater. Sci.-Polym. Ed.* **2000,** 11, (6), 547-569.

99. Alexander, S. *J. Phys.* **1977,** 38, (8), 977-981.

100. Degennes, P. G. *Macromolecules* **1981,** 14, (6), 1637-1644.

101. Degennes, P. G. *Macromolecules* **1982,** 15, (2), 492-500.

102. Degennes, P. G. *Ann. Chim.* **1987,** 77, (3-4), 389-410.

103. Jeon, S. I.; Andrade, J. D. *J. Colloid Interface Sci.* **1991,** 142, (1), 159-166.

104. Jeon, S. I.; Lee, J. H.; Andrade, J. D.; Degennes, P. G. *J. Colloid Interface Sci.* **1991,** 142, (1), 149-158.

105. Prime, K. L.; Whitesides, G. M. *J. Am. Chem. Soc.* **1993,** 115, (23), 10714-10721.

106. Szleifer, I. *Curr. Opin. Colloid Interface Sci.* **1996,** 1, (3), 416-423.

107. Szleifer, I. *Curr. Opin. Solid State Mat. Sci.* **1997,** 2, (3), 337-344.

108. Szleifer, I. *Physica A* **1997,** 244, (1-4), 370-388.

109. Szleifer, I. *Biophys. J.* **1997,** 72, (2), 595-612.

110. Halperin, A. *Langmuir* **1999,** 15, (7), 2525-2533.

111. Besseling, N. A. M.; Lyklema, J. *J. Phys. Chem.* **1994,** 98, (44), 11610-11622.

112. Besseling, N. A. M.; Scheutjens, J. *J. Phys. Chem.* **1994,** 98, (44), 11597-11609.

113. Besseling, N. A. M.; Lyklema, J. *Pure Appl. Chem.* **1995,** 67, (6), 881-888.

114. Besseling, N. A. M. *Langmuir* **1997,** 13, (7), 2113-2122.

115. Vanoss, C. J.; Good, R. J.; Chaudhury, M. K. *J. Colloid Interface Sci.* **1986,** 111, (2), 378-390.

116. Wang, R. L. C.; Kreuzer, H. J.; Grunze, M. *J. Phys. Chem. B* **1997,** 101, (47), 9767-9773.

117. Harder, P.; Grunze, M.; Dahint, R.; Whitesides, G. M.; Laibinis, P. E. *J. Phys. Chem. B* **1998,** 102, (2), 426-436.

118. Li, L. Y.; Chen, S. F.; Jiang, S. Y. *J. Biomater. Sci.-Polym. Ed.* **2007,** 18, (11), 1415-1427.

119. Kingshott, P.; Thissen, H.; Griesser, H. J. *Biomaterials* **2002,** 23, (9), 2043-2056.

120. Neugebauer, D. *Polym. Int.* **2007,** 56, (12), 1469-1498.

121. Chen, Y. J.; Kang, E. T.; Neoh, K. G.; Wang, P.; Tan, K. L. *Synth. Met.* **2000,** 110, (1), 47-55.

122. Wang, P.; Tan, K. L.; Kang, E. T. *J. Biomater. Sci.-Polym. Ed.* **2000,** 11, (2), 169-186.

123. Zhang, F.; Kang, E. T.; Neoh, K. G.; Wang, P.; Tan, K. L. *Biomaterials* **2001,** 22, (12), 1541-1548.

124. Zou, X. P.; Kang, E. T.; Neoh, K. G. *Plasmas Polym.* **2002,** 7, (2), 151-170.

125. Yu, W. H.; Kang, E. T.; Neoh, K. G.; Zhu, S. P. *J. Phys. Chem. B* **2003,** 107, (37), 10198-10205.

126. Lee, S. B.; Koepsel, R. R.; Morley, S. W.; Matyjaszewski, K.; Sun, Y. J.; Russell, A. J. *Biomacromolecules* **2004,** 5, (3), 877-882.

127. Ma, H. W.; Hyun, J. H.; Stiller, P.; Chilkoti, A. *Adv. Mater.* **2004,** 16, (4), 338-+.

128. Wu, Y. Z.; Huang, Y. Y.; Ma, H. W. *J. Am. Chem. Soc.* **2007,** 129, (23), 7226-+.

129. Mrksich, M.; Sigal, G. B.; Whitesides, G. M. *Langmuir* **1995,** 11, (11), 4383-4385.

130. Wuelfing, W. P.; Gross, S. M.; Miles, D. T.; Murray, R. W. *J. Am. Chem. Soc.* **1998,** 120, (48), 12696-12697.

131. Jo, S.; Park, K. *Biomaterials* **2000,** 21, (6), 605-616.

132. Papra, A.; Gadegaard, N.; Larsen, N. B. *Langmuir* **2001,** 17, (5), 1457-1460.

133. Zhang, Y.; Kohler, N.; Zhang, M. Q. *Biomaterials* **2002,** 23, (7), 1553-1561.

134. Abbasi, F.; Mirzadeh, H.; Katbab, A. A. *Polym. Int.* **2001,** 50, (12), 1279-1287.

135. Gupta, V. K.; Abbott, N. L. *Science* **1997,** 276, (5318), 1533-1536.

136. Hodneland, C. D.; Lee, Y. S.; Min, D. H.; Mrksich, M. *Proc. Natl. Acad. Sci. U. S. A.* **2002,** 99, (8), 5048-5052.

137. Kumar, N.; Hahm, J. I. *Langmuir* **2005,** 21, (15), 6652-6655.

138. Ratner, B. D. *Biosens. Bioelectron.* **1995,** 10, (9-10), 797-804.

139. Lee, J.; Martic, P. A.; Tan, J. S. *J. Colloid Interface Sci.* **1989,** 131, (1), 252-266.

140. Lee, J. H.; Kopecek, J.; Andrade, J. D. *J. Biomed. Mater. Res.* **1989,** 23, (3), 351-368.

141. Amiji, M.; Park, K. *Biomaterials* **1992,** 13, (10), 682-692.

142. Green, R. J.; Tasker, S.; Davies, J.; Davies, M. C.; Roberts, C. J.; Tendler, S. J. B. *Langmuir* **1997,** 13, (24), 6510-6515.

143. Neff, J. A.; Caldwell, K. D.; Tresco, P. A. *J. Biomed. Mater. Res.* **1998,** 40, (4), 511-519.

144. Kenausis, G. L.; Voros, J.; Elbert, D. L.; Huang, N. P.; Hofer, R.; Ruiz-Taylor, L.; Textor, M.; Hubbell, J. A.; Spencer, N. D. *J. Phys. Chem. B* **2000,** 104, (14), 3298-3309.

145. Huang, N. P.; Michel, R.; Voros, J.; Textor, M.; Hofer, R.; Rossi, A.; Elbert, D. L.; Hubbell, J. A.; Spencer, N. D. *Langmuir* **2001,** 17, (2), 489-498.

146. Pasche, S.; De Paul, S. M.; Voros, J.; Spencer, N. D.; Textor, M. *Langmuir* **2003,** 19, (22), 9216-9225.

147. Dynarowicz-Latka, P.; Dhanabalan, A.; Oliveira, O. N. *Adv. Colloid Interface Sci.* **2001,** 91, (2), 221-293.

148. Gaines, G. L. *Insoluble Monolayers at Liquid-Gas Interfaces.* Wiley-Interscience: New York, 1966; p 386.

149. Mohwald, H. *Annu. Rev. Phys. Chem.* **1990,** 41, 441-476.

150. Petty, C. M. *Langmuir-Blodgett Films: An Introduction*. Cambridge University Press: Cambridge, 1996; p 234.

151. Hlady, V.; Jogikalmath, G. *Colloid Surf. B-Biointerfaces* **2007,** 54, (2), 179-187.

152. Majewski, J.; Kuhl, T. L.; Gerstenberg, M. C.; Israelachvili, J. N.; Smith, G. S. *J. Phys. Chem. B* **1997,** 101, (16), 3122-3129.

153. Majewski, J.; Kuhl, T. L.; Kjaer, K.; Gerstenberg, M. C.; Als-Nielsen, J.; Israelachvili, J. N.; Smith, G. S. *J. Am. Chem. Soc.* **1998,** 120, (7), 1469-1473.

154. Baekmark, T. R.; Wiesenthal, T.; Kuhn, P.; Albersdorfer, A.; Nuyken, O.; Merkel, R. *Langmuir* **1999,** 15, (10), 3616-3626.

155. Kuhl, T. L.; Majewski, J.; Howes, P. B.; Kjaer, K.; von Nahmen, A.; Lee, K. Y. C.; Ocko, B.; Israelachvili, J. N.; Smith, G. S. *J. Am. Chem. Soc.* **1999,** 121, (33), 7682-7688.

156. Wiesenthal, T.; Baekmark, T. R.; Merkel, R. *Langmuir* **1999,** 15, (20), 6837-6844.

157. Tsukanova, V.; Salesse, C. *Macromolecules* **2003,** 36, (19), 7227-7235.

158. Ohe, C.; Goto, Y.; Noi, M.; Arai, M.; Kamijo, H.; Itoh, K. *J. Phys. Chem. B* **2007,** 111, (7), 1693-1700.

159. Kim, K.; Kim, C.; Byun, Y. *J. Biomed. Mater. Res.* **2000,** 52, (4), 836-840.

160. Du, H.; Chandaroy, P.; Hui, S. W. *Biochim. Biophys. Acta-Biomembr.* **1997,** 1326, (2), 236-248.

161. Chen, C. S.; Mrksich, M.; Huang, S.; Whitesides, G. M.; Ingber, D. E. *Science* **1997,** 276, (5317), 1425-1428.

162. Kane, R. S.; Takayama, S.; Ostuni, E.; Ingber, D. E.; Whitesides, G. M. *Biomaterials* **1999,** 20, (23-24), 2363-2376.

163. Fodor, S. P. A.; Read, J. L.; Pirrung, M. C.; Stryer, L.; Lu, A. T.; Solas, D. *Science* **1991,** 251, (4995), 767-773.

164. Mrksich, M.; Whitesides, G. M. *Trends Biotechnol.* **1995,** 13, (6), 228-235.

165. Blawas, A. S.; Reichert, W. M. *Biomaterials* **1998,** 19, (7-9), 595-609.

166. MacBeath, G.; Schreiber, S. L. *Science* **2000,** 289, (5485), 1760-1763.

167. Templin, M. F.; Stoll, D.; Schrenk, M.; Traub, P. C.; Vohringer, C. F.; Joos, T. O. *Trends Biotechnol.* **2002,** 20, (4), 160-166.

168. Yadavalli, V. K.; Koh, W. G.; Lazur, G. J.; Pishko, M. V. *Sens. Actuator B-Chem.* **2004,** 97, (2-3), 290-297.

169. Dietrich, C.; Schmitt, L.; Tampe, R. *Proc. Natl. Acad. Sci. U. S. A.* **1995,** 92, (20), 9014-9018.

170. Britt, D. W.; Mobius, D.; Hlady, V. *Phys. Chem. Chem. Phys.* **2000,** 2, (20), 4594-4599.

171. Mallik, S.; Plunkett, S. D.; Dhal, P. K.; Johnson, R. D.; Pack, D.; Shnek, D.; Arnold, F. H. *New J. Chem.* **1994,** 18, (3), 299-304.

172. Shnek, D. R.; Pack, D. W.; Sasaki, D. Y.; Arnold, F. H. *Langmuir* **1994,** 10, (7), 2382-2388.

173. Gritsch, S.; Neumaier, K.; Schmitt, L.; Tampe, R. *Biosens. Bioelectron.* **1995,** 10, (9-10), 805-812.

174. Ng, K.; Pack, D. W.; Sasaki, D. Y.; Arnold, F. H. *Langmuir* **1995,** 11, (10), 4048-4055.

175. Ng, K. M.; Pack, D. W.; Chen, C. T.; Arnold, F. H. *Faseb J.* **1995,** 9, (6), A1459-A1459.

176. Fang, J. Y.; Knobler, C. M. *Langmuir* **1996,** 12, (5), 1368-1374.

177. Frey, W.; Schief, W. R.; Pack, D. W.; Chen, C. T.; Chilkoti, A.; Stayton, P.; Vogel, V.; Arnold, F. H. *Proc. Natl. Acad. Sci. U. S. A.* **1996,** 93, (10), 4937-4941.

178. Fang, J. Y.; Knobler, C. M.; Gingery, M.; Eiserling, F. A. *J. Phys. Chem. B* **1997,** 101, (43), 8692-8695.

179. Pack, D. W.; Arnold, F. H. *Chem. Phys. Lipids* **1997,** 86, (2), 135-152.

180. Pack, D. W.; Chen, G. H.; Maloney, K. M.; Chen, C. T.; Arnold, F. H. *J. Am. Chem. Soc.* **1997,** 119, (10), 2479-2487.

181. Pack, D. W.; Ng, K.; Maloney, K. M.; Arnold, F. H. *Supramol. Sci.* **1997,** 4, (1-2), 3-10.

182. Maloney, K. M.; Schief, W. R.; Pack, D. W.; Frey, W.; Arnold, F. H.; Vogel, V. *Coord. Chem. Rev.* **1999,** 183, 3-18.

183. Du, X. Z.; Hlady, V.; Britt, D. *Biosens. Bioelectron.* **2005,** 20, (10), 2053-2060.

184. Du, X. Z.; Wang, Y. C.; Ding, Y. H.; Guo, R. *Langmuir* **2007,** 23, (15), 8142-8149.

185. Xia, Y. N.; Whitesides, G. M. *Annu. Rev. Mater. Sci.* **1998,** 28, 153-184.

186. Xia, Y. N.; Whitesides, G. M. *Angew. Chem., Int. Ed. Engl.* **1998,** 37, (5), 551-575.

187. Huang, Y. G. Y.; Zhou, W. X.; Hsia, K. J.; Menard, E.; Park, J. U.; Rogers, J. A.; Alleyne, A. G. *Langmuir* **2005,** 21, (17), 8058-8068.

188. Lee, T. W.; Jeon, S.; Maria, J.; Zaumseil, J.; Hsu, J. W. P.; Rogers, J. A. *Adv. Funct. Mater.* **2005,** 15, (9), 1435-1439.

189. Lee, J. N.; Park, C.; Whitesides, G. M. *Anal. Chem.* **2003,** 75, (23), 6544-6554.

190. Makamba, H.; Kim, J. H.; Lim, K.; Park, N.; Hahn, J. H. *Electrophoresis* **2003,** 24, (21), 3607-3619.

191. Psaltis, D.; Quake, S. R.; Yang, C. H. *Nature* **2006,** 442, (7101), 381-386.

192. Whitesides, G. M. *Nature* **2006,** 442, (7101), 368-373.

193. El-Ali, J.; Sorger, P. K.; Jensen, K. F. *Nature* **2006,** 442, (7101), 403-411.

194. Huang, B.; Wu, H. K.; Bhaya, D.; Grossman, A.; Granier, S.; Kobilka, B. K.; Zare, R. N. *Science* **2007,** 315, (5808), 81-84.

195. Huang, Y. Y.; Castrataro, P.; Lee, C. C.; Quake, S. R. *Lab Chip* **2007,** 7, (1), 24-26.

196. Bartzoka, V.; McDermott, M. R.; Brook, M. A. *Adv. Mater.* **1999,** 11, (3), 257-+.

197. Malpass, C. A.; Millsap, K. W.; Sidhu, H.; Gower, L. B. *J. Biomed. Mater. Res.* **2002,** 63, (6), 822-829.

198. Mata, A.; Fleischman, A. J.; Roy, S. *Biomed. Microdevices* **2005,** 7, (4), 281-293.

199. Chen, K. Y.; Kuo, J. F.; Chen, C. Y. *J. Biomater. Sci.-Polym. Ed.* **1999,** 10, (12), 1183-1205.

200. Belanger, M. C.; Marois, Y. *J. Biomed. Mater. Res.* **2001,** 58, (5), 467-477.

201. Chen, Z.; Ward, R.; Tian, Y.; Malizia, F.; Gracias, D. H.; Shen, Y. R.; Somorjai, G. A. *J. Biomed. Mater. Res.* **2002,** 62, (2), 254-264.

202. Park, J. H.; Bae, Y. H. *Biomaterials* **2002,** 23, (8), 1797-1808.

203. Unger, M. A.; Chou, H. P.; Thorsen, T.; Scherer, A.; Quake, S. R. *Science* **2000,** 288, (5463), 113-116.

204. Boxshall, K.; Wu, M. H.; Cui, Z.; Cui, Z. F.; Watts, J. F.; Baker, M. A. *Surf. Interface Anal.* **2006,** 38, (4), 198-201.

205. Lee, J.; Kim, M. J.; Lee, H. H. *Langmuir* **2006,** 22, (5), 2090-2095.

206. Ocvirk, G.; Munroe, M.; Tang, T.; Oleschuk, R.; Westra, K.; Harrison, D. J. *Electrophoresis* **2000,** 21, (1), 107-115.

207. Dou, Y. H.; Bao, N.; Xu, J. J.; Chen, H. Y. *Electrophoresis* **2002,** 23, (20), 3558-3566.

208. Decher, G.; Hong, J. D.; Schmitt, J. *Thin Solid Films* **1992,** 210, (1-2), 831-835.

209. Decher, G.; Lvov, Y.; Schmitt, J. *Thin Solid Films* **1994,** 244, (1-2), 772-777.

210. Decher, G. *Science* **1997,** 277, (5330), 1232-1237.

211. Hu, S. W.; Brittain, W. J. *Macromolecules* **2005,** 38, (15), 6592-6597.

212. Efimenko, K.; Wallace, W. E.; Genzer, J. *J. Colloid Interface Sci.* **2002,** 254, (2), 306-315.

213. Schnyder, B.; Lippert, T.; Kotz, R.; Wokaun, A.; Graubner, V. M.; Nuyken, O. *Surf. Sci.* **2003,** 532, 1067-1071.

214. Olah, A.; Hillborg, H.; Vancso, G. J. *Appl. Surf. Sci.* **2005,** 239, (3-4), 410-423.

215. Hu, S. W.; Ren, X. Q.; Bachman, M.; Sims, C. E.; Li, G. P.; Allbritton, N. *Anal. Chem.* **2002,** 74, (16), 4117-4123.

216. Hu, S. W.; Ren, X. Q.; Bachman, M.; Sims, C. E.; Li, G. P.; Allbritton, N. L. *Langmuir* **2004,** 20, (13), 5569-5574.

217. Hu, S. W.; Ren, X. Q.; Bachman, M.; Sims, C. E.; Li, G. P.; Allbritton, N. L. *Anal. Chem.* **2004,** 76, (7), 1865-1870.

218. Wang, Y. L.; Lai, H. H.; Bachman, M.; Sims, C. E.; Li, G. P.; Allbritton, N. L. *Anal. Chem.* **2005,** 77, (23), 7539-7546.

219. Patrito, N.; McCague, C.; Chiang, S.; Norton, P. R.; Petersen, N. O. *Langmuir* **2006,** 22, (8), 3453-3455.

220. Barbier, V.; Tatoulian, M.; Li, H.; Arefi-Khonsari, F.; Ajdari, A.; Tabeling, P. *Langmuir* **2006,** 22, (12), 5230-5232.

221. Yu, K.; Han, Y. C. *Soft Matter* **2006,** 2, (8), 705-709.

222. Neys, P. E. F.; Severeyns, A.; Vankelecom, I. F. J.; Ceulemans, E.; Dehaen, W.; Jacobs, P. A. *J. Mol. Catal. A-Chem.* **1999,** 144, (2), 373-377.

223. Huang, B.; Wu, H. K.; Kim, S.; Kobilka, B. K.; Zare, R. N. *Lab Chip* **2006,** 6, (3), 369-373.

224. Luo, Y. Q.; Huang, B.; Wu, H.; Zare, R. N. *Anal. Chem.* **2006,** 78, (13), 4588-4592.

225. Xiao, Y.; Yu, X. D.; Xu, J. J.; Chen, H. Y. *Electrophoresis* **2007,** 28, (18), 3302-3307.

CHAPTER 3

PROTEIN INSERTION AND PATTERNING OF PEG BEARING LANGMUIR MONOLAYERS[†]

3.1 ABSTRACT

Protein adsorption to multi-component lipid monolayers is presented as a means of inducing protein specific binding pockets or imprints, in surfaces. Adsorption of the acidic protein ferritin to Langmuir monolayers of cationic dioctadecyldimethylammonium bromide (DOMA), nonionic methyl stearate (SME), and poly(ethylene glycol) (PEG) bearing phospholipids is investigated as a model system. The number, size, and distribution of protein binding pockets (domains of SME and DOMA in a PEG matrix) are defined by controlling the molar ratios, miscibility, and lateral mobility of the lipids. Protein patterning of binary SME:DOMA monolayers is limited by protein-protein interactions that hinder desorption to regenerate the protein induced template. The incorporation of PEG bearing phospholipids as a third lipid component is introduced as a successful approach to reduce protein aggregates in the monolayer template. Atomic force microscopy and fluorescence microscopy are employed to study protein adsorption to the ternary monolayers, which exhibit a user defined distribution of protein with fewer protein-protein interactions, thus facilitating protein desorption and regeneration of the protein binding pockets.

[†] Coauthored by Harshil Dhruv, Revathi Pepalla, Mundeta Taveras, and David W. Britt

3.2 Introduction

Molecular imprinting tailors specific recognition sites in polymeric materials or inorganic matrixes by using template molecules.[1, 2] Traditionally, molecular imprinting involves cross-linking of functionalized monomers assembled around a template target molecule, followed by extraction of the template, creating binding sites that are complementary in shape, structure, and surface properties. In simple terms, molecular imprinting technology can be described as making "artificial locks" for "molecular keys."[3] This method has tremendous potential in various fields such as, construction of biosensors,[4] separations,[5-7] catalysis,[8] and in the synthesis of artificial antibodies.[9]

Traditionally, molecular imprint polymers (MIPs) are most applicable in recognizing small molecules such as drugs[10] and amino acids,[11] with specificity high enough for separating enantiomers.[12] However, when forming imprints against "large" molecules such as proteins, there are still many limitations associated with MIPs, like maintaining the integrity of the imprint site while extracting the original template molecule, permanent entrapment of the template molecule, slow mass transfer of analytes through the network polymer, and difficulty in characterizing the heterogeneous polymers. This has fostered interest in the development of novel and alternative imprinting methods such as two-dimensional, or in-plane, protein imprinting.

One means of planar protein imprinting is to simply restrict a bulk imprinting method to an interface. With this approach, surfaces expressing protein binding pockets have been created by a sequential process where proteins are first adsorbed onto a sacrificial surface (mica), then coated with a recognition element (disaccharide), followed

by plasma polymerization, removal of mica, and dissolution of protein, thus leaving behind sugar coated nano-pits that are complementary in shape and chemistry (hydrogen bonding) to the template protein.[13] Alternatively, a more direct and biomimetic approach can be followed by allowing the protein to adsorb to a fluid interface containing the recognition elements, such as multi-component lipid monolayers at the air/water interface[14-16] or supported bilayers.[17] For this type of two dimensional imprinting, the protein "must select" the recognition elements (e.g. through electrostatic interactions of protein residues with lipid head groups) and induce a local demixing of the lipids as predicted through mean-field theory,[18] as demonstrated for directed mineralization.[19, 20]

In our previous work with collaborators, we have adsorbed the acidic protein ferritin to mixed cationic / nonionic lipid monolayers in an effort to induce charge patterns in the fluid monolayers.[15, 16] However, the success was limited by a large fraction of irreversibly bound protein on the patterned monolayers, attributed in part to strong protein-protein interactions (aggregation) during the patterning process. Clearly, a population of irreversibly bound protein complicates assessment of the imprinting procedure, while solvents and detergents strong enough to elute the protein may lead to disruption of the imprint site. Here, we introduce poly(ethylene glycol) (PEG) bearing lipids as a third component to the nonionic methyl stearate (SME) and cationic dioctadecyldimethylammonium bromide (DOMA) binary fluid monolayer previously investigated. The incorporation of PEG bearing lipids into this planar imprinting method is designed to limit protein-protein interactions, narrow binding site affinities, and eliminate non-imprint-mediated adsorption. Moreover, the number of binding sites can be pre-programmed in the monolayer as the adsorbing protein competes with PEG chains for

space, triggering a "mushroom to brush" transition as previously observed at the air/water interface.[21, 22] In this conformationally restricted brush state, the PEG chains define binding pockets complimentary to adsorbed protein size and shape while the SME and DOMA head groups form the floor of the binding pocket as depicted in Figure 3.1. With this ternary mixed lipid monolayer, it is demonstrated that the number, size, and distribution of binding sites for a target protein are user-defined by controlling the molar ratios, miscibility, and lateral mobility of the lipids.

3.3 Experimental

3.3.1 Lipids. Methyl stearate (SME) (99 % GC, Fluka), dioctadecyldimethylammonium bromide (DOMA, or DODAB) (99 % Tech Grade, TCI), and 1,2-Distearoyl-*sn*-Glycero-3-Phosphoethanolamine-N-[Methoxy(Polyethylene glycol)-350] as ammonium salt (PEG350) (M.W.= 1131; 99 % in chloroform, Avanti Polar Lipids), were prepared as 1mM stock solutions in chloroform (99% HPLC grade, Merck) and stored at 4 ºC (Structure of all lipids are presented in Appendix A). PEG350 has seven ethylene glycol (EG) units, which, when tightly packed form a brush layer that is sufficient to inhibit non-specific adsorption;[23-27] however, longer PEG chain lengths are commercially available (Avanti Polar Lipids) and are being investigated in ongoing studies. Binary lipid mixtures of SME and DOMA were first prepared in a 2:1 molar ratio hereafter referred to as "SD". Our previous[15, 28] work demonstrated that SME and DOMA are highly miscible, therefore miscibility analysis here considers only the mixing of PEG350 with SD, the latter essentially being treated as a single component to facilitate analysis of the ternary system. A series of PEG350:SD lipid mixtures were prepared by

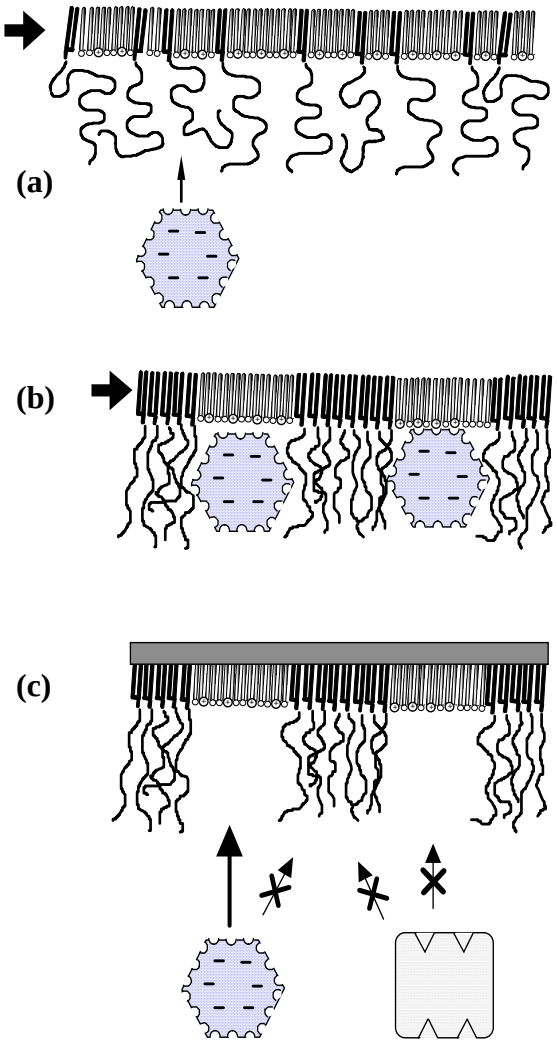

Figure 3.1. Schematic of entrapment and imprinting of protein using functionalized lipid monolayers cospread with PEG-bearing lipids at air/water interface of a Langmuir trough. **(a)** Protein (ferritin) adsorption induces de-mixing and a PEG "mushroom to brush" transition, while surface pressure is maintained to prevent protein insertion into alkyl-tail region, yet allow nonionic SME/cationic DOMA head-groups to laterally diffuse to form favorable hydrogen bonding and electrostatic interactions with protein residues **(b)** Protein adsorption is self-limiting as the PEG brush is impenetrable. Slow condensation of the silane head-groups and close-packing of alkyl-tails preserves the imprint structure **(c)** Immobilization of the monolayer to solid hydrophobic support, followed by elution of imprint protein, resulting in 'frozen' imprint. PEG brush inhibits non-specific binding outside of imprint sites while imprint cavity shape and functionalized lipid head group distribution, favor rebinding of original imprint protein.

volumetrically mixing the 1 mM stock solutions of SD with PEG-350 prior to spreading at the air/water interface. Bulk mixing of the lipids (in contrast to co-spreading the lipids at the air/water interface) significantly enhances monolayer miscibility.[28]

3.3.2 Protein. Horse spleen ferritin (76 mg/mL, Type 1, Sigma), was diluted to 2 mg/mL in HPLC grade water (Sigma) and stored at 4°C prior to use. Alexafluor 546 (Molecular Probes) was conjugated to ferritin for experiments where visualization of the protein gross distribution on the monolayers was desired. Protein was injected below the Langmuir monolayers yielding a final concentration of 2.0 μg/ml as previously described.[16]

3.3.3 Monolayer Preparation and Transfer. Monolayer experiments were carried out on a glass and PTFE Langmuir trough of surface area of 550 × 220 mm^2 (Kibron, Inc.), maintained at 21°C by circulating water through a metal plate below the trough. The subphase was double was HPLC grade water (Sigma) (surface tension ~ 72 mN/m). Langmuir monolayers of SD, PEG-350, and their mixtures were prepared by spreading the lipids dropwise on the air/water interface of the trough, using a 50 μL Hamilton Gastight syringe, and allowing 10 min for solvent (chloroform) evaporation. The monolayers were then compressed at a rate of 5 $Å^2$/molecule/min until the desired surface pressure was reached (e.g. for protein injection into the subphase and film transfer) or until film collapse (for generating isotherms). The trough was kept free of surface-active materials by cleaning with ethanol, and then thoroughly rinsing with double distilled water after each experiment. Monolayers were transferred horizontally onto an octadecyltrichorosilane (OTS) modified glass coverslip by a modified Langmuir-Schaeffer method.[29] OTS substrates were prepared by cleaning the glass coverslip in a

piranha etch solution (3:1 ratio of 98% H_2SO_4: H_2O_2) for 1 hr and then rinsed with double distilled water and dried at 80°C. Care must be taken when using piranha solution as it is a strong oxidant and reacts violently with organic contaminants. The hydrophilic cover slides were transferred into a 0.5 mM OTS in toluene solution for 15 min and then thoroughly rinsed in toluene followed by double distilled water. This yields a uniformly hydrophobic surface with water contact angles between 98° -105°. Lipid monolayers immobilized on the OTS-coverslip were maintained hydrated for fluorescence and AFM imaging.

3.3.4 AFM and Fluorescence Microscopy. A Nanoscope III Bioscope (Digital Instruments, Inc.) was used to image hydrated monolayers in contact mode. Cantilevers (Park Scientific Instruments) with a relatively low spring constant of 0.01 N/m were employed to reduce disruption of protein by the AFM tip. An inverted Fluorescence microscope (Nikon Eclipse TE2000-S) with 100 W Hg-lamp and 40X (Nikon ELWD DM 40X / 0.60 CFI Plan Fluor) and 100X / 1.40 oil (Nikon CFI Plan Apochromat,) objectives was used to study adsorption and distribution of Alexafluor 546 labeled ferritin on the monolayers illuminated through the Nikon TRITC filter cube. Images were captured with a Nikon DXM1200 color CCD camera operated with ACT-1 (Nikon) software from a PC with frame-grabber. A parallel plate flow cell was constructed by laying a piranha cleaned glass slide on top of the monolayer containing coverslip (under water), followed by removal from water and sealing the edges with a rapid drying enamel while leaving two small gaps for injection and removal of protein and rinse solutions.

Fluorescence studies of floating monolayers were carried out by doping the PEG-350:SD lipid mixtures with 2 mol % of the fluorescent lipid: 1-Oleoyl-2-[12-[(7-nitro-2-

1,3-benzoxadiazol-4-yl)amino]dodecanoyl]-sn-Glycero-3-Phosphoethanolamine (18:0 NBD-PE; Avanti Polar Lipids). Monolayers were spread on a KSV microscopy trough (KSV Ltd.) and imaged with a Nikon upright microscope equipped with ELWD 40X / 0.60 objective. Images were captured using a 12-bit Peltier-cooled CCD camera (MicroMax, Princeton Instruments) driven by IP-Lab software on a PC with a frame-grabber.

3.4 Results and Discussion

3.4.1 Monolayer Properties and Surfactant Miscibility. The molecular organization or packing of pure and multi-component lipid films at the air/water interface of a Langmuir trough can be inferred from the profile of the surface pressure-molecular area (π-A) isotherms. The π-A isotherms of monolayers of PEG350, SD, and PEG350:SD

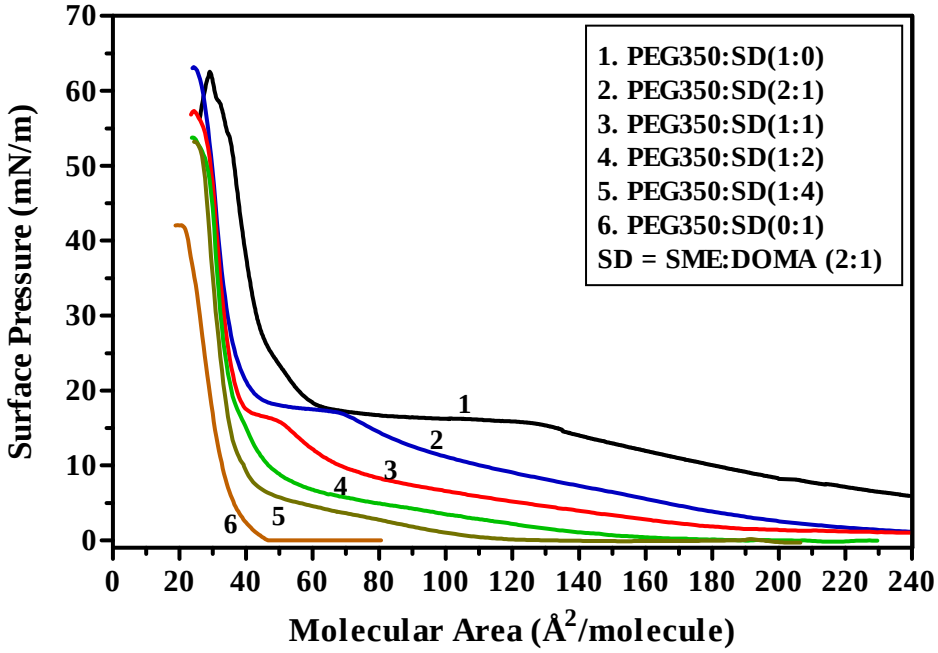

Figure 3.2. Surface pressure - molecular area isotherms of phospholipids bearing PEG, (PEG350), the binary mixture of SME:DOMA 2:1, (SD) and ternary mixture of PEG350:SD prepared at the indicated molar ratios.

mixtures (molar ratios 2:1, 1:1, 1:2, 1:4) are shown in Figure 3.2. The PEG350 isotherm is biphasic, exhibiting an expanded region of high compressibility (beginning near 325 $Å^2$/molecule, not shown in figure) where the PEG chains compete with the alkyl-tails for space at the air/water interface.[30] As the film is compressed, the chains are forced into the subphase, resulting in an extended plateau region between 15 and 20 mN/m corresponding to the PEG mushroom to brush transition. Above 20 mN/m the alkyl-tails come into close contact and the PEG chains are in an extended brush conformation, with a limiting molecular area near 55 $Å^2$/molecule as previously reported.[30] As SD is introduced to PEG350, the isotherms gradually shift to lower molecular areas and the plateau region representing the mushroom to brush transition diminishes proportionally.

Mixing diagrams (Figure 3.3) constructed from the π-A isotherms (Appendix A) provide additional insight into lipid miscibility at select surface pressures. A transition from non-additive mixing at low packing densities (10 mN/m data) towards additive

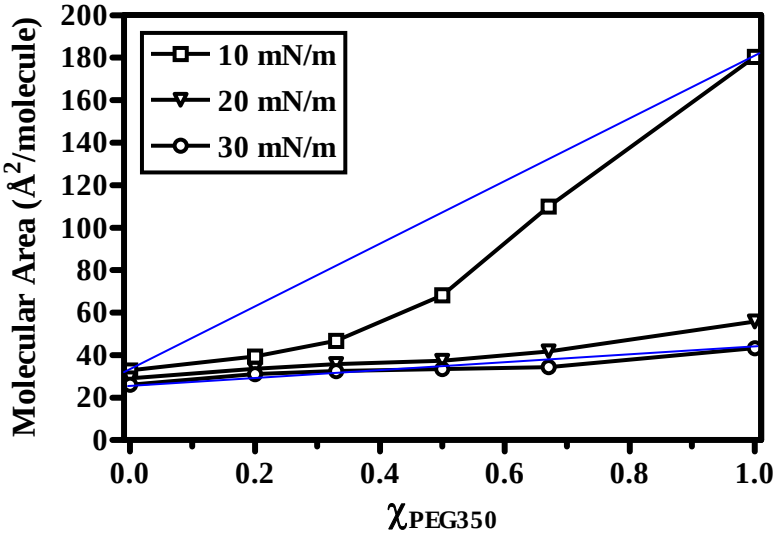

Figure 3.3. Miscibility analysis of PEG350:SD monolayers at the indicated surface pressures. The straight line represents additive mixing for the 10 and 30 mN/m data.

mixing at high packing densities (20 and 30 mN/m data) is observed. In the non-additive mixing regime, the mixtures occupy less area than predicted from the sum of the components (i.e. all the data points fall below a line representing ideal additive behavior). As the lipids are compressed, the areas of the mixtures approach the line representing ideal additive mixing behavior. This latter behavior can either be ascribed to lipid demixing upon compression (i.e. ideally immiscible), or intimate lipid mixing (ideally miscible). The latter case is anticipated due to all lipids having identical alkyl-tail lengths as well as probable charge pairing of the quaternary ammonium group of DOMA with the phosphate of PEG350.

The phase behavior of the mixed monolayers is visualized from in-situ fluorescence images of the films at air/water interface (Figure 3.4), which reveal the

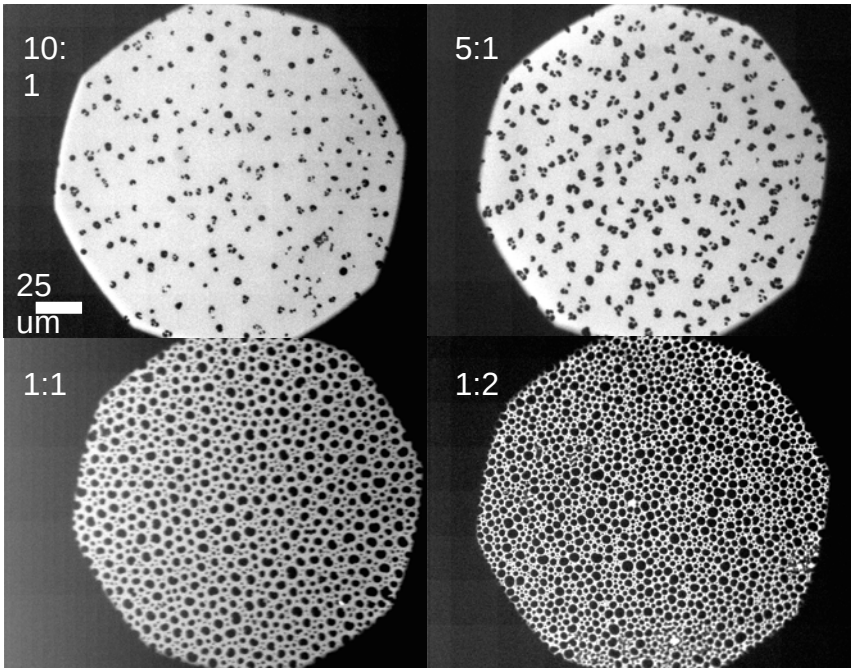

Figure 3.4. Fluorescence micrographs (40X) of Langmuir monolayers of PEG350:SD (molar ratios indicated in figure) doped with 2% NBD-PE. Films prepared at 20mN/m surface pressure.

presence of micron-sized domains in the films. As the SD content of the monolayers is increased, the domains increase in density and adopt a more rounded appearance, but do not coalesce. Pure PEG350 films were uniformly fluorescent (image not shown), further indicating the domains are a result of the addition of SD. While it may be tempting to ascribe the domains as SD rich phases, this is not supported by AFM analysis of the monolayers (Figure 3.5). A height profile across this image reveals that the domains are actually some 2.5 nm taller than the surrounding phase—If the domains corresponded to phase separated regions of SD surrounded by a matrix of PEG350 then an opposite height profile would be expected as the PEG350 brush extends approximately 2.5 nm (7 EG units) beyond the head-groups. The height difference is thus ascribed to condensed phase nucleation and growth from an expanded phase matrix as is commonly observed upon compression of single component lipid monolayers (i.e. the liquid expanded to liquid condensed phase transition). However, in the case of this ternary lipid mixture, nucleation

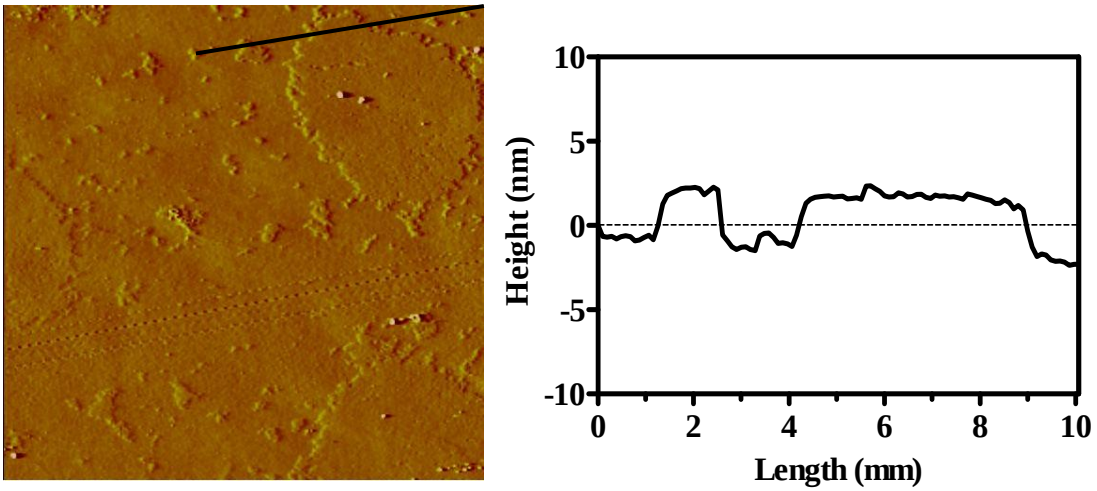

Figure 3.5. AFM image (25 × 25 μm^2) of a PEG350:SD 1:2 monolayer horizontally transferred at 12 mN/m to a hydrophobic coverslip. A line profile reveals that the domains observed in the fluorescence analysis are ~2.5 nm taller than the surrounding phase.

of condensed domains may induce a localized transition of the PEG chains into a brush layer. This is further supported by fluorescence microscopy analysis of the gross distribution of protein on mixed monolayers as discussed next.

3.4.2 Protein Adsorption to Ternary Monolayers. Protein imprinting of the monolayer films was carried out at surface pressures sufficient to restrict protein adsorption to the lipid headgroups and prevent insertion into the hydrophobic alkyl tail region, where protein unfolding is possible as previously reported for albumin penetration into PEG bearing monolayers.[21, 22] The distribution of ferritin on several different mixed monolayers prepared at 20 mN/m is observed in the fluorescence microscopy images shown in Figure 3.6. Gross monolayer morphology is clearly visualized as the protein preferentially adsorbs to the regions surrounding the domains, further indicating that the

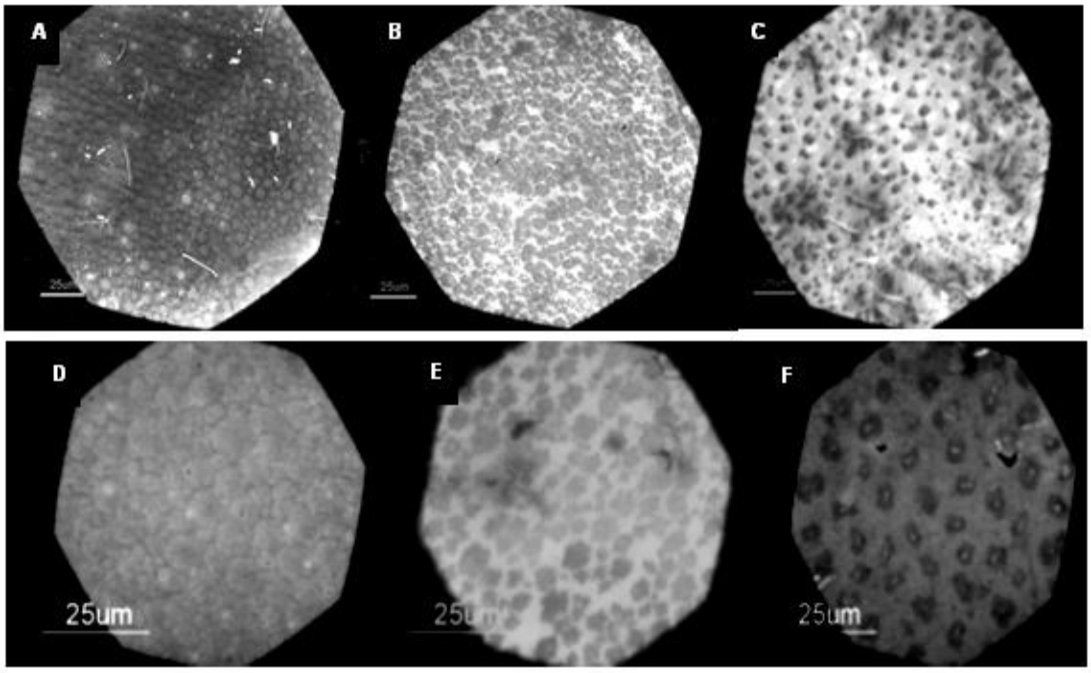

Figure 3.6. Fluorescence microscopy analysis of Alexafluor ferritin distribution on PEG350:SD monolayer films (at indicated molar ratios). Top row: 40× objective. Bottom row: 100× objective. Films horizontally transferred at 20 mN/m to hydrophobic coverslips.

domains are not an SD-rich phase.

Ferritin adsorption to the mixed monolayers is driven by a strong affinity for the SD lipid head-groups, which is regulated by the local density of protein repellent PEG chains. Ferritin is highly negatively charged and binds strongly to mixed cationic / neutral monolayers of SD when adsorbing from a pure water subphase at pH 5.5.[15, 16] However, on SD monolayers, protein-protein interactions interplay with protein-lipid interactions, resulting in ferritin aggregates that are irreversibly bound, even when rinsing with dilute acid.[16] For the ternary monolayers employed here, PEG350 is introduced to limit protein-protein interactions without interfering with the intended pairing of protein residues with the SD headgroups. This mediating role of the PEG350 lipid in defining single protein binding pockets is assessed through AFM analysis (Figure 3.7) of the ternary monolayers pre- and post-imprinting.

The pre-imprinting morphology of the ternary monolayer (Figure 3.7 (a)) reveals a surface exhibiting numerous defects and pinholes that are 1.5 – 2.5 nm deep, consistent with the thickness expected for PEG chains containing 7 EG units. The post-imprinting morphology (Figure 3.7 (b), (c)) reveals both vacant and protein-filled binding pockets. Removal of protein from the binding pockets by the AFM tip was also observed, demonstrating the reversibility of binding that is a prerequisite for assessing imprint affinity. The pre- and post-imprinting monolayer morphologies are distinct, indicating that allowing protein to interact with this monolayer while it is laterally mobile at the air/water interface forces lipid restructuring, as protein seeks SD head-groups while competing for space with the PEG chains. This can be viewed as a unique self-assembly approach to protein arraying,[31-36] where the amount and distribution of protein is guided

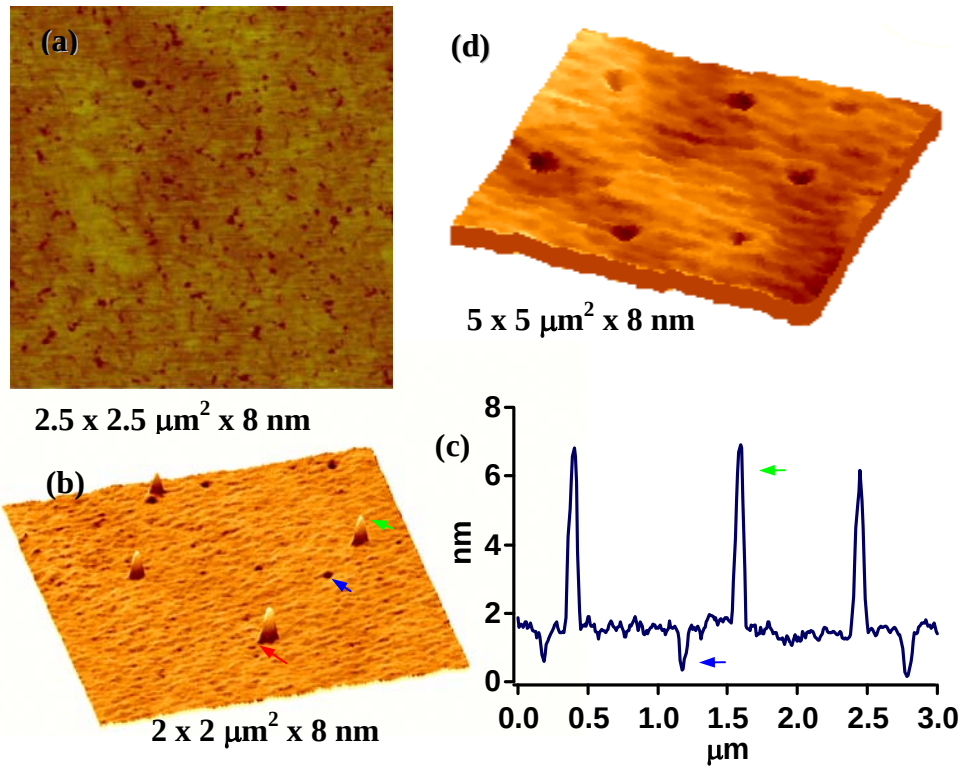

Figure 3.7. Self-assembly driven protein arraying of the PEG350:SD 1:2 monolayer. (a) Pre-imprint monolayer morphology exhibiting numerous defects and pinholes. (b) Post-imprint morphology revealing ferritin residing in the protein-sized pockets. (c) A line profile across the image in B reveals vacant pockets that are 1.5-2.5 nm deep. Compression of the protein by the AFM tip (contact mode in solution) reduces the protein height from the expected 12 nm to ~8 nm. (d) Doubling the SD content leads to a corresponding increase in the binding pocket dimensions (300-400 nm diameter).

by a strictly self-limiting adsorption process in which protein not only occupies (and defines) its own binding site but in the process eliminates other potential binding sites by forcing PEG into a brush conformation. In this manner, local binding events may lead to global transitions in the fluid monolayer. Further control over monolayer morphology is attained by varying the lipid ratios, permitting the size of the binding pockets to be tuned as shown in Figure 3.7 (d) where the SD content is twice that in Figure 3.7 (b). Increasing the number of protein binding sites without increasing the size is a question of the interplay of protein-lipid interactions and lipid mixing behavior, which can be further tuned through varied subphase temperature, introduction of *n*-alkanes as volatile lubricating agents, and extended film incubation time at a given surface pressure.

3.5 Conclusions

The introduction of poly(ethylene glycol) bearing lipid to the neutral SME/cationic DOMA (SD) lipid mixtures at the air/water interface has been employed to reduce protein-protein interactions on the monolayer in an effort to define single protein binding sites. The intrinsic inertness of the PEG brush layer in the mixed lipid monolayer reduces nonspecific adsorption of proteins to the monolayer, while the SME and DOMA headgroups define favorable binding sites for adsorption of ferritin. Molecular area mixing diagrams support a high miscibility of the lipids, revealing a transition from nonadditive to additive mixing behavior upon film compression. Fluorescence microscopy reveals a micron-scale phase behavior in the ternary monolayers consistent with an expanded to condensed phase transition and not lipid demixing. Atomic force microscopy indicates that ferritin adsorption induces local restructuring of the fluid

monolayer, resulting in the creation of protein-sized binding pockets, the dimensions of which can be fine-tuned by changing the molar ratios of the lipids. Applying this two-dimensional protein imprinting approach, ongoing work will investigate imprint site affinity through protein adsorption/desorption kinetics on monolayers transferred to the quartz crystal microbalance.

3.6 References

1. Wulff, G. *Angew. Chem.-Int. Edit. Engl.* **1995,** 34, (17), 1812-1832.

2. Mosbach, K.; Ramstrom, O. *Bio-Technology* **1996,** 14, (2), 163-170.

3. Ramström, O. Molecular Imprinting Technology. http://www.smi.tu-berlin.de/story/MIT.htm

4. Vidyasankar, S.; Arnold, F. H. *Curr. Opin. Biotech.* **1995,** 6, (2), 218-224.

5. Sellergren, B.; Lepisto, M.; Mosbach, K. *J. Am. Chem. Soc.* **1988,** 110, (17), 5853-5860.

6. Vidyasankar, S.; Ru, M.; Arnold, F. H. *J. Chromatogr. A* **1997,** 775, (1-2), 51-63.

7. Piletsky, S. A.; Alcock, S.; Turner, A. P. F. *Trends Biotechnol.* **2001,** 19, (1), 9-12.

8. Davis, M. E.; Katz, A.; Ahmad, W. R. *Chem. Mat.* **1996,** 8, (8), 1820-1839.

9. Wulff, G. Molecular imprinting - a way to prepare effective mimics of natural antibodies and enzymes. In *Nanoporous Materials Iii*, Sayari, A. J. M., Ed. Elsevier Science Bv: Amsterdam, 2002; Vol. 141, pp 35-44.

10. Ye, L.; Haupt, K. *Anal. Bioanal. Chem.* **2004,** 378, (8), 1887-1897.

11. Whitcombe, M. J.; Alexander, C.; Vulfson, E. N. *Synlett* **2000**, (6), 911-923.

12. Yu, C.; Ramstrom, O.; Mosbach, K. *Anal. Lett.* **1997,** 30, (12), 2123-2140.

13. Shi, H. Q.; Tsai, W. B.; Garrison, M. D.; Ferrari, S.; Ratner, B. D. *Nature* **1999,** 398, (6728), 593-597.

14. Pack, D. W.; Arnold, F. H. *Chem. Phys. Lipids* **1997,** 86, (2), 135-152.

15. Britt, D. W.; Mobius, D.; Hlady, V. *Phys. Chem. Chem. Phys.* **2000,** 2, (20), 4594-4599.

16. Du, X. Z.; Hlady, V.; Britt, D. *Biosens. Bioelectron.* **2005,** 20, (10), 2053-2060.

17. Bondurant, B.; Last, J. A.; Waggoner, T. A.; Slade, A.; Sasaki, D. Y. *Langmuir* **2003,** 19, (5), 1829-1837.

18. May, S.; Harries, D.; Ben-Shaul, A. *Biophys. J.* **2000,** 79, (4), 1747-1760.

19. Gidalevitz, D.; Weissbuch, I.; Kjaer, K.; Alsnielsen, J.; Leiserowitz, L. *J. Am. Chem. Soc.* **1994,** 116, (8), 3271-3278.

20. Litvin, A. L.; Samuelson, L. A.; Charych, D. H.; Spevak, W.; Kaplan, D. L. *J. Phys. Chem.* **1996,** 100, (44), 17708-17708.

21. Britt, D.; Jogikalmath, G.; Hlady, V. Protein interactions with monolayers at the air-water interface. In *Biopolymers at Interfaces*, 2nd ed.; Malmsten, M., Ed. Marcel Dekker Inc: New York, 2003; pp 415-434.

22. Jogikalmath, G. Ph.D. Thesis, University of Utah, Salt Lake City, UT, 2003.

23. Prime, K. L.; Whitesides, G. M. *Science* **1991,** 252, (5009), 1164-1167.

24. Sofia, S. J.; Premnath, V.; Merrill, E. W. *Macromolecules* **1998,** 31, (15), 5059-5070.

25. Halperin, A. *Langmuir* **1999,** 15, (7), 2525-2533.

26. Ostuni, E.; Chapman, R. G.; Holmlin, R. E.; Takayama, S.; Whitesides, G. M. *Langmuir* **2001,** 17, (18), 5605-5620.

27. Yam, C. M.; Lopez-Romero, J. M.; Gu, J. H.; Cai, C. Z. *Chem. Commun.* **2004**, (21), 2510-2511.

28. Goodman, T.; Bussmann, E.; Williams, C.; Taveras, M.; Britt, D. *Langmuir* **2004,** 20, (9), 3684-3689.

29. Buijs, J.; Britt, D. W.; Hlady, V. *Langmuir* **1998,** 14, (2), 335-341.

30. Kuhl, T. L.; Majewski, J.; Howes, P. B.; Kjaer, K.; von Nahmen, A.; Lee, K. Y. C.; Ocko, B.; Israelachvili, J. N.; Smith, G. S. *J. Am. Chem. Soc.* **1999,** 121, (33), 7682-7688.

31. Sigal, G. B.; Bamdad, C.; Barberis, A.; Strominger, J.; Whitesides, G. M. *Anal. Chem.* **1996,** 68, (3), 490-497.

32. Hodneland, C. D.; Lee, Y. S.; Min, D. H.; Mrksich, M. *Proc. Natl. Acad. Sci. U. S. A.* **2002,** 99, (8), 5048-5052.

33. Houseman, B. T.; Huh, J. H.; Kron, S. J.; Mrksich, M. *Nat. Biotechnol.* **2002,** 20, (3), 270-274.

34. Houseman, B. T.; Mrksich, M. *Chem. Biol.* **2002,** 9, (4), 443-454.

35. Cha, T.; Guo, A.; Jun, Y.; Pei, D. Q.; Zhu, X. Y. *Proteomics* **2004,** 4, (7), 1965-1976.

36. Gu, J. H.; Yam, C. M.; Li, S.; Cai, C. Z. *J. Am. Chem. Soc.* **2004,** 126, (26), 8098-8099.

CHAPTER 4

PROTEIN PATTERNING OF MULTICOMPONENT PEG BEARING LANGMUIR MONOLAYERS: INFLUENCE OF LIPID MISCIBILITY, PHASE BEHAVIOR AND PEG CHAIN LENGTH

4.1 Abstract

Langmuir-Schaffer films of cationic dioctadecyldimethylammonium bromide (DOMA), nonionic methyl stearate (SME), and PEG bearing phospholipids with different chain length of PEG moiety (DSPE-PEG_{350}, DSPE-PEG_{750}, DSPE-PEG_{1000}) are presented as a means to create different protein adsorption patterns. The miscibility of mixed lipid Langmuir monolayers was assessed from surface pressure and surface potential measurements of the monolayer films. Miscibility analysis of mixed lipid films indicated that PEG chain length has a profound effect on lipid packing at the air/water interface, even though they have similar lipid moieties. Phase behavior of the lipid monolayers was evaluated by fluorescence microscopy, using labeled lipids and proteins to provide contrast. Surface pressure – Area (π–A) isotherms of mixed lipid monolayers exhibited plateaus indicative of a liquid expanded (LE) to liquid condensed (LC) phase transition. Fluorescence microscopy confirmed the presence of micron-sized LC domains exhibiting diminished protein adsorption (PEG in a tightly packed brush state), while the surrounding LE regions exhibited higher protein adsorption (PEG in a mushroom state). For longer chain length PEG lipids or higher molar concentrations of short chain PEG lipids, the LC domains disappeared and the bound protein was more uniformly

distributed over the film. Thus, the interfacial activity of the PEG chains during monolayer formation appears to greatly influence the final phase behavior of the compressed monolayer, where longer PEG chains diminish the LC phase for a fixed ratio of lipids. Thus, this method affords a self-assembly approach of creating programmable surfaces with user defined protein adsorption patterns through varying molar ratios and miscibility of lipids.

4.2 Introduction

End-grafted chains of polyethylene glycol (PEG) are used extensively as an antifouling coating to improve materials biocompatibility for both *in vivo* and *ex vivo* applications.[1-5] The widespread use of PEG arises from its protein repellent nature, low toxicity, and low immunogenicity.[2, 6, 7] The biological inertness of PEG is generally attributed to chain hydrophilicity and water structure, steric hindrance associated with chain mobility, as well as lack of ionic charges.[1, 2, 5-14] Consequently, PEG has been extensively studied as biocompatible material suitable for creating protein resistant surface coatings for biological applications.[1, 2, 4, 6-14] A number of studies and literature reviews addressed the potential and realized aspects of tethered PEG chains and their effectiveness in resisting protein adsorption.[1, 6-8, 12-19]

Optimal protein repellency is achieved as the PEG surface density increases, forcing the chains into a "brush" configuration. The PEG grafting density and brush layer thickness greatly influence the extent and dynamics of protein adsorption.[3, 4, 9, 10, 13, 15-17, 19] There are numerous physical and chemical approaches to form PEG layers with high surface density on a variety of surfaces to impart non-fouling character. Here we apply

the Langmuir monolayer technique to precisely control the packing density of PEG-bearing lipids and investigate the influence of PEG chain length on the phase behavior generated by introducing protein-binding lipids into the PEG-lipid monolayer. In this manner we create patterned surfaces in which the amount and distribution of target protein on the monolayer is defined by the lipid ratios, PEG chain length, and film packing density.

Further, an array of studies involving polymer-lipid conjugate (lipopolymers) monolayers and vesicles can be found in the literature, which focus mainly on development of protein resistant surfaces with relevance to biomaterials applications,[1, 4, 8, 9, 12, 20] and on development of sterically stabilized vesicles for drug delivery[21-23] with enhanced biocompatibility. Lipopolymer assemblies also open new prospects for the development of protein selective surfaces and biosensors with enhanced sensitivity, allowing the control over the access of the biomolecules to the receptors present in the lipopolymer matrix,[11, 24] and the suppression of non-specific adsorption of proteins to the surfaces.[25, 26]

The phase behavior of PEG-bearing Langmuir monolayers is a unique method that affords a better understanding of the protein repellent nature of PEG layers. Jogikalmath and Hlady have applied the Langmuir trough technique to investigate the phase behavior and protein interactions with single-component monolayers of PEG-bearing polymers.[4] Further, Tsukanova and Salesse suggested a relationship and rationale behind the phase behavior and protein repellency of PEG chains through Langmuir monolayers of PEG-lipids.[27] It is well established in the literature that the PEG lipopolymers exhibit complex surface activity and monolayer phase behavior due to

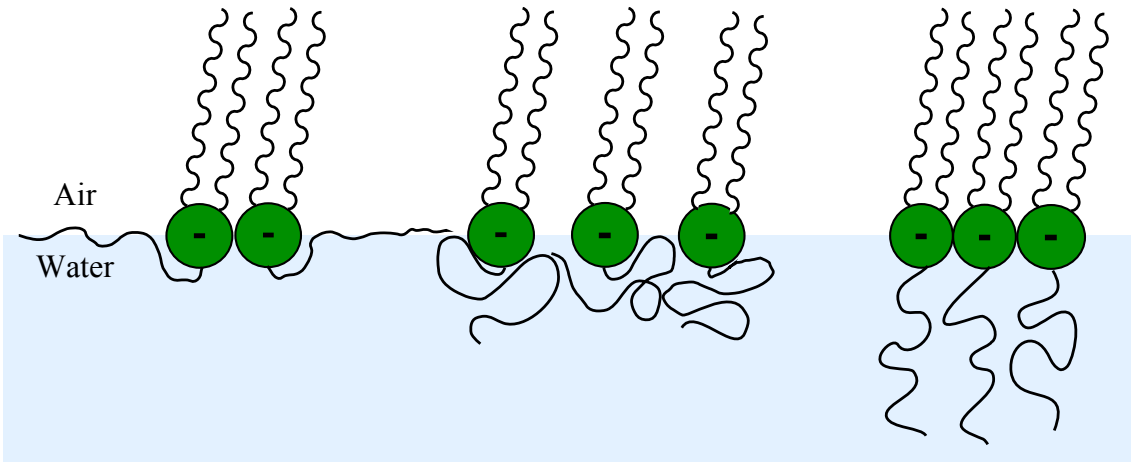

Figure 4.1. Conformational states of lipid conjugated PEG chains: pancake, mushroom, and brush (from left to right).

amphiphilicity of PEG as well as of the lipids to which PEG is tethered.[24, 28-38] The PEG chains of water insoluble PEG-lipid conjugates (lipopolymers) residing on the air/water interface are expected to stretch into a "brush" conformation from a "mushroom" conformation (Figure 4.1) when compressed by Langmuir trough barriers due to the increase in surface density.[24, 27, 29, 31] Also, based on this postulation, it is suggested that PEG brushes are more effective in providing a steric repulsive barrier and reducing protein adsorption when highly stretched and hydrated.[2, 3, 7, 9, 10, 12, 14, 17, 19, 39] However, the conformational changes of PEG chains which take place at the air/water interface in a Langmuir monolayer system as a consequence of lipopolymer compression is still a matter of debate and despite a number of efforts, there have been no results that clearly describe the relationship between the conformation of lipid conjugated PEG chains and their behavior at the air/water interface.[27, 31-33, 38, 40]

Here, we focus on development of a generic platform for protein patterning/detection through multi-component Langmuir monolayers comprised of protein binding lipids dispersed in a matrix of protein-repellent PEG-bearing lipids. In

this bottom-up approach, properties of the resulting protein selective surface are defined by the lipid molar ratios, their physical properties such as alkyl-tail length and saturation, head-group size and charge, and preparation conditions such as temperature, film compression rate, and subphase properties. Combined, these properties determine lipid phase behavior and miscibility, which define the size and distribution of protein binding lipid domains within the inert PEG-lipid matrix.

We have shown that PEG bearing lipids acted as inert matrix when present in the neutral methyl stearate (SME)/cationic dioctadecyldimethylammonium bromide (DOMA) lipid mixtures at the air/water interface to define specific protein binding sites and reduce non-specific protein interactions on the monolayer.[26, 41] However, only modest selectivity for protein binding to the resulting surfaces was achieved, attributed to the lower steric barrier imparted by smaller PEG chain length (M.W. 350 daltons).

In the present study, we employ higher MW PEG chains (PEG_{750}, and PEG_{1000}) as well as PEG_{350} as matrix lipids and report on the phase behavior and protein patterning exhibited when mixed with the protein binding lipids. We present a detailed miscibility analysis of these ternary lipid films prepared at several molar ratios and demonstrate a strong influence of PEG chain length on lipid miscibility and phase behavior. While the influence of alkyl-tail lengths (and mismatch in mixed films) is well-known to influence phase behavior, the findings presented here are significant in that introducing longer PEG chains, to provide a greater steric barrier against protein adsorption, also leads to dramatic differences in the size and distribution of domains within the mixed monolayers. We demonstrated that, increasing PEG chain length to provide greater inhibition of non-specific binding concomitantly leads to a decrease in the size of protein binding

SME/DOMA domains as compared to shorter PEG lengths in otherwise identical monolayers.

4.3 Experimental

4.3.1 Lipids. Methyl stearate (SME) (99% GC, Fluka), dioctadecyldimethylammonium bromide (DOMA, or DODAB) (99% Tech Grade, TCI), 1,2-distearoyl-*sn*-glycero-3-phosphoethanolamine-*N*-[methoxy(poly(ethylene glycol))-350] as the ammonium salt (PEG_{350}) (M.W. = 1131; 99% in chloroform, Avanti Polar Lipids), 1,2-distearoyl-*sn*-glycero-3-phosphoethanolamine-*N*-[methoxy(poly(ethylene glycol))-750] as the ammonium salt (PEG_{750}) (M.W. = 1131; 99% in chloroform, Avanti Polar Lipids), and 1,2-distearoyl-*sn*-glycero-3-phosphoethanolamine-*N*-[methoxy(poly(ethylene glycol))-1000] as the ammonium salt (PEG_{1000}) (M.W. = 1131; 99% in chloroform, Avanti Polar Lipids) were prepared as 1 mM stock solutions in chloroform (99% HPLC grade, Merck) and stored at 4 ºC (Molecular structure of all lipids are presented in Appendix A). Binary lipid mixtures of SME and DOMA were first prepared in a 2:1 molar ratio hereafter referred to as "SD". Miscibility analysis here considers only the mixing of $PEG_{350/750/1000}$ with SD, the latter essentially being treated as a single component based on previous studies illustrating the high miscibility of SME with DOMA.[42, 43] A series of $PEG_{350/750/1000}$:SD lipid mixtures were prepared by volumetrically mixing the 1 mM stock solutions of SD with $PEG_{350/750/1000}$ prior to spreading at the air/water interface.

4.3.2 Protein. Bovine serum albumin, Alexafluor® 594 conjugate (5 mg, Invitrogen) was diluted to 1 mg/mL in HPLC grade water (Sigma) and stored at 4 ºC

prior to adsorption on transferred monolayers. Protein was injected in a custom-made poly(dimethylsiloxane) (PDMS) (Sylgard 184 Silicone elastomer kit, Dow Corning) flow cell containing a hydrated monolayer, yielding a final concentration of 5.0 μg/ml, and allowed to adsorb for 1 hr followed by thorough rinsing with double distilled water to remove any loosely bound protein.

4.3.3 Monolayer Preparation and Transfer. Monolayer experiments were carried out on a PTFE Langmuir trough with surface area of 55 × 220 mm^2 (μTroughS, Kibron, Inc.), maintained at 25 ± 0.5 ºC by circulating water through a metal plate below the trough. The subphase was HPLC grade water (Sigma) (surface tension ~72 mN/m, at 25 ºC). Langmuir monolayers of SD, $PEG_{350/750/1000}$, and their mixtures were prepared by spreading the lipids dropwise on the air/water interface of the trough, using a 50 μL Hamilton Gastight syringe, and allowing 10 min for solvent (chloroform) evaporation. The monolayers were then compressed at a rate of 20 mm/min until the desired surface pressure was reached (e.g. 25 mN/m for film transfer) or until film collapse (for generating π-A isotherms). The surface potential versus surface area (ΔV-A) isotherms were recorded during the compression isotherm with the vibrating plate technique (μSpot, Kibron, Inc.). All π-A and ΔV-A isotherms were repeated three times to verify reproducibility. The standard deviation for the values of ΔV at collapse was less than ±15 mV. The trough was kept free of surface-active materials by cleaning with 70% ethanol and then thoroughly rinsing with double distilled water after each experiment.

Monolayers held at 25 mN/m were transferred horizontally onto an octadecyltrichorosilane (OTS) modified glass coverslip by a Langmuir-Schaeffer (LS) method in which the OTS-coverslip is pushed through the monolayer into a small

polystyrene petridish in the subphase and maintained hydrated for all analysis. OTS substrates were prepared by cleaning the glass coverslip (25 mm diameter, Fisher Scientific) in a piranha etch solution (3:1 ratio of 98% H_2SO_4/H_2O_2) for 1 hr, rinsing with double distilled water, and drying at 80 ºC. Care must be taken when using piranha solution as it is a strong oxidant and reacts violently with organic contaminants. OTS silanized glass substrates were prepared by immersing acid cleaned hydrophilic coverslips in a 0.5 mM solution of OTS in bicyclohexyl (Sigma) for 12 h followed by rinsing with chloroform and then 5 min of ultrasonication in methanol followed by rinsing under double distilled water. This yields a uniformly hydrophobic surface with water contact angles of 103-106º.

4.3.4 AFM and Fluorescence Microscopy. A Nanoscope III Bioscope (Digital Instruments, Inc.) was used to image hydrated monolayers in contact mode. Cantilevers (Park Scientific Instruments) with a relatively low spring constant of 0.01 N/m were employed to reduce disruption of protein by the AFM tip. An inverted fluorescence microscope (Nikon Eclipse TE2000-S) with 100 W Hg-lamp, Filter Cubes G-2A (excitation filter at 510 – 560 nm, a dichroic mirror at 570 nm and an emission filter at 595 nm) and B-2A (excitation filter at 450 – 490 nm, a dichroic mirror at 505 nm and an emission filter at 520 nm) and, 40×/0.60 N.A. (Nikon ELWD CFI Plan Fluor) and 100×/1.40 N.A. oil (Nikon CFI Plan Apochromat) objectives was used to image transferred monolayers. Images were captured with a Nikon DXM1200 color CCD camera operated with ACT-1 (Nikon) software from a PC with frame-grabber.

Monolayer phase behavior was revealed by doping the $PEG_{350/750/1000}$:SD lipid mixtures with 2 mol % of the fluorescent lipid: 1-oleoyl-2-[12-[(7-nitro-2-1,3-

benzoxadiazol-4-yl)amino]dodecanoyl]-*sn*-glycero-3-phosphoethanolamine (18:1 NBD-PE; Avanti Polar Lipids). Adsorption and distribution of Alexafluor® 594 BSA conjugate to the lipid monolayers was investigated to assess protein adsorption patterns. All protein adsorption studies were carried out in a custom-made PDMS flow cell. All the images were captured at 5 sec exposure time except for PEG_{1000}:SD (2:1) where longer exposure time was necessary to obtain fluorescence in image, and thus fluorescence analysis was employed as a qualitative assessment of protein-monolayer interactions.

4.3.5 Image Analysis. Area fraction occupied by liquid condensed (LC) domains in fluorescence micrographs of $PEG_{350/750/1000}$:SD lipid mixtures was calculated using NIH ImageJ software. Further hypothetical value of area fraction occupied by LC domains, if LC domains are phase separated regions of SD lipids, at surface pressure of 25 mN/m were also calculated based on the following equation for comparison with actual area fraction occupied by LC domains, as determined by image analysis.

$$\%\ \text{Area Fraction of LC Domains} = \text{Mole Fraction of SD Lipids} \times \frac{\text{Molecular Area of SD Lipids at 25 mN/m}}{\left(\text{Molecular Area of SD Lipids at 25 mN/m}\right) + \left(\text{Molecular Area of PEG Lipids at 25 mN/m}\right)} \times 100$$

4.4 Results and Discussion

4.4.1 Monolayer Properties and Mixing Behavior: Pure DSPE-PEG Films. The molecular organization or packing of pure and multicomponent lipid films at the air/water interface of a Langmuir trough was inferred from the profile of the surface pressure-molecular area (π-A) and surface potential-molecular area (ΔV-A) isotherms. While the hydrophobic moiety (lipid tails) of the three PEG lipids investigated here are the same (DSPE), differences in π-A (Figure 4.2 (a)) and ΔV-A (Figure 4.3) relationships

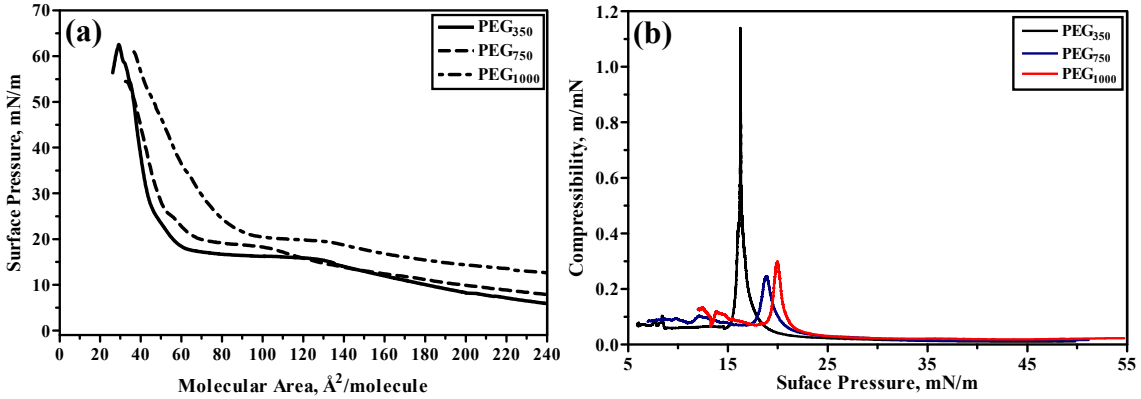

Figure 4.2. (a) Surface pressure-molecular area (π-*A*) isotherms and **(b)** Compressibility as a function of surface pressure for PEG_{350}, PEG_{750}, and PEG_{1000} lipids. The peak in compressibility plot represents the plateau region of the π–*A* isotherms in Figure 2(a).

for different lipopolymers arise from different lengths of PEG chains. The pure $PEG_{350/750/1000}$ isotherms exhibit an expanded region of high compressibility (> 140 $Å^2$/molecule) where the PEG chains compete with the alkyl tails for space at the air/water interface[40] followed by a plateau region, then a region of reduced compressibility as the PEG chains are forced into a bush-layer in the subphase and the limiting molecular area defined by the alkyl tails is reached. The plateau region is attributed to a combination of alkyl tail transition (liquid expanded (LE) to liquid condensed (LC))[32, 44] and a transition associated with reduced conformational mobility of the PEG chains.[4] As PEG chain length increases for DSPE-PEG, a more expanded π-*A* isotherm is observed due to the higher number of ethylene oxide monomers occupying space at the air-water interface. As the monolayers of PEG_{350} and PEG_{750} are compressed, their isotherms approach limiting areas near ~55$Å^2$/molecule, a value observed for pure DSPE monolayers,[40] indicating that the maximum density of the PEG chains in the brush is limited by the area of closed packed lipids. For PEG_{1000} expanded type behavior is observed even at very high surface pressures (π > 40 mN/m), indicating that the longer PEG chains may

compete with alkyl tails for space at air/water interface even at higher surface pressures, which is frequently discussed and disputed in the literature as a "mushroom to brush"[40, 45] transition. It may also be that for higher M.W. PEG lipids the monolayer packing is controlled through PEG chain packing in the subphase and not through alkyl tail packing due to lack in free area,[32, 33] which is further supported by X-ray diffraction data indicating that PEG chains tends to interdigitize and form a weak network when composed of ≥ 14 EO units[40, 46, 47] (as in the case for PEG_{750} (16 EO units) and PEG_{1000} (22 EO units)).

Additional evidence for this phenomenon can be obtained from the compressibility, $C = A^{-1}(dA/d\pi)$ of the PEG lipids plotted vs. the surface pressure, π (Figure 4.2 (b)), where the size of the peak is correlated to the strength of alkyl chain condensation.[35, 48] Figure 4.2 (b) shows the largest peak for PEG_{350}, while PEG_{750} and PEG_{1000} show smaller peaks of similar size, indicating that there is a stronger coupling between alkyl chains of adjacent molecules of lower M.W. PEG lipids (PEG_{350}) and weaker coupling between alkyl chains of adjacent molecules of higher M.W. PEG lipids (PEG_{750}, and PEG_{1000}). Thus, it can be inferred from Figure 2(a) and (b) that the volume of the polymer moiety of the PEG lipids profoundly influences the overall behavior of π-*A* relationships as the alkyl tail length is held constant. This effect has unique implications on the mixing and phase behavior of the PEG lipids with other lipids as will be discussed later.

The surface potential-molecular area (ΔV-*A*) relationships, shown in Figure 4.3, exhibited unique behavior that point out certain distinctive molecular packing properties of PEG lipids. The surface potential at film collapse increases with PEG M.W., yielding

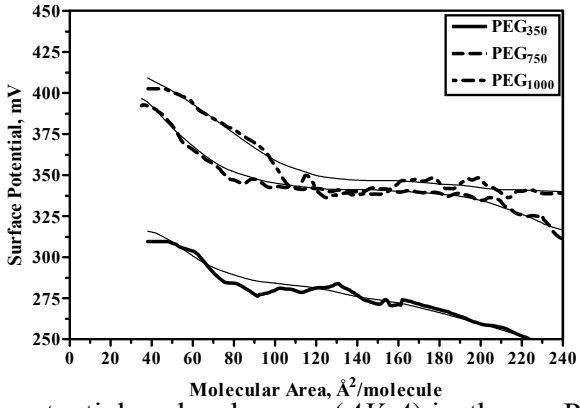

Figure 4.3. Surface potential-molecular area (ΔV-A) isotherms PEG_{350}, PEG_{750}, and PEG_{1000} lipids.

310, 390, and 400 mV for PEG_{350}, PEG_{750}, and PEG_{1000}, respectively. Further, the ΔV-A isotherms of PEG_{750} and PEG_{1000} are nearly identical with a very small difference in ΔV_{max} (~ 10 mV) as compared to the ΔV-A isotherm of PEG_{350} which demonstrates approximately 100 mV lower ΔV_{max} value. In contrast, PEG350 and PEG750 π–A isotherms are nearly identical while PEG1000 is shifted to higher molecular area and pressure (Figure 2(a)). This increase of ΔV_{max} in PEG750 and PEG1000 as compared to the PEG350 and increase of occupied molecular area at specific pressure in PEG1000 as compared to the PEG350 and PEG750 indicates the critical contribution of the PEG chain length, water structure associated with the PEG chains, and alkyl tail dipole moment density to the overall ΔV value.

A quantitative relationship between measured ΔV values and normal (orthogonal) components of group dipole moment can be established through the Demchak-Fort three-layer capacitor model,[27, 49] which is written as

$$\Delta V = \frac{1}{\varepsilon_0 A}\left(\frac{\mu_{\text{hydrophobic tail}}}{\varepsilon_{\text{hydrophobic tail}}} + \frac{\mu_{\text{polar head}}}{\varepsilon_{\text{polar head}}} + \frac{\mu_{H_2O}}{\varepsilon_{H_2O}}\right) + \psi_0$$

where ε_0 is the permittivity of the vacuum, A is the area per molecule, μ_i is the normal components of the effective dipole moment of each layer in a monolayer, ε_i is the effective dielectric constant of each layer, and ψ_0 is the electric double layer potential.[27, 49] Based on the Demchak-Fort model the surface potential behavior of the DSPE-PEG lipids can be explained as depicted in Figure 4.4: (i) Decrease in electric double layer potential magnitude (ψ_0) (less negative) for PEG_{750} and PEG_{1000} due to increase in local PEG concentration near lipid head group which decreases the local dielectric constant (ε) of the medium surrounding the lipid head group (pure PEG dielectric constant , e = 11, compared with water e = 80)[27]. (ii) Increase in bulk like (disordered) water (as demonstrated through sum frequency generation (SFG) spectroscopy of PEG lipids at the air-water interface by Ohe et.al.)[38] because of interdigitation of PEG chains (as illustrated through X-ray diffraction measurement by Kuhl et al.)[40] for PEG_{750} and PEG_{1000}, which decreases (less negative) the effective water dipole moment value.[50] (iii) Increase in alkyl tail end methyl dipole moment contribution because of more orthogonal orientation of the alkyl tails with increase in PEG chain length of lipopolymer.[40]

4.4.2 Monolayer Properties and Mixing Behavior: Mixed DSPE-PEG/SD Films. From the analysis of pure PEG lipid films a strong influence of PEG chain length on lipid packing is observed. This influence becomes more apparent as simple lipids (SD) are introduced to the PEG lipid films. PEG lipid-SD mixtures were investigated in order to develop films having protein binding domains (SD) distributed in a protein repellent matrix (PEG lipids). The different PEG chain lengths were selected to investigate the effect of PEG M.W. (in mixed films) on protein repellency as well as phase behavior. The π-*A* and *ΔV-A* and isotherms of $PEG_{350/750/1000}$:SD mixtures (molar ratios 2:1, 1:2,

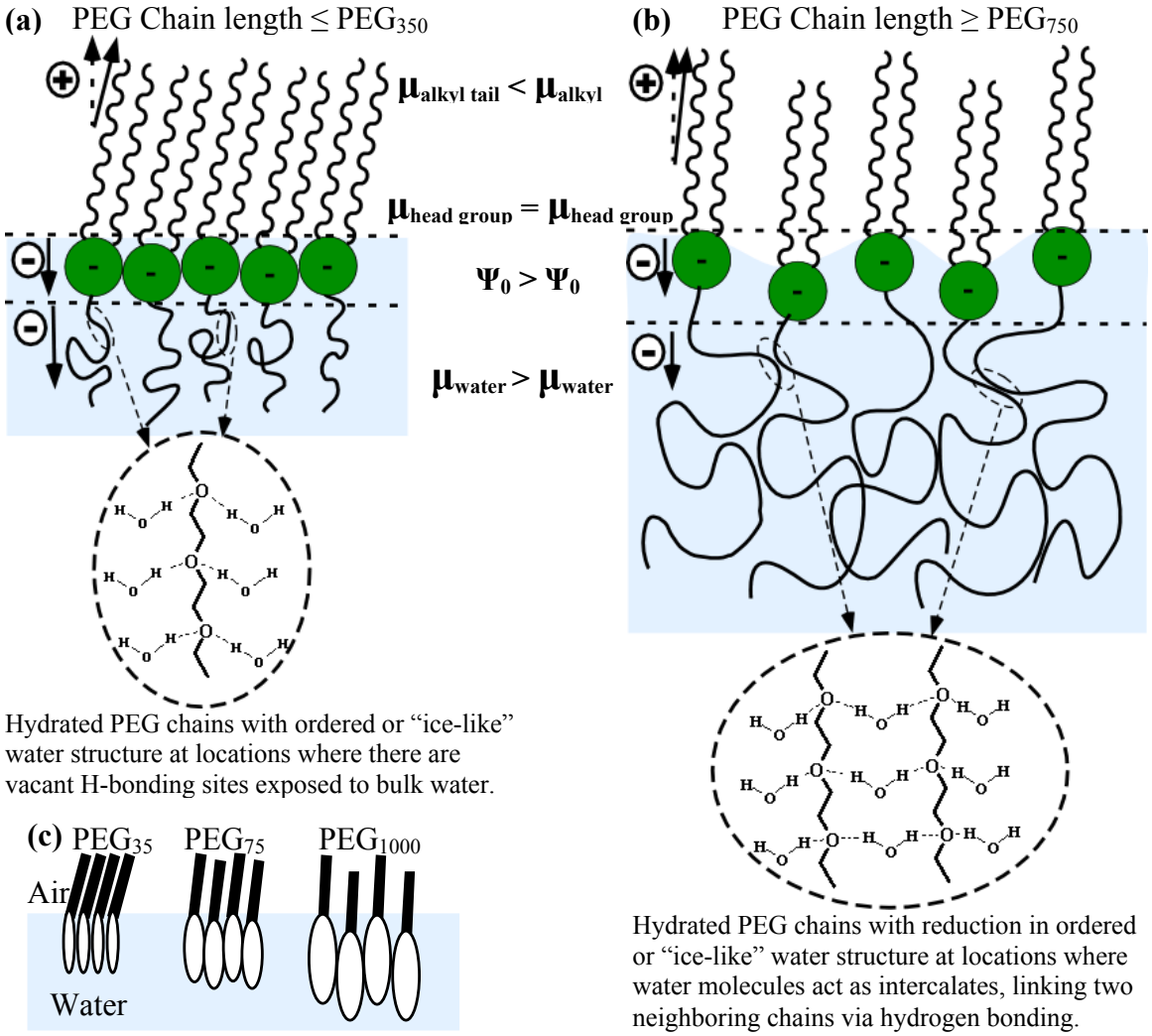

Figure 4.4. Schematic of a possible molecular model to explain the observed surface potential behavior amongst different M.W. PEG lipids as the PEG chains are compressed to a "brush-like" conformation. **(a)** When M.W. of PEG chains is ≤ 350 daltons and **(b)** When M.W. of PEG chains is ≥ 750 daltons. **(c)** Schematic illustrating more orthogonal orientation (decrease in tilt angle) of alkyl tails in lipid molecule as PEG chain length increases. (Figure adapted from Ref. 28 and 47)

1:3) along with isotherms of pure films at 25 ± 0.5 ºC are shown in Figure 4.5(a–f). As SD is introduced to PEG lipids, the π-A isotherms (Figure 4.5 (a–c))gradually shift to lower molecular areas and the plateau region representing the PEG "mushroom to brush" transition diminishes proportionally. The ΔV-A relationships, shown in Figure 4.5(d–f), demonstrates that as SD is introduced to PEG lipids ΔV_{max} increases proportionally due to the quaternary ammonium headgroup of DOMA. However, a prominent feature that surfaced through the π-A isotherms was that increasing PEG chain length from PEG_{350} to PEG_{750} results in more densely packed mixed monolayer films. It can be observed from the decrease in the molecular area gap (clearly visible in miscibility diagrams, Figure 6) separating the isotherm of the pure SD curve from those of PEG lipid–SD mixtures. Conversely, as PEG chain length increases from PEG_{750} to PEG_{1000}, less densely packed mixed films are observed. This phenomenon specifically reveals that as PEG chain length increases, it influences miscibility as well as packing of the lipids at the air/water interface even at high surface pressures, where all PEG chains are expected to be completely submerged into the water subphase. These specific molecular events are explained in more detail in the following miscibility analysis and tentative molecular packing behavior model for the DSPE-$PEG_{350/750/1000}$:SD mixtures.

Mixing diagrams (Figure 4.6) constructed from π-A and ΔV-A isotherms for the three PEG chain lengths provide a more detailed view of lipid miscibility and PEG chains behavior at the air/water interface over a range of surface pressures. Figure 4.6 (a–d) shows the miscibility diagrams of the mean area per molecule in the films composed of SD and PEG lipids versus DSPE-PEG lipid molar fraction in the mixture at selected surface pressures. The 0 and 1 χ_{PEG} values are removed from these mixing diagrams to

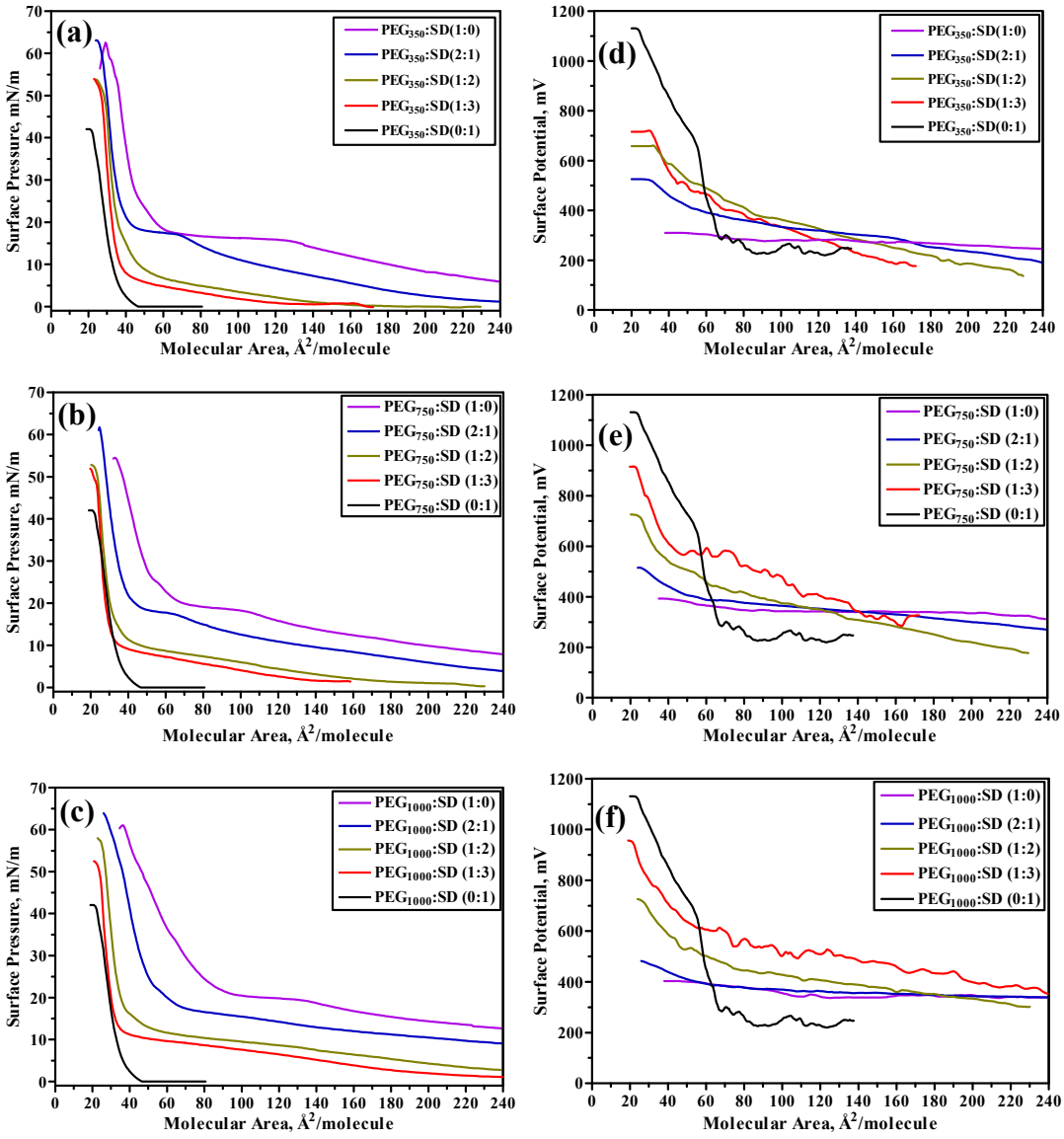

Figure 4.5. (a–c) Surface pressure-molecular area (π-*A*) and **(d–f)** surface potential-molecular area (*ΔV*-*A*) isotherms of SD and of its mixture with PEG_{350} (a, d), PEG_{750} (b, e), and PEG_{1000} (c, f). Molar ratios of PEG:SD mixtures are 2:1, 1:2, and 1:3.

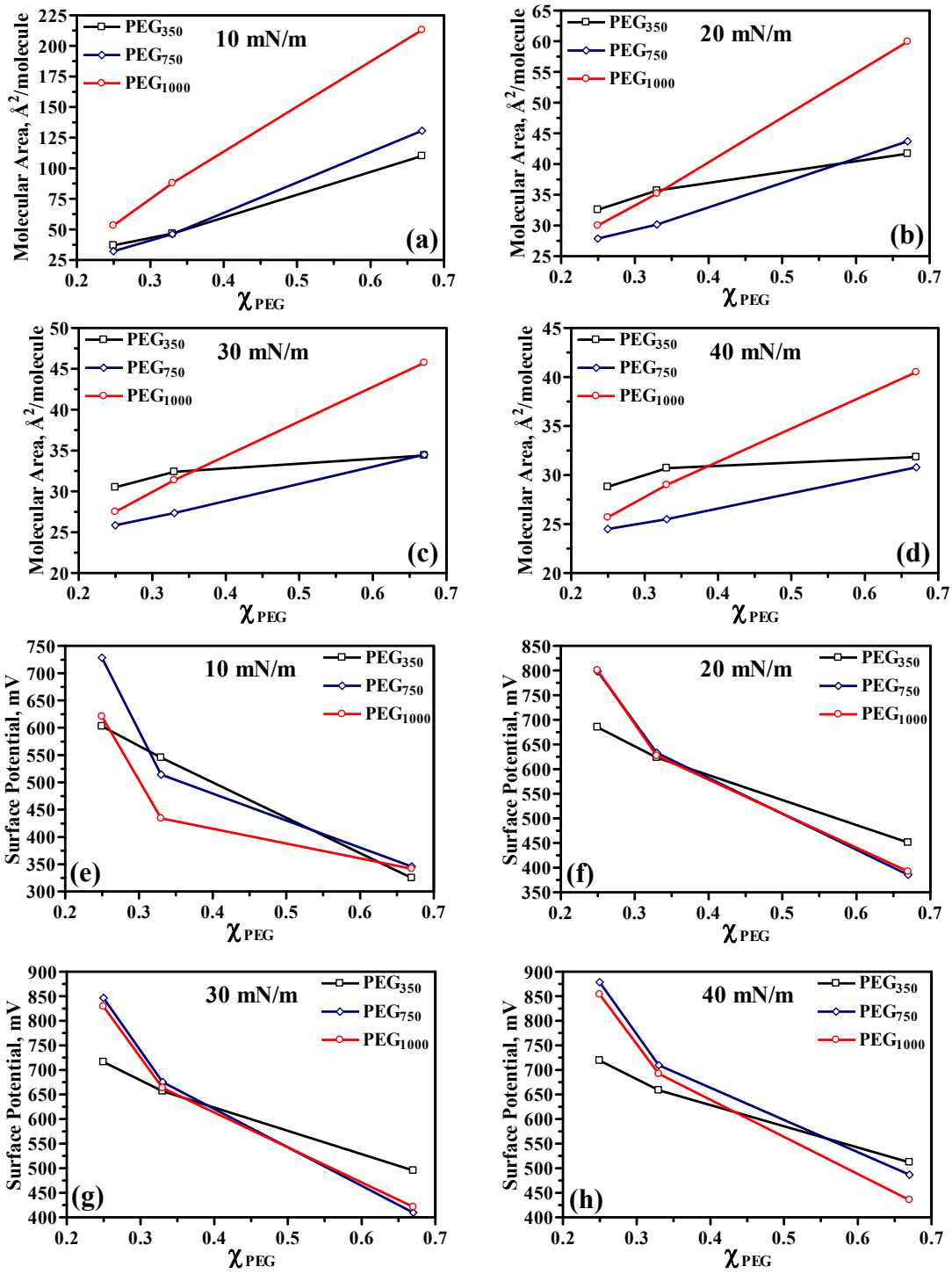

Figure 4.6. (a–h) Miscibility analysis of PEG:SD monolayers. Mixing diagrams constructed from the isotherms in Figure 4.5 (a–f) at indicated surface pressures.

better visualize the distinct trends seen upon introducing SD lipids into the three different M.W. PEG lipids.

In Figure 4.6 (a) (at 10 mN/m) the area trend upon increasing SD appears to be that of SD acting as a diluent, reducing PEG-PEG repulsion, allowing PEG_{1000} to converge to an area near that of $PEG_{350/750}$ for $\chi_{PEG} \sim 0.2$ (extrapolating). Further, it is important to note here that PEG_{750} and PEG_{350} converge at $\chi_{PEG} \sim 0.33$ upon adding SD and appear to cross-over for $\chi_{PEG} < 0.33$. This cross-over effect is even more pronounced at higher surface pressures up to 40 mN/m. The unexpected trend observed here is that the higher M.W. PEG_{1000} occupies a lower area than low M.W. PEG_{350} for $0.33 < \chi_{PEG} < 0.38$ in 20 to 40 mN/m range (Figure 4.6 (b–d)). The unique significance of the mixed PEG:SD film area vs. PEG M.W. shows that a longer PEG chain can be employed (to provide better inhibition of non-specific binding), while maintaining the same protein binding to repulsive surface area ratio attained with lower M.W. PEG lipids mixed with SD. While reduction of PEG-PEG interaction upon introduction of SD can be attributed to high lipid miscibility, thus diluting the PEG surface density, this does not account for $PEG_{750/1000}$:SD mixtures occupying lower molecular area than PEG_{350}:SD mixtures.

One possible explanation for these differences in mixing behavior can be given through two different molecular packing events occurring at the air/water interface due to the different PEG lipid concentrations: (i) For $\chi_{PEG} \leq 0.33$ the surface area available to the lipids actually increases for $PEG_{750/1000}$:SD as compared to PEG_{350}:SD at high surface pressures because the bulkier polymer chains of $PEG_{750/1000}$ may pull the lipopolymer further into the water subphase, when the films are highly compressed, leading to a roughening of the monolayer that allows for assembly of more densely packed films as

lipids are essentially staggered.[29, 31, 40, 45] This is depicted in Figure 4.6 (b). Here, molecular packing is essentially driven through the lipid headgroup size as well as through the alkyl tail packing, because lateral interactions between PEG chains in the subphase are reduced by incorporating higher concentrations of SD lipids. Thus SD acts as a diluent to improve monolayer packing by reducing PEG-PEG interactions, and for longer PEG chains a monolayer roughening effect allows the lipids to occupy an even lesser area. (ii) Conversely, for $\chi_{PEG} \geq 0.67$ the above stated phenomenon fails to describe the mixing behavior of PEG:SD mixtures. This is attributed to the behavior of PEG chains with increasing number of EO (ethylene oxide) monomers at the air/water interface and as discussed earlier in the manuscript that for higher PEG chain length PEG lipids, bulkier PEG chains virtually control the packing of the monolayer film through lateral interaction between PEG chains in the subphase, which ultimately produces less densely packed films with higher areas per lipid molecule.

Similar behavior is also observed in surface potential mixing diagrams (Figure 4.6 (e-h)), where an "isopotential" is seen at $\chi_{PEG} \sim 0.33$ for all three PEG lengths. Also, at $\chi_{PEG} < 0.33$ the cross-over in molecular areas, where PEG_{350}:SD mixtures occupy greater areas than the $PEG_{750/1000}$:SD mixed films, results in a decrease in surface potential, likely due to a less efficient packing of lipid dipoles. A more orthogonal lipid orientation and/or altered structure of PEG associated water may also contribute to the increased surface potential of the $PEG_{750/1000}$:SD mixtures ($\chi_{PEG} \leq 0.33$) as compared to PEG_{350}:SD mixtures at the same mixing ratios.[38] Further, at higher PEG lipid concentration ($\chi_{PEG} \geq 0.67$), ΔV almost varies in close proportion to the lipid packing density of the mixtures and also supports the previous supposition that as molecular

weight of the PEG chain increases monolayer packing is driven through the polymer chains with alky tails forced in a more orthogonal orientation even though there is ample space for the alkyl tails to retain a high number of gauche isomers (as demonstrated through Infrared Reflection-Absorption Spectroscopy (IRAS) by Baekmark et al.).[32, 33]

4.4.3 Phase Behavior. Pure PEG lipid monolayers are devoid of phase behavior as evidenced by fluorescence microscopy (data not shown). SD monolayers exhibit a rich phase behavior of 1-10 micron sized circular domains.[42] The phase behavior of the mixed monolayers is visualized from the fluorescent images of the films doped with 2 mol% NBD-PE and transferred horizontally at 25mN/m to a hydrophobic coverglass (Figure 4.7). Fluorescence micrographs reveal the presence of micron-sized domains, whose size tends to decrease with increasing PEG chain length (left to right in Figure 4.7) and increasing PEG mole fraction (bottom to top in Figure 4.7). The decrease in domain density is expected with increasing PEG lipid concentration in mixed films as pure PEG lipid films display no phase behavior. These differences in the phase behavior of mixed monolayer films may be attributed to the decrease in line tension of the lipids in mixed monolayer films caused by the change in lipid packing, because of the change in the concentration and M.W. of DSPE-PEG lipids.

The film compression hinders diffusion of fluorescent lipids at lower areas per lipid molecule, where interaction between higher M.W. PEG chains decreases the lateral mobility of the other lipid molecules[51, 52] (SD, NBD-PE) leads to a blurring of domain boundaries in surrounding phase as seen clearly in Figure 4.7 (b) ,(e), and (f). For PEG_{1000}, $\chi_{PEG} = 0.67$ (Figure 4.7 (c)) the domains are absent or of dimension beyond the resolution of the fluorescence microscope. These observations indicate that the phase

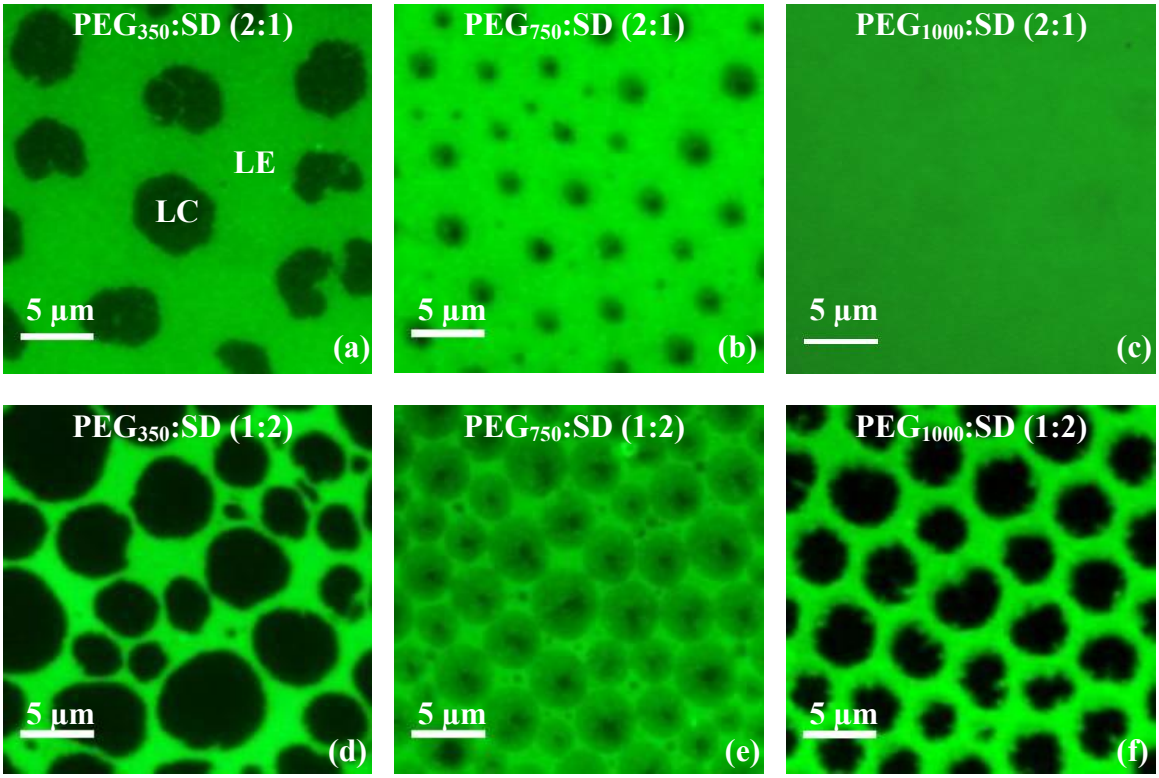

Figure 4.7. (a–f) Fluorescence micrographs of Langmuir films of $PEG_{350/750/1000}$:SD (molar ratios indicated in figure) doped with 2% NBD-PE. All images captured with 100X oil immersion objective and samples were kept hydrated while imaging. Films horizontally transferred at 25mN/m to hydrophobic substrate.

behavior arises from the SD lipids, while domain size is a function of PEG chain length. Phase separation (i.e. demixing) of SD from PEG lipids is not supported by image analysis (Figure 4.8). A ratio of area occupied by LC domains has been calculated and is plotted versus the M.W. of PEG chains in Figure 4.8 (a) and (b), for χ_{PEG} = 0.67 and 0.33 respectively. For $PEG_{350/750/1000}$:SD (χ_{PEG} = 0.67) and $PEG_{350/750/1000}$:SD (χ_{PEG} = 0.33) lipid mixtures if LC domains are phase separated regions of SD then the area fraction occupied by the LC domains should be ~13%/~12%/~9% and ~26%/~25%/~17% respectively (i.e. the mole fraction x molecular area fraction of the SD lipids in the mixture, calculated based on the area occupied by the pure lipid films at 25 mN/m (SD= 35 $Å^2$/molecule, PEG_{350} = 55 $Å^2$/molecule, PEG_{750} = 60 $Å^2$/molecule, and PEG_{1000} = 100 $Å^2$/molecule)). However, as observed in the Figure 4.8 (a), for PEG_{350}:SD (χ_{PEG} = 0.67) the area fraction occupied by LC domains is ~28%, which is significantly higher than the expected area fraction of ~13% if phase separated. Further, as PEG chain length increases the area fraction occupied by LC domains significantly decreases more than the predicted area faction (if phase separated), indicating that LC domains are not phase separated

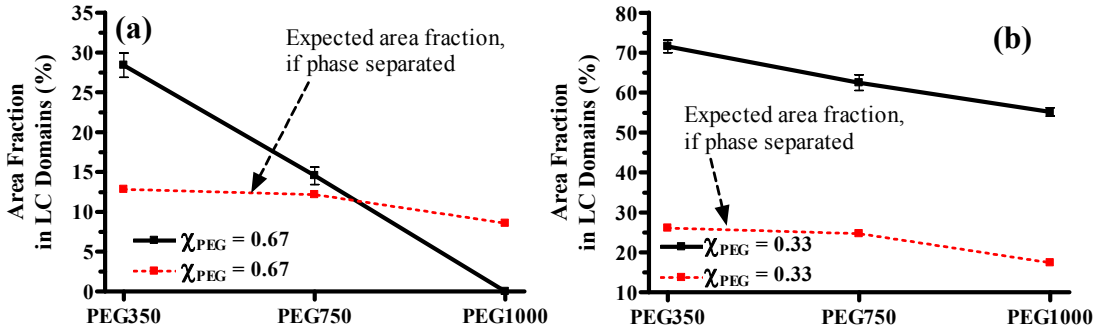

Figure 4.8. (a) & (b) Image analysis of the fluorescence micrographs (Figure 4.8. (a–f)) showing area occupied by liquid condensed (LC) domains. Error bars represent standard error of mean.

regions of SD lipids and the DSPE-$PEG_{350/750/100}$ and SD lipids are miscible.

For all PEG:SD lipid mixtures (χ_{PEG} = 0.33) (Figure 4.8 (b)) the area fraction occupied by LC domains is significantly higher than expected area fraction if phase separated. This phase behavior for all PEG:SD lipid mixtures is thus ascribed to condensed phase nucleation and growth from an expanded phase matrix, as is commonly observed upon compression of single-component lipid monolayers (i.e. the liquid expanded (LE) to liquid condensed (LC) phase transition). However, in the case of PEG bearing lipids, nucleation of condensed domains (though addition of other lipids) may induce a localized transition of the PEG chains into a closely packed brush layer. The nucleation of condensed domains in a monolayer containing PEG-bearing lipids presents a means of inducing the mushroom to brush transition as discrete events within micron-sized domains.[41] This is further supported by fluorescence microscopy analysis of the gross distribution of protein on mixed monolayers as well as AFM analysis as discussed in next section.

Based on the miscibility analysis and observed phase behavior, the packing of the DSPE-PEG:SD lipid mixtures at the air/water interface can be described by two different models based on the molar concentrations of DSPE-PEG lipids in the DSPE-PEG:SD lipid mixture as presented in Figure 4.9: (i) At lower PEG lipid concentration, i.e. $\chi_{PEG} \leq$ 0.33, the packing of lipids is ascribed to headgroup size with roughening of monolayer for bulkier PEG chains ($\geq PEG_{750}$) and alkyl tail packing. (ii) At higher PEG lipid concentration, i.e. $\chi_{PEG} \geq 0.67$, the packing of lipids is essentially driven through headgroup size and alkyl tail packing for low M.W. PEG chains ($\leq PEG_{350}$) and through polymer chains for high M.W PEG chains ($\geq PEG_{750}$) with roughening of the monolayer.

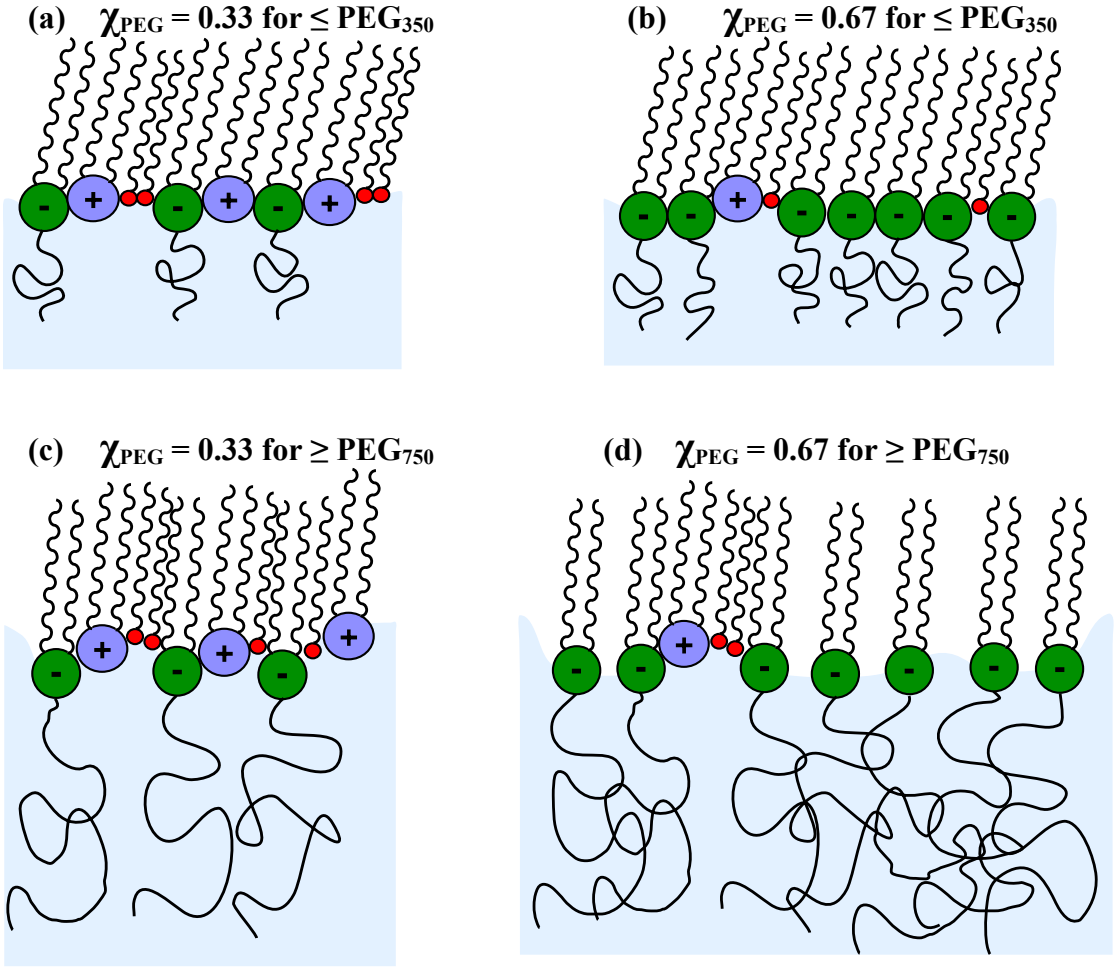

Figure 4.9. Schematic of a possible molecular model illustrating packing of PEG:SD lipid mixtures at the air/water interface based on the M.W. and molar concentration of the PEG lipids. When M.W. of PEG chains is ≤ 350 daltons: **(a)** for χ_{PEG} = 0.33 and **(b)** for χ_{PEG} = 0.67 lipid packing is ascribed to head group size and alkyl tail packing. When M.W. of PEG chains is ≥ 750 daltons: **(c)** for χ_{PEG} = 0.33 lipid packing is ascribed to head group size and alkyl tail packing and **(d)** for χ_{PEG} = 0.67 lipid packing is ascribed to polymer chain packing in the subphase.

4.4.4 Protein Adsorption and Patterning. Protein distribution on the mixed lipid monolayers was visualized through fluorescent BSA adsorption to transferred films (Figure 4.10). All the images were captured at the same exposure times for qualitative estimation of the protein affinity to the respective mixed lipid films. As observed in the fluorescence micrographs BSA preferentially adsorbs to the LE regions with less adsorption to LC domains, further indicating that the LC domains are not a SD rich phase. BSA adsorption to the mixed monolayers is driven by a strong electrostatic affinity for the SD lipid headgroups, which is countered by the local density of the protein repellent PEG chains. It is depicted by the fluorescent micrographs that BSA tends to adsorb less in LC domains indicating that LC domains are either PEG rich phases or phases with PEG in a tightly packed brush state, as PEG chains have a greater tendency to repel protein when in tightly packed brush state (i.e. high local surface density of PEG chains) as compared to the mushroom state (i.e. low local surface density of PEG chains).[2, 4, 12, 53]

The efficiency of PEG in repelling protein is mainly dependent on two characteristics, i.e. density of the PEG chains on surface and length of the PEG chains. [2, 17] This theory is further supported by the fluorescent micrographs presented here (Figure 4.10), where the total fluorescence intensity decreases as PEG chain length increases for given lipid mixtures, suggesting that longer PEG chain length provide better steric barrier against protein adsorption in effectively screening the SD head groups from protein.

It can also be observed for PEG_{350}:SD (χ_{PEG} = 0.67) and (χ_{PEG} = 0.33) (Figure 4.10 (a) and (d)) that considerable amount of protein adsorbs to the LC domains, which is mainly attributed to the electrostatic protein adsorption to the SD lipids and non-specific

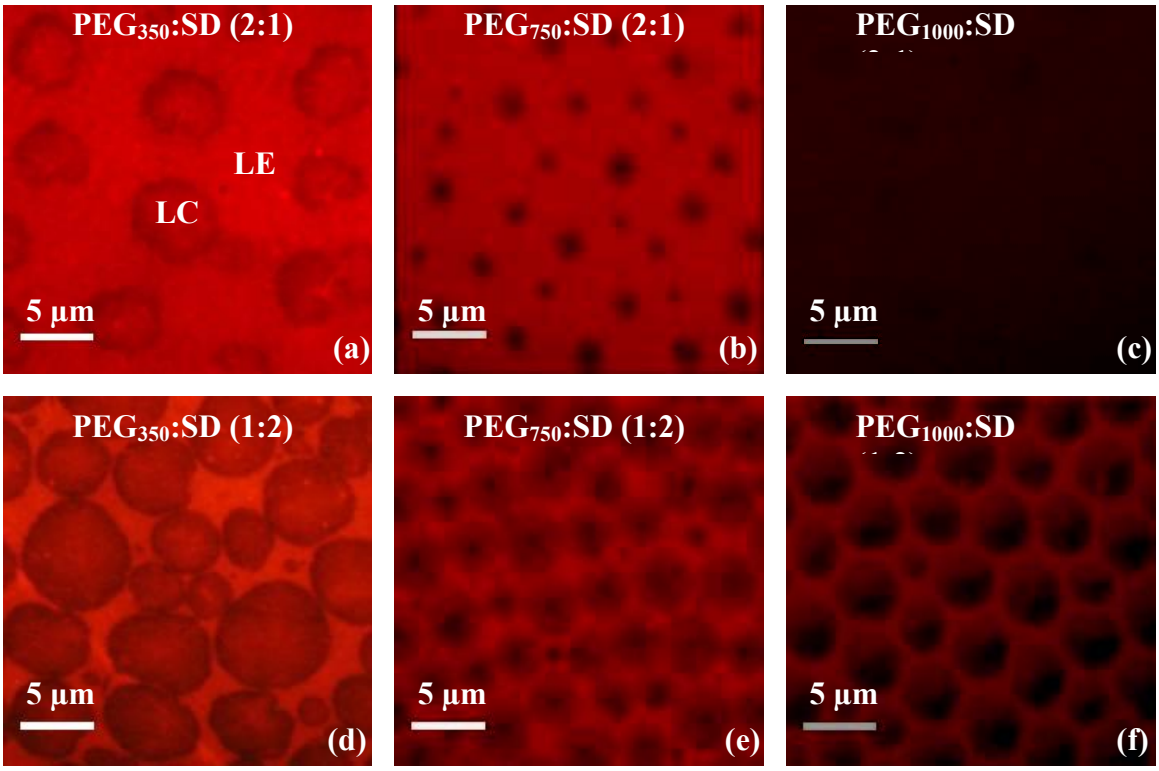

Figure 4.10. (a–f) Fluorescence microscopy analysis of Fluorescent BSA distribution on $PEG_{350/750/1000}$:SD monolayer films (at indicated molar ratios). Films horizontally transferred at 25 mN/m to hydrophobic coverslips.

protein adsorption to the PEG chains and other protein molecules because of lesser steric barrier imparted through smaller chain length PEG lipids. However, as PEG chain length increases, overall protein adsorption to the monolayer film as well as protein adsorption to the LC domain also decreases, demonstrating the significant role played by PEG chain length in reducing non-specific protein adsorption. This is clearly evident from the lower fluorescence intensity of protein on PEG_{1000}:SD (χ_{PEG} = 0.67) (Figure 4.10 (c)) lipid film, where no phase behavior was observed.

Lower protein adsorption to the LC domains and higher adsorption to the LE region of the mixed lipid monolayer films further supports the possibility of localized "mushroom to brush" transition in the monolayer. This phenomena of a localized "mushroom to brush" transition is indicated by AFM microscopy of PEG_{350}:SD (χ_{PEG} = 0.67) (Figure 11). AFM analysis (Figure 4.11 (a) and (b)) illustrates that LC domains are ~ 3.5 nm taller than LE, roughly correspond to PEG_{350} chain (~ 1.5-2.5 nm) extended into brush because 3.5 nm height difference also includes height differences between LC and LE domains (~0.5 nm)[43] and adsorbed protein on LC domains. It is further noted that protein is easily displaced from the LC domain by the AFM tip (Figure 11 (c) and (d)) suggesting that protein is very weakly bound on the LC domains.

Fluorescence microscopy analysis reveals that mixed films of protein repellent DSPE-PEG and protein adsorbing SD lipids with similar molar ratios, but different PEG chain length ($PEG_{350/750/1000}$) dramatically changes phase behavior of the mixed lipid films and thus provides an interesting self-assembly approach of controlling protein patterns via phase behavior of the respective lipid mixtures. Further, our approach presents an unique technique to achieve localized "mushroom to brush" transition as

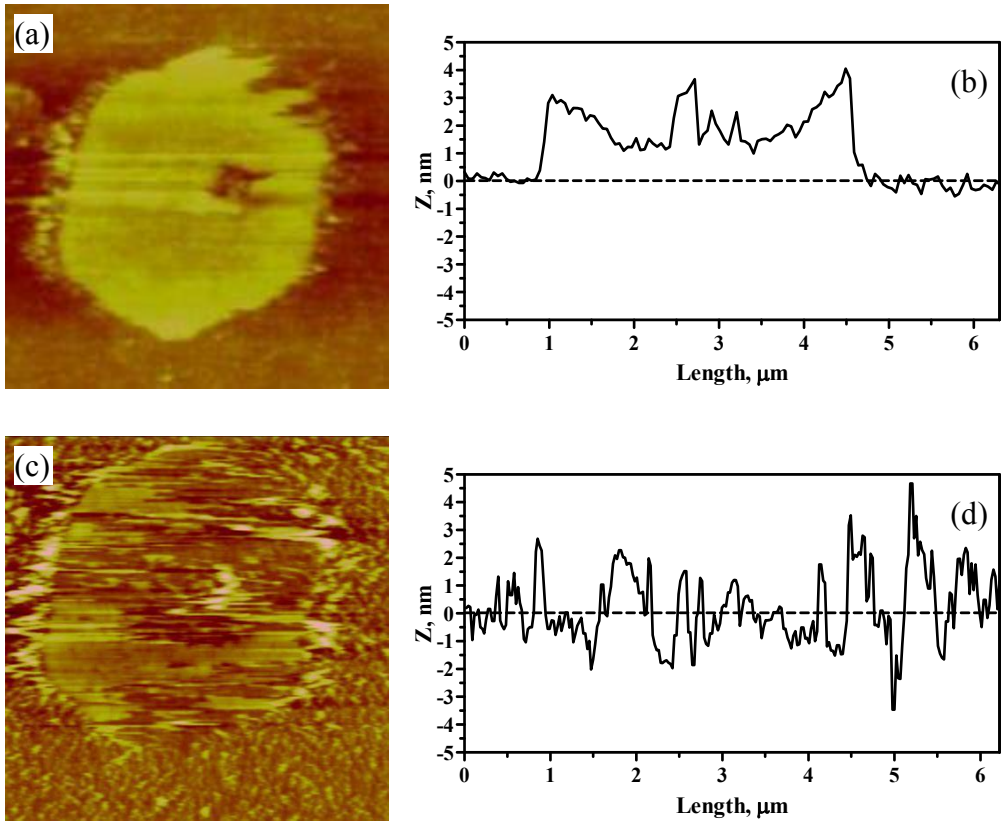

Figure 4.11. AFM analysis of PEG_{350}:SD ($\chi_{PEG} = 0.67$). **(a)** 5 X 5 μm^2 topography image displaying morphology of LC domain and surrounding LE regions. **(b)** Line profile across the image in (a). **(c)** 5 X 5 μm^2 topography image in the similar scan area as the image in (a) displaying that protein is easily displaced from LC domain **(d)** Line profile across the image in (c).

discussed earlier, that is LC domains represents the areas where PEG chains are in tightly packed "brush" state with less protein adsorption as compared to LE regions where PEG chains are less densely packed and may be in "mushroom" or "extended-mushroom" states with more protein adsorption. This outcome of self-assembly approach may serve as an interesting tool for development of protein arrays, protein sensors, etc. Further, SD lipids can be replaced by other protein specific lipids or lipid mixtures to create protein selective surfaces with defined adsorption patterns.

4.5 Conclusion

The miscibility of cationic dioctadecyldimethylammonium bromide (DOMA), nonionic methyl stearate (SME), and PEG bearing phospholipids with different chain length of PEG moiety (DSPE-PEG_{350}, DSPE-PEG_{750}, DSPE-PEG_{1000}) was investigated through surface pressure-area *(π-A)* and surface potential-area (ΔV-A) measurements. Molecular area mixing diagram support a high miscibility of the lipids, revealing a transition from non-additive to additive mixing behavior upon film compression for all lipid mixtures with different PEG chain lengths. Further, detailed miscibility analysis through molecular area and surface potential mixing diagram revealed that PEG chain length has a very profound effect on lipid packing behavior of mixed lipid films at the air/water interface, i.e. at lower PEG lipid concentration ($\chi_{PEG} \leq 0.33$), the packing of lipids is ascribed to headgroup size with roughening of monolayer for bulkier PEG chains ($\geq PEG_{750}$) and alkyl tail packing while at higher PEG lipid concentration ($\chi_{PEG} \geq 0.67$), the packing of lipids is essentially driven through headgroup size and alkyl tail packing for low M.W. PEG chains ($\leq PEG_{350}$) and through polymer chains for high M.W

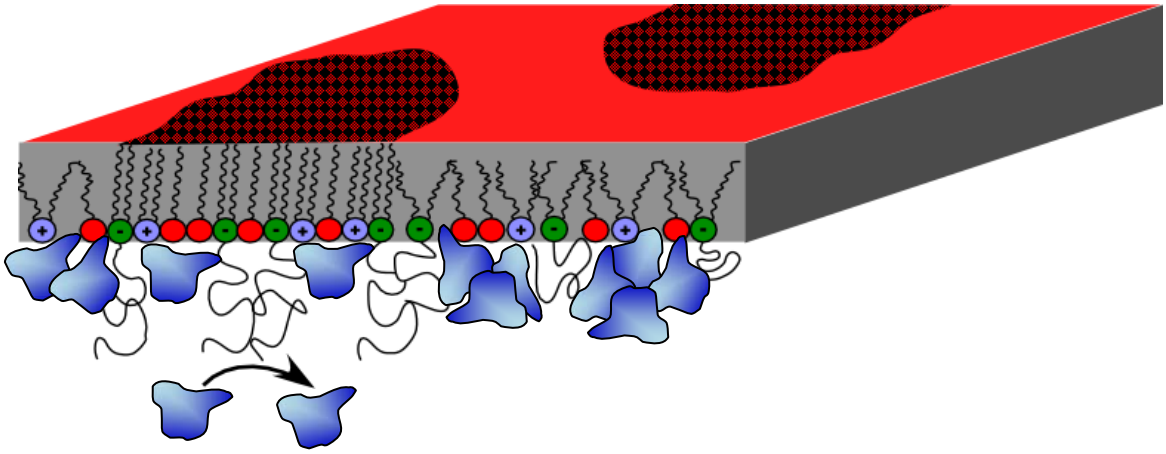

Figure 4.12. Schematic illustration of discrete "mushroom to brush" transition. LC domains shows less protein adsorption with PEG chains in tightly packed "brush" state as compared to LE regions depict high protein adsorption with PEG chain in "mushroom or extended mushroom" state.

PEG chains ($\geq PEG_{750}$) with roughening of the monolayer.

Fluorescence microscopy analysis reveals that mixed films of DSPE-PEG and SD lipids with similar molar ratios, but different PEG chain lengths ($PEG_{350/750/1000}$) dramatically changes phase behavior of the mixed lipid films, i.e., as PEG chain length and mole fraction increases LC domain size decreases and completely disappears for DSPE-PEG_{1000}:SD (χ_{PEG} = 0.67). Further, protein adsorption study revealed that LC domains exhibits diminished protein adsorption while the surrounding LE regions exhibits higher protein adsorption. This variable protein adsorption indicates that LC domains represents the areas where PEG chains are in tightly packed "brush" state as compared to LE regions where PEG chains are less densely packed and may be in "mushroom" or "extended-mushroom" state, which is further supported by AFM analysis. Thus, this self-assembly approach present a unique technique to achieve localized "mushroom to brush" transition (Figure 12) and user defined protein adsorption

patterns.

4.6 References

1. Harris, J. M. ed. *Poly(Ethylene Glycol) Chemistry: Biotechnical and Biomedical Applications.* Plenum Press: New York, 1992; p 485.

2. Sheth, S. R.; Leckband, D. *Proc. Natl. Acad. Sci. U. S. A.* **1997,** 94, (16), 8399-8404.

3. Bosker, W. T. E.; Iakovlev, P. A.; Norde, W.; Stuart, M. A. C. *J. Colloid Interface Sci.* **2005,** 286, (2), 496-503.

4. Hlady, V.; Jogikalmath, G. *Colloid Surf. B-Biointerfaces* **2007,** 54, (2), 179-187.

5. Zhao, H. X.; Dubielecka, P. M.; Soderlund, T.; Kinnunen, P. K. J. *Biophys. J.* **2002,** 83, (2), 954-967.

6. Zhu, B.; Eurell, T.; Gunawan, R.; Leckband, D. *J. Biomed. Mater. Res.* **2001,** 56, (3), 406-416.

7. Efremova, N. V.; Sheth, S. R.; Leckband, D. E. *Langmuir* **2001,** 17, (24), 7628-7636.

8. Desai, N. P.; Hubbell, J. A. *Biomaterials* **1991,** 12, (2), 144-153.

9. Jeon, S. I.; Andrade, J. D. *J. Colloid Interface Sci.* **1991,** 142, (1), 159-166.

10. Jeon, S. I.; Lee, J. H.; Andrade, J. D.; Degennes, P. G. *J. Colloid Interface Sci.* **1991,** 142, (1), 149-158.

11. Needham, D.; McIntosh, T. J.; Lasic, D. D. *Biochim. Biophys. Acta* **1992,** 1108, (1), 40-48.

12. Lee, J. H.; Lee, H. B.; Andrade, J. D. *Prog. Polym. Sci.* **1995,** 20, (6), 1043-1079.

13. Sofia, S. J.; Premnath, V.; Merrill, E. W. *Macromolecules* **1998,** 31, (15), 5059-5070.

14. Leckband, D.; Sheth, S.; Halperin, A. *J. Biomater. Sci.-Polym. Ed.* **1999,** 10, (10), 1125-1147.

15. Bijsterbosch, H. D.; Dehaan, V. O.; Degraaf, A. W.; Mellema, M.; Leermakers, F. A. M.; Stuart, M. A. C.; Vanwell, A. A. *Langmuir* **1995,** 11, (11), 4467-4473.

16. McPherson, T.; Kidane, A.; Szleifer, I.; Park, K. *Langmuir* **1998,** 14, (1), 176-186.

17. Halperin, A. *Langmuir* **1999,** 15, (7), 2525-2533.

18. Currie, E. P. K.; Norde, W.; Stuart, M. A. C. *Adv. Colloid Interface Sci.* **2003,** 100, 205-265.

19. Norde, W.; Gage, D. *Langmuir* **2004,** 20, (10), 4162-4167.

20. Dori, Y.; Bianco-Peled, H.; Satija, S. K.; Fields, G. B.; McCarthy, J. B.; Tirrell, M. *J. Biomed. Mater. Res.* **2000,** 50, (1), 75-81.

21. Blume, G.; Cevc, G. *Biochim. Biophys. Acta* **1990,** 1029, (1), 91-97.

22. Klibanov, A. L.; Maruyama, K.; Torchilin, V. P.; Huang, L. *FEBS Lett.* **1990,** 268, (1), 235-237.

23. Lasic, D. D.; Martin, F. J.; Gabizon, A.; Huang, S. K.; Papahadjopoulos, D. *Biochim. Biophys. Acta* **1991,** 1070, (1), 187-192.

24. Baekmark, T. R.; Elender, G.; Lasic, D. D.; Sackmann, E. *Langmuir* **1995,** 11, (10), 3975-3987.

25. Stelzle, M.; Weissmuller, G.; Sackmann, E. *J. Phys. Chem.* **1993,** 97, (12), 2974-2981.

26. Turner, N. W.; Wright, B. E.; Hlady, V.; Britt, D. W. *J. Colloid Interface Sci.* **2007,** 308, (1), 71-80.

27. Tsukanova, V.; Salesse, C. *J. Phys. Chem. B* **2004,** 108, (30), 10754-10764.

28. Baekmark, T. R.; Wiesenthal, T.; Kuhn, P.; Bayerl, T. M.; Nuyken, O.; Merkel, R. *Langmuir* **1997,** 13, (21), 5521-5523.

29. Majewski, J.; Kuhl, T. L.; Gerstenberg, M. C.; Israelachvili, J. N.; Smith, G. S. *J. Phys. Chem. B* **1997,** 101, (16), 3122-3129.

30. Kuhl, T. L.; Majewski, J.; Wong, J. Y.; Steinberg, S.; Leckband, D. E.; Israelachvili, J. N.; Smith, G. S. *Biophys. J.* **1998,** 75, (5), 2352-2362.

31. Majewski, J.; Kuhl, T. L.; Kjaer, K.; Gerstenberg, M. C.; Als-Nielsen, J.; Israelachvili, J. N.; Smith, G. S. *J. Am. Chem. Soc.* **1998,** 120, (7), 1469-1473.

32. Baekmark, T. R.; Wiesenthal, T.; Kuhn, P.; Albersdorfer, A.; Nuyken, O.; Merkel, R. *Langmuir* **1999,** 15, (10), 3616-3626.

33. Wiesenthal, T.; Baekmark, T. R.; Merkel, R. *Langmuir* **1999,** 15, (20), 6837-6844.

34. Frank, C. W.; Naumann, C. A.; Knoll, W.; Brooks, C. F.; Fuller, G. G. *Macromol. Symp.* **2001,** 166, 1-12.

35. Naumann, C. A.; Brooks, C. F.; Fuller, G. G.; Lehmann, T.; Ruhe, J.; Knoll, W.; Kuhn, P.; Nuyken, O.; Frank, C. W. *Langmuir* **2001,** 17, (9), 2801-2806.

36. Xu, Z.; Holland, N. B.; Marchant, R. E. *Langmuir* **2001,** 17, (2), 377-383.

37. Tsukanova, V.; Salesse, C. *Macromolecules* **2003,** 36, (19), 7227-7235.

38. Ohe, C.; Goto, Y.; Noi, M.; Arai, M.; Kamijo, H.; Itoh, K. *J. Phys. Chem. B* **2007,** 111, (7), 1693-1700.

39. Kuhl, T. L.; Majewski, J.; Alcantar, N.; Hu, Y.; Smith, G.; Israelachvili, J. N. *Biophys. J.* **2000,** 78, (1), 489A-489A.

40. Kuhl, T. L.; Majewski, J.; Howes, P. B.; Kjaer, K.; von Nahmen, A.; Lee, K. Y. C.; Ocko, B.; Israelachvili, J. N.; Smith, G. S. *J. Am. Chem. Soc.* **1999,** 121, (33), 7682-7688.

41. Dhruv, H.; Pepalla, R.; Taveras, M.; Britt, D. W. *Biotechnol. Prog.* **2006,** 22, (1), 150-155.

42. Britt, D. W.; Mobius, D.; Hlady, V. *Phys. Chem. Chem. Phys.* **2000,** 2, (20), 4594-4599.

43. Goodman, T.; Bussmann, E.; Williams, C.; Taveras, M.; Britt, D. *Langmuir* **2004,** 20, (9), 3684-3689.

44. Foreman, M. B.; Coffman, J. P.; Murcia, M. J.; Cesana, S.; Jordan, R.; Smith, G. S.; Naumann, C. A. *Langmuir* **2003,** 19, (2), 326-332.

45. Majewski, J.; Kuhl, T. L.; Wong, J. Y.; Smith, G. S. *Rev. Mol. Biotech.* **2000,** 74, (3), 207-231.

46. Tatsuo, M. *Journal of Polymer Science* **1961,** 55, (161), 215-231.

47. J. L. Koenig, A. C. A. *J. Polym. Sci., Part A-2: Polym. Phys.* **1970,** 8, (10), 1787-1796.

48. Coffman, J. P.; Naumann, C. A. *Macromolecules* **2002,** 35, (5), 1835-1839.

49. Dynarowicz-Latka, P.; Dhanabalan, A.; Oliveira, O. N. *Adv. Colloid Interface Sci.* **2001,** 91, (2), 221-293.

50. Nickolov, Z. S.; Britt, D. W.; Miller, J. D. *J. Phys. Chem. B* **2006,** 110, (31), 15506-15513.

51. Ke, P. C.; Naumann, C. A. *Langmuir* **2001,** 17, (16), 5076-5081.

52. Naumann, C. A.; Knoll, W.; Frank, C. W. *Biomacromolecules* **2001,** 2, (4), 1097-1103.

53. Du, H.; Chandaroy, P.; Hui, S. W. *Biochim. Biophys. Acta-Biomembr.* **1997,** 1326, (2), 236-248.

CHAPTER 5

A FACILE ONE STEP APROACH FOR SYNTHESIS OF HYDROPHILIC AND PROTEIN REPELLENT POLY(DIMETHYLSILOXANE)

5.1 Abstract

Poly(dimethylsiloxane) (PDMS) substrates were modified with block copolymers comprised of poly(ethylene oxide) (PEO) and PDMS segments (PDMS-b-PEO 600) by two methods: (1) the block copolymer was mixed in with the PDMS during polymerization; (2) the block copolymer was allowed to insert into solvent swollen PDMS monoliths. In both cases van der Waals force and hydrophobic interactions between the PDMS monolith and PDMS segments in block copolymers were sufficient to lead to a stable hydrophilic surface, as shown by time dependent contact angle analysis. The surface fraction of PEO on the PDMS surface can be controlled by the cross-linking density of the PDMS matrix and concentration of PEO containing block copolymers used in the modification procedure. Further, surface modification of PDMS substrates with the bulk modification method using a range of PDMS-PEO block copolymers, suggested that surface segregation of the block copolymers is mainly dependent on their molecular weight. Atomic Force Microscopy (AFM) analysis of control and PEO tethered PDMS surfaces reveals a significant increase in surface roughness of bulk modified PDMS substrates. All modified PDMS surfaces exhibited reduced fibrinogen adsorption as compared to controlled PDMS surfaces. Thus, the bulk modification method serves as a very simple, rapid, and cost-effective approach for fabrication of hydrophilic and protein

repellent PDMS elastomer.

5.2 Introduction

Poly(Dimethylsiloxane) (PDMS) is widely used in soft lithography applications,[1-5] microfluidic devices,[6-12] and biological systems[13-16] including blood contacting surfaces.[17-20] PDMS is a choice material given a range of favorable properties, including[7]: (1) low temperature polymerization conditions and low viscosity allowing PDMS to flow into micro-scale patterns on template surfaces; (2) good mechanical properties and tunable elasticity, favoring preservation of micro-scale features imprinted in the PDMS from a master template, allowing applications in microfluidic chips and even facilitated mechanical pumping of fluids within microchannels;[3, 21] (3) high optical transparency down to 280 nm, allowing for applications in bio-analyte detection over a wide range of wavelengths;[9] (4) low biological activity and toxicity, which favors applications in medicine and novel methods such as cell patterning;[10] (5) high gas permeability, necessary for oxygen delivery to growing cells in a closed systems such as a bioreactors.[22]

While the mechanical, optical, and gas transport properties of PDMS are very favorable, the high hydrophobicity of the polymer often limits applications. Complications include: (1) significant non-specific protein adsorption limiting its application in biomedical and biosensor devices;[13] (2) resistance to flow of polar liquids in the microchannels of a microfluidic device;[7] and (3) swelling in presence of organic solvents.[23]

A variety of surface modification strategies have been developed to render the

PDMS surface hydrophilic and protein repellent using hydrophilic polymers, such as poly(ethyleneglycol) (PEG), to increase the applicability of PDMS. Further, these PDMS surface modification strategies can be divided into three broad categories, namely physisorption, covalent modification, and physical entanglement. Surface modification of PDMS with physisorption mainly involves use of charged surfactants[24, 25] and polyelectrolyte multilayers, (PEMs)[26-28] and is driven by hydrophobic interaction and electrostatic force respectively. However, this simple method yields modified PDMS surfaces exhibiting low stability and can only withstand lower shear stress.[7]

Covalent coupling of hydrophilic polymers to the PDMS surface generates stable and desirable surface properties, but it is difficult to achieve because PDMS is chemically inert. Covalent coupling methods for surface modification of PDMS can be generally divided into two classifications known as grafting-from and grafting-to approaches.[29] The grafting-from approach employs active species existing on the PDMS surface to initiate the polymerization of monomers from the surface, while in the case of the grafting-to approach, performed polymer chains carrying reactive groups at the end or the side chains are covalently coupled to the surface. In the grafting-to approach, the first step is generally to render the surface reactive through exposure to oxygen plasma[1] or ultraviolet ozone (UVO)[30, 31] etching, resulting in a glass-like silicate layer with chemically reactive groups (–OH) on the surface. Additional surface modification is achieved via chemical coupling of target molecules to the –OH following standard protocols. However, the underlying glass-like layer remains brittle, limiting its applications where elasticity is required, and has also been found to be unstable when stored in air.[32] In the grafting-from approach of covalent coupling, UV energy has been widely applied for surface graft

polymerization of polymers with the aid of a photoinitiator or photosensitizer.[33-37] Additionally, graft polymerization through exposure to radiation has also been investigated for surface modification of PDMS with hydrophilic polymers.[38, 39] Recently, a novel chemical cross-linking method for functional surface modification of PDMS was described by Wu et al.,[40] where a vinyl terminated initiator was mixed with liquid PDMS prepolymer prior to curing, resulting in an initiator integrated PDMS surface, which can be later utilized for desirable functionalization of PDMS surface using surface initiated–atom transfer radical polymerization (SI–ATRP). However, these covalent coupling methods require multiple reaction steps and are time consuming, which can be costly and inefficient.

The physical entanglement technique presents a very elegant approach for modification of PDMS surfaces. This method takes advantage of PDMS swelling in presence of certain organic solvents. In this approach, the first step is swelling of a cross-linked PDMS monolith in an amphiphilic copolymer (usually with PDMS segment as anchor group) solution, followed by deswelling to embed / anchor the amphiphilic copolymers on the surface of the cross-linked PDMS. When amphiphilic copolymer molecules are tethered, van der Waals force and hydrophobic interactions between the PDMS monolith and PDMS segments in block copolymers lead to a hydrophilic surface; however, we have discovered that the stability of the entangled amphiphile layer when stored in aqueous solutions is rather low. To our knowledge, only two such studies have been reported in the literature utilizing physical entanglement through swelling-deswelling for surface functionalization of PDMS. Han et al.[41] first reported the use of this method to immobilize PDMS-b-PEO molecules on PDMS surface and demonstrated

increased hydrophilicity of PDMS surface. Further, Seo et al.[42] used ABA type block copolymer of poly(2-methacryloyloxyethylphosphorylcholine) (MPC) and PDMS (MPC-PDMS-MPC) to synthesize phosphorylcholine terminated PDMS surfaces via swelling-deswelling protocol and demonstrated significant reduction in protein adsorption as compared to native PDMS surface. They also demonstrated increased hydrophilicity of PDMS surfaces. However, this method is very time consuming and requires an organic solvent such as chloroform to sufficiently swell the PDMS.

Further, a few studies[43-46] have also been reported in the literature where functionalization of the PDMS surface was achieved by bulk modification of PDMS through a premixing method, i.e., addition of the functional molecules to the liquid PDMS prepolymer prior to curing. This premixing method was first utilized by Neys et al.[43] to create catalytic PDMS films with porphyrin doping of the PDMS prepolymer. Further, Zare and coworkers[44] investigated bulk modification of PDMS for protein immobilization on PDMS surface through addition of biotinylated phospholipids (1,2-dioleoyl-sn-glycero-3-phosphoethanolamine-N-(biotinyl) (Bio–DOPE)) to PDMS prepolymer. Zare and coworkers[45] fabricated bulk-modified PDMS microchips by adding a carboxylic acid (undecylenic acid) to the prepolymer prior to curing. This study mainly focused on introducing charged groups to increase the electro osmotic flow (EOF) in PDMS microchannels, which ultimately results in improvement of the separation efficiency and reduction of peak broadening in PDMS microfluidic devices. However, in both studies by Zare et. al. additive doped PDMS showed similar hydrophobicity behavior as native PDMS. Further, in a recent study, Xiao et al.[46] investigated bulk modification of PDMS microchips by addition of an amphiphilic copolymer poly(lactic

acid)-poly(ethyleneglycol) (PLA-PEG) for reducing hydrophobicity as well as the non-specific protein adsorption to PDMS microchannels. They demonstrated that due to the non-ionic nature of the PEG EOF within bulk modified PDMS microchannels was decreased and non-specific protein (myoglobin) adsorption was also reduced drastically owing to excellent protein repellent properties of PEG.

In the present study, we further expand on the bulk modification approach for PDMS surface functionalization by employing copolymers of PDMS and poly(ethyleneoxide) (PEO) as additives in an effort to create protein repellent and hydrophilic PDMS surfaces. Furthermore, use of PDMS-PEO block copolymer offers two significant advantages as compared to other additives that have been explored to date: (1) PDMS-PEO block copolymer additives are highly miscible with the PDMS prepolymer owing to its PDMS segment and (2) van der Waals force and hydrophobic interactions between the PDMS monolith and PDMS segments in block copolymers will lead to a more stable PEO layer on the PDMS surface.

In particular, we have investigated the effectiveness of a low molecular weight amphiphilic block copolymer PDMS-b-PEO (M.W. 600, Polysciences, Inc.) in surface functionalization of PDMS through the bulk modification approach as well as through swelling-deswelling method for comparison. Further, it has been demonstrated through dynamic water contact angle analysis and adsorption of bovine fibrinogen on modified PDMS surfaces that our bulk modification approach serves as a more effective technique for fabrication of hydrophilic and protein repellent PDMS as compared to swelling-deswelling approach. Additionally, in this study we have also investigated the effect of mixing block copolymers of PMDS-PEO with a range of molecular weights and

geometries (mainly AB and ABA type of block copolymers) to PDMS prepolymer before curing and demonstrated that molecular weight, geometry, and composition of these amphiphilic block copolymers dictate the degree of surface segregation and consequently the surface functionalization of PDMS surfaces through the bulk modification approach.

5.3 Experimental

5.3.1 Materials. Sylgard®184, an elastomer PDMS kit containing two parts (polymer base and curing agent) was purchased from Dow Corning. Block copolymers of PDMS and PEO were purchased mainly from Polysciences, Inc. and Gelest, Inc., composition and geometry of which are summarized in Table 5.1. Chloroform (HPLC grade), absolute ethanol and acetone (HPLC grade) were purchased from Sigma-Aldrich. Bovine fibrinogen (≥70% protein basis) was obtained as lyophilized from Sigma Aldrich. Micro BCA assay kit was obtained from Pierce Chemicals for quantifying the amount of adsorbed protein. Standard bovine fibrinogen solution was obtained from Innovative Research, (Novi, MI) and used to construct standard curve in Micro BCA assay for precisely calculating the amount of adsorbed protein.

5.3.2 Preparation of PDMS Monoliths for Swelling-Deswelling Experiments. PDMS monoliths of different cross-linking density were prepared by mixing polymer base and curing agent of Sylgrad® 184 kit in different mass ratios of 5:1, 10:1, and 20:1. The mixtures were then stirred in a glass beaker using a glass rod. Trapped air bubbles resulting from the agitation of the mixture were removed by storing the mixture in a refrigerator for 12 hrs at ≤ 4 ºC (polymerization process of PDMS is strictly temperature dependent and at low temperatures it does not occur). The PDMS monoliths

Table 5.1. Summary of Composition and Geometry of Different PDMS-PEO Amphiphilic Block Copolymers Used.

Block Copolymer	Molecular Weight	% Non-siloxane	Structure	Source
PDMS-b-PEO 600	600	75	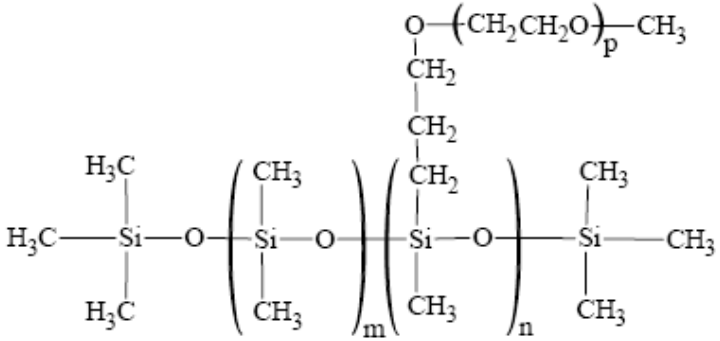	Polysciences, Inc.
PDMS-b-PEO 600 (G)	560-590	60-70		Gelest, Inc.
PDMS-b-PEO 1000	900-1100	80		Gelest, Inc.
PDMS-b-PEO 3000	3000	80		Polysciences, Inc.
PDMS-b-PEO 3000 (G)	2500-3500	50-55		Gelest, Inc.
PDMS-b-PEO 10000	8000-12000	25		Gelest, Inc.
PDMS-b-PEO 5000	4500-5500	85-90	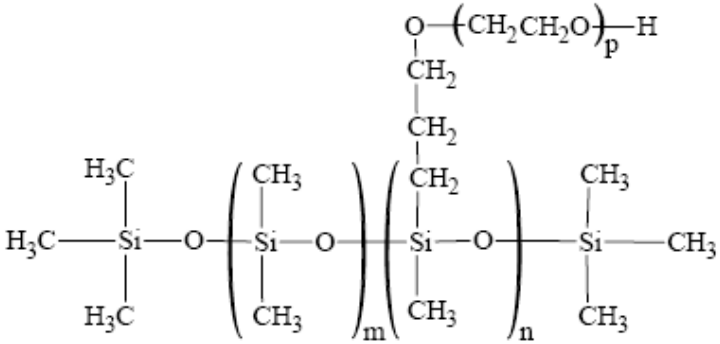	Gelest, Inc.

PDMS-b-PEO 600 (I)	500-700	-*	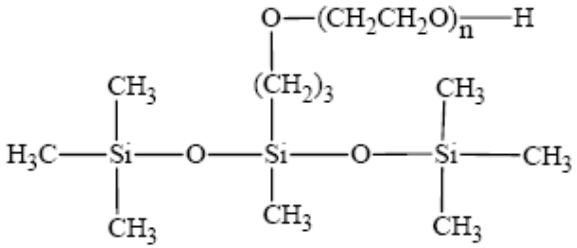	Gelest, Inc.
PDMS-PEO 1000	900-1000	-†	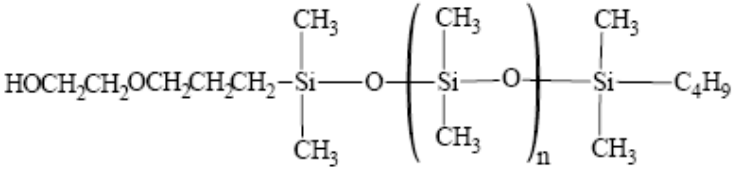	Gelest, Inc.
PEO-PDMS-PEO 4000	3500-4500	60	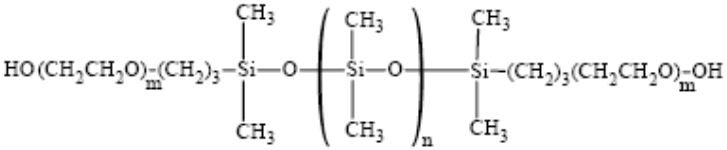	Gelest, Inc.
PEO-PDMS-PEO 1000	1000-1250	-‡		Gelest, Inc.

* PDMS-b-PEO 600 (I) is a symmetric amphiphilic block copolymer, where PDMS chain is composed of just two dimethylsiloxane units.
† PDMS-PEO 1000 contains two ethyleneoxide (EO) units.
‡ PEO-PDMS-PEO 1000 contains two ethyleneoxide (EO) units, i.e. m=1 in structural formula.

were prepared by casting the mixtures into a flat polystyrene Petri dish and cured at 70 ºC for 4 hrs. Subsequently, the PDMS monoliths (~2 mm thick) were cut into pieces of desired size (1.5 cm X 1.5 cm) and used for swelling-deswelling experiments.

5.3.3 Fabrication of PEO Tethered Layer on PDMS Surface by Swelling-Deswelling Method. This method is illustrated in scheme 5.1(a). Briefly, PDMS slabs were first immersed in chloroform solution for 24 hrs to remove residual cross-linker and unreacted monomers, followed by drying under vacuum at about 80 ºC for 12 hrs before any further treatment. These PDMS slabs were immersed in PDMS-b-PEO 600 chloroform solution of desired concentration, i.e. 1%, 2%, 3%, and 5% (V/V), for 5 days to allow the PDMS block of amphiphilic block copolymer to penetrate into the PDMS matrix (Scheme 5.1(a)). Under these conditions, swelling reached equilibrium (until the dimensions of PDMS did not change with time). After removal from the chloroform solution, the PDMS slabs were placed in a vacuum oven at about 80 ºC for 12 hrs to remove the solvent from the PDMS network. Finally, to remove excess or loosely bound PDMS-b-PEO 600 on the surface, the PDMS slabs were sonicated in the chloroform solution for 10 sec. It was then placed in a vacuum oven at about 80 ºC for 12 hrs to remove the residual solvent (Scheme 5.1(a), the dimension of PDMS returned to its original value). Subsequently, the PDMS slabs were rinsed by absolute ethanol for 45 min and allowed to air dry at room temperature. These PDMS slabs were used for further analysis purposes.

5.3.4 Fabrication of PEO Tethered Layer on PDMS Surface by Bulk Mixing Method. This method is illustrated in scheme 5.1(b). Briefly, PDMS polymer base and curing agent of Sylgrad® 184 kit were mixed in mass ratios of 10:1. Desired volume of

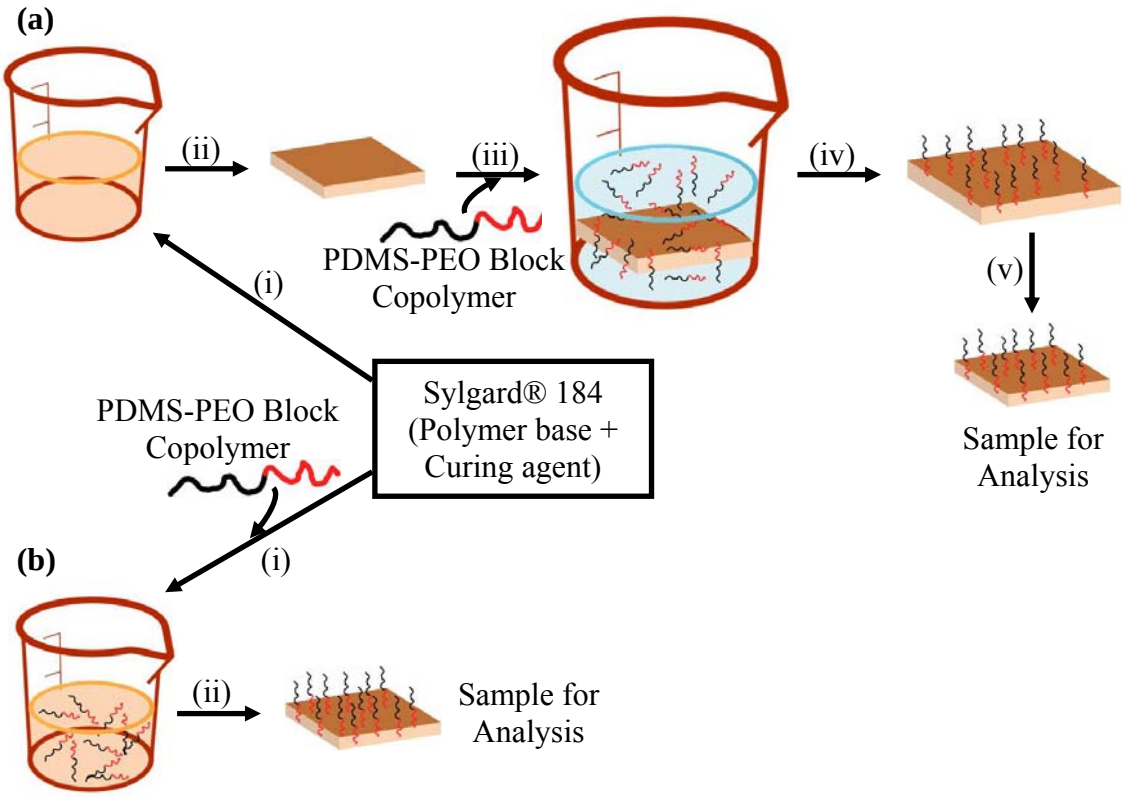

Scheme 5.1. (a) Fabrication of PEO Tethered Layer on PDMS Surface by Swelling-Deswelling Method. (i) Mix Polymer base with curing agent in desired mass ratio of 5:1/10:1/20:1. (ii) Mix thoroughly and remove air bubbles by storing it at temperatures ≤ 4 °C for 12 hrs. Followed by heat curing at 70 °C for 4 hrs. (Cured elastomer slabs were first immersed in chloroform solution for 24 hrs to remove residual cross-linker and unreacted monomers, followed by drying under vacuum at about 80 ºC for 12 hrs before any further treatment). (iii) Immerse the cured elastomer in desired concentration chloroform solution of block copolymer for 5 days. (iv) Remove the swelled elastomer from chloroform solution. (v) Drying in vacuum oven at 80 °C followed by 10 sec sonication in chloroform solution. Further, Drying in vacuum oven at 80 °C again to remove the solvent followed by rinsing with absolute ethanol for 45 min. **(b) Fabrication of PEO Tethered Layer on PDMS Surface by Bulk Mixing Method.** (i) Mix polymer base, curing agent and block copolymer in desired ratio (polymer base and curing agent mixed in mass ration of 10:1) of 10:1:0.1 to 0.5 (1 to 5 %V/W). (ii) Mix thoroughly and remove air bubbles by storing it at temperatures ≤ 4 °C for 12 hrs. Followed by heat curing at 70 °C for 4 hrs.

amphiphilic block copolymer PDMS-b-PEO 600 was then added in the polymer base and curing agent mix to achieve the final concentration of 1%, 2%, 3%, and 5% (V/W) in the mixtures. The mixtures were then stirred in a glass beaker using a glass rod. The trapped air bubbles resulting from the agitation of the mixture were removed by storing the mixture in refrigerator for 12 hrs at ≤ 4 ºC (polymerization process of PDMS is strictly temperature dependent and at low temperatures it does not occur). The block copolymer integrated PDMS monoliths were prepared by casting the mixtures into a flat polystyrene Petri dish and cured at 70 ºC for 4 hrs. Further, all different PDMS-PEO block copolymer integrated PDMS monoliths were prepared in the same way by mixing respective block copolymer at 1% (V/W) concentration in PDMS polymer base and curing agent mix (mass ratio of 10:1). Subsequently, the PDMS monoliths (~2 mm thick) were cut into pieces of desired size (1.5 cm X 1.5 cm) followed by thorough rinsing with acetone. These samples were used for analysis.

5.3.5 Sample Characterization. ***Water Contact Angle.*** The static contact angles of double distilled water droplets at the polymer-air interface were measured at room temperature (RT) using VCA Optima (AST Products, Inc.) system equipped with an autodispenser, video camera, and drop-shape analysis software. A 1 µL droplet of double distilled water was dispensed on PDMS surface and the static contact angles were measured at regular time intervals for 195 seconds (All measurements were performed in triplicate). PDMS surfaces with tethered PDMS-PEO block copolymers represent a dynamic surface where wettability changes very rapidly. Thus, time dependent contact angle analysis serves as a better measure to determine surface properties of such PDMS monoliths.

Optical Density. Optical density of all PDMS samples were determined by measuring absorbance at 400 nm in a 24-well plate with a UV-Vis Spectrophotometer (Multiskan Spectrometer, Thermofisher). All samples were prepared with similar thicknesses (~ 2 mm) and then transferred to 24-well plate for absorbance measurement to avoid any disparity in the data.

Atomic Force Microscopy. A Nanoscope III Bioscope (Digital Instruments, Inc.) was used to image all PDMS surfaces in tapping mode. A tapping mode cantilever BS-TAP300 (Force constant = 40 N/m) was used for imaging all surfaces.

5.3.6 Protein Adsorption. All PDMS samples (in triplicates) were pre-equilibrated in phosphate buffered saline (PBS) (pH 7.4) for 12 hrs before carrying out the protein adsorption experiment. 1 mg/ml Bovine fibrinogen solution was prepared in PBS (pH 7.4) for adsorption studies. Further, pre-equilibrated PDMS samples were immersed inside this protein solution and allowed protein to adsorb for 4 hrs with constant shaking. After 4 hrs of protein adsorption PDMS samples were removed from the protein solution and washed carefully in PBS (pH 7.4) for 15 min twice. Further, all PDMS samples were sonicated in PBS + 1% sodium dodecyl sulfate (SDS) solution for 30 min to desorb protein. This solution was analyzed with Micro-BCA assay for quantifying the amount of adsorbed protein. Standard curve for the Micro-BCA assay was constructed using a commercially available standard bovine fibrinogen solution for accurate determination of protein quantity.

5.4 Results and Discussion

5.4.1 Water Contact Angle Analysis of PEO Tethered PDMS Substrates.

Time dependant contact angle analysis has traditionally been used for determining the swelling behavior in hydrogels[47] and the quality paper materials.[48] However, in these studies, decrease in water contact angle over period of time is mainly attributed to the absorption of water on the surface given the nature of these types of material surfaces. Further, Kasemura and coworkers[49, 50] reported a dynamic contact angle analysis for copolymer films having both hydrophobic and hydrophilic side chains using the Wilhelmy plate technique, and demonstrated the time dependent change in advancing and receding contact angles through varying the dipping velocity of the Wilhelmy plate. They also demonstrated that, time dependent change in advancing and receding contact angle is due to the reorientation of hydrophilic moiety of the copolymer to the polymer/water interface when copolymer film comes in contact with water through XPS analysis of dried and hydrated copolymer films. Further, Ji et al.[51] reported a time dependent static contact angle analysis to determine the surface restructuring of polystyrene-graft-omega-stearyl-poly(ethylene oxide) (PS-g-SPEO) films. Consequently, time dependent contact angle analysis can serve as a useful tool in determining the properties of PDMS surfaces modified with PDMS-PEO block copolymers, which also has hydrophobic and hydrophilic moieties.

Temporal variation in sessile drop water contact angles on PDMS surfaces modified by PDMS-b-PEO 600, prepared through swelling-deswelling and bulk modification methods, are shown in Figure 5.1. As depicted in the data, water contact angle on all modified surfaces decreased significantly over the time of 195 sec as compared to unmodified PDMS surface, except for surfaces of 10:1 cross-linking density PDMS monoliths modified using 1% PDMS-b-PEO 600 through the swelling-deswelling

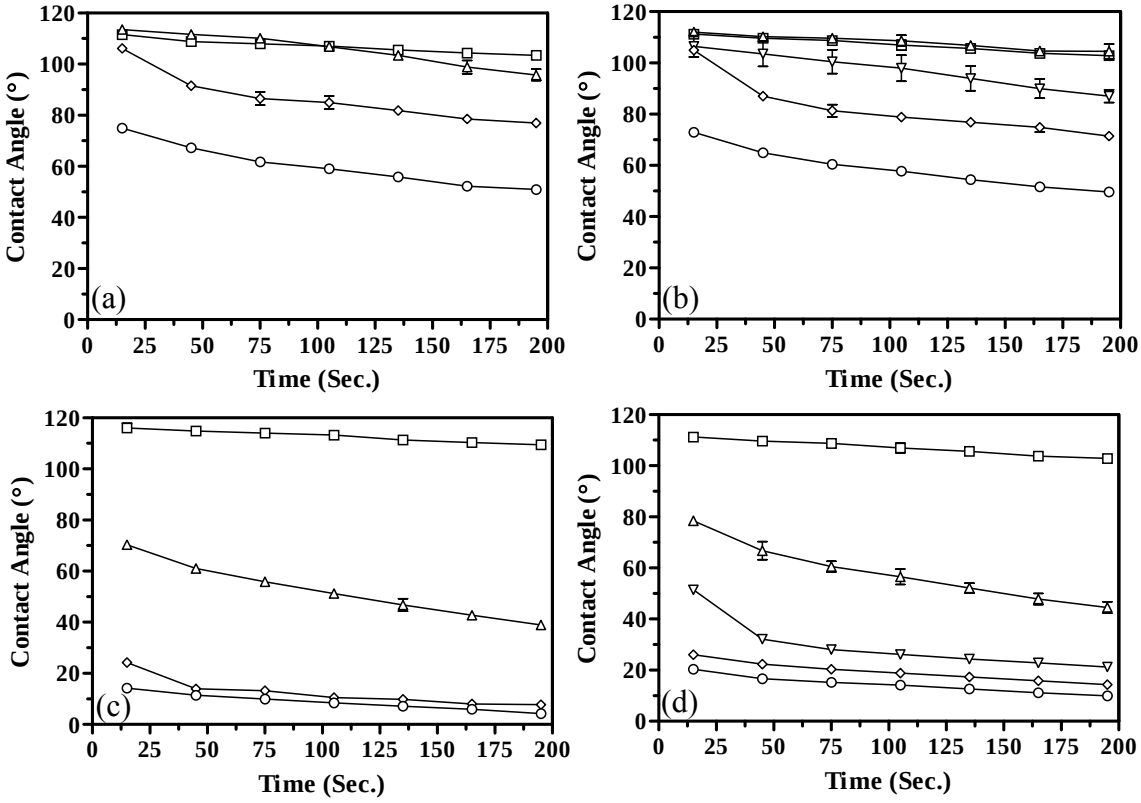

Figure 5.1. Temporal variation in water contact angle behavior on modified PDMS surfaces. (a) 5:1 cross-linking density, (b) 10:1 cross-linking density, and (c) 20:1 cross-linking density PDMS substrates modified through swelling-deswelling method using 1% (–△–), 2% (–▽–), 3% (–◇–), and 5% (–○–) PDMS-b-PEO 600. (d) PDMS substrates modified with bulk mixing method using 1% (–△–), 2% (–▽–), 3% (–◇–), and 5% (–○–) PDMS-b-PEO 600. Open squares (–□–) in all graphs show contact angle behavior on unmodified PDMS substrates. Error bars represent the standard error of mean (n=3).

method. This time dependent change in water contact angle behavior can be attributed to the adsorption and reorientation of the hydrophilic PEO moieties to the polymer surface/water interface to reduce interfacial free energy when a modified PDMS surface comes in contact with water.[49]

Additional evidence for this phenomenon can be obtained from the detailed drop shape analysis. Figure 5.2 illustrates change in water contact angle (Figure 5.2(a)), change in base width (or diameter) of a water droplet (Figure 5.2(b)), and change in volume of a water droplet (Figure 5.2(c)) over the period of 195 sec. for selected samples, i.e. unmodified PDMS (Figure 5.2(d)), 1% PDMS-b-PEO 600 prepared through bulk mixing method (Figure 5.2(e)), and 1% PDMS-b-PEO 600 prepared through swelling-deswelling method on 20:1 cross-linking density PDMS monolith (Figure 5.2(f)). It can be observed from Figure 5.2(c) that the volume of water droplet on unmodified PDMS and modified PDMS surfaces remains similar without any significant differences. However, diameter of the water droplet changes significantly over the period of 195 sec for modified PDMS surface as compared to unmodified PDMS surface, indicates that the water droplet is spreading over the modified PDMS surfaces. This water droplet behavior on modified PDMS surfaces represents the adsorption and reorientation of PEO moieties on the polymer/water interface rather than absorption of water on the polymer surface. This is because change in water contact angle over period of time due to absorption of water will be marked by a substantial decrease in volume with no increase in base diameter of the water droplet.[52]

Further, it is also demonstrated that in surface modification of PDMS monoliths through the swelling-deswelling method, concentration of block copolymer PDMS-b-

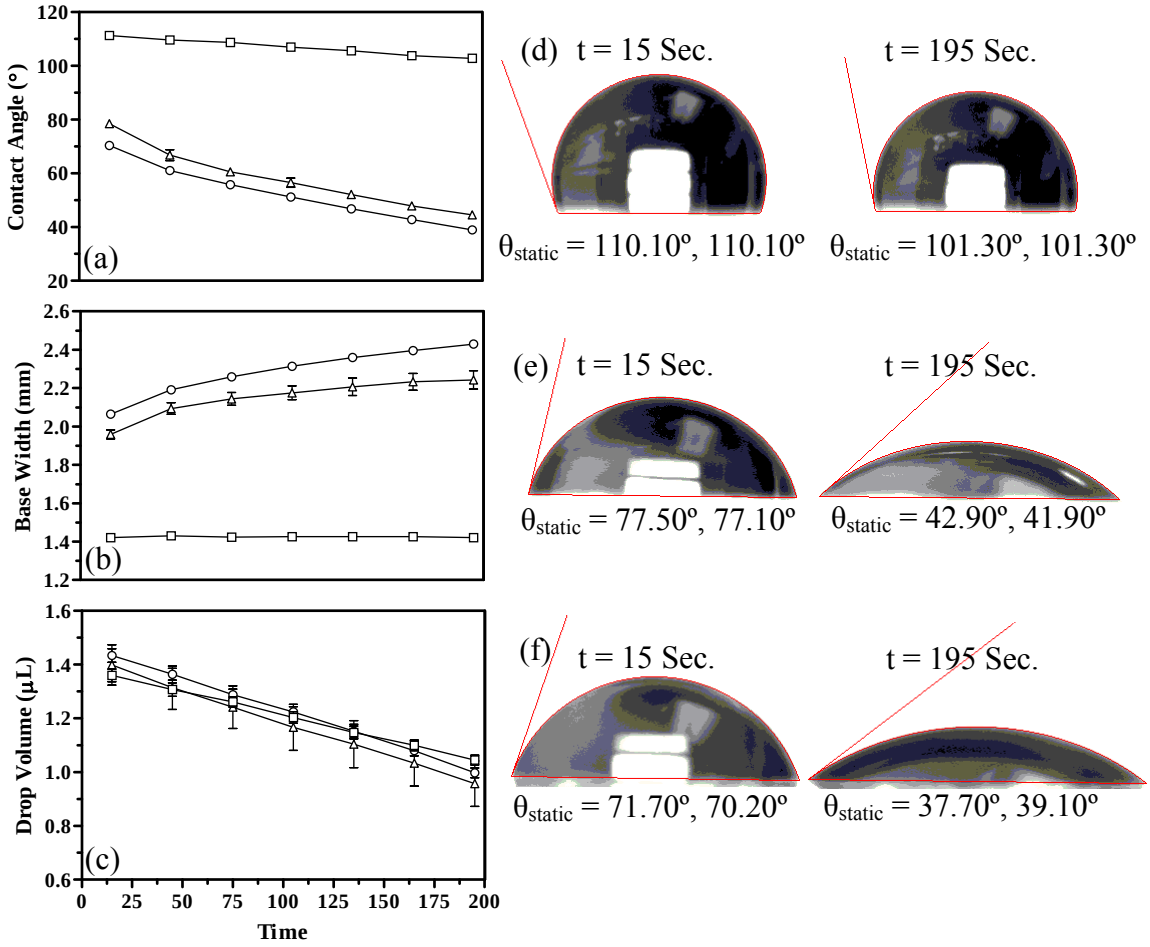

Figure 5.2. Drop shape analysis of water droplet on selected PDMS surfaces, i.e. unmodified PDMS (–□–), bulk modified PDMS using 1% PDMS-b-PEO 600 (–△–), and 20:1 cross-linking density PDMS modified through swelling-deswelling method using 1% PDMS-b-PEO 600 (–○–). Change in (a) water contact angle, (b) base width of a water droplet (droplet diameter), and (c) volume of water droplet over the period of 195 sec are presented. Example images depicting drop shape of (d) unmodified PDMS, (e) bulk modified PDMS using 1% PDMS-b-PEO 600, and (f) 20:1 cross-linking density PDMS modified through swelling-deswelling method using 1% PDMS-b-PEO 600 at t = 15 sec and t = 195 sec. All error bars represent standard error of mean (n=3).

PEO 600 and cross-linking density of PDMS monoliths significantly influences the water contact angle of the surface (Figure 5.1(a) to (c)). The contact angle on modified PDMS substrates decreases as concentration of block copolymer solutions increase and cross-linking density of PDMS monolith decreases indicating higher surface fraction of PEO molecules. It has been previously demonstrated that as cross-linking density of PDMS monoliths decreases, the mean molecular weight of the chain segments (M_c) between the cross-links increases, and thus % swelling in chloroform increases for lower cross-linking density monoliths.[41, 53] This is also because the higher degree of swelling PDMS monoliths with lower cross-linking density allows more block copolymer surfactants to get tethered inside PDMS monolith. Further, increased surface fraction of PEO molecules with increasing PDMS-b-PEO 600 concentration can be explained through higher diffusion of block copolymers in PDMS monoliths at higher concentrations.

Swelling-deswelling experiments with higher molecular weight block copolymer (PEO-PDMS-PEO 4000) at 2% concentration in chloroform solution alters the contact angle behavior of only 20:1 cross-linking density PDMS monoliths and fails to modify 5:1 and 10:1 cross-linking density PDMS substrate surface (Figure 5.3). This finding suggests that higher molecular weight block copolymers cannot diffuse through swelled PDMS monoliths of higher cross-linking density, which demonstrates a lower degree of swelling. It also demonstrates that size of the block copolymers and cross-linking density of PDMS monoliths play a very important role in altering the surface properties of PDMS substrates with the swelling-deswelling method. However, contradictory results were exhibited by Seo et al.,[42] where they successfully modified surface properties of 10:1

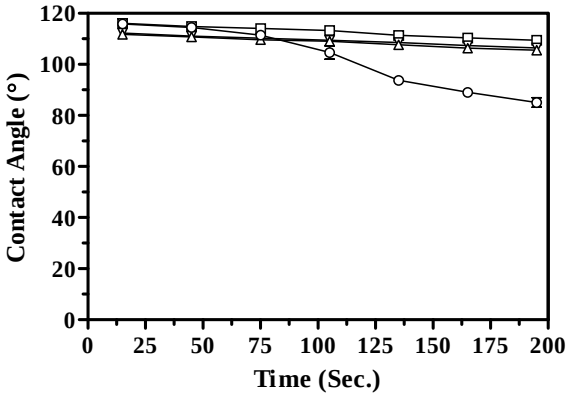

Figure 5.3. Water contact angle behavior on, 5:1 cross-linking density (–▽–), 10:1 cross-linking density (–△–), and 20:1 cross-linking density (–◇–) PDMS surfaces modified through swelling-deswelling method using 2% PEO-PDMS-PEO 4000. pen squares (–□–) show contact angle behavior on unmodified PDMS substrates. Error bars represent the standard error of mean (n=3).

cross-linking density PDMS monoliths with high molecular weight (M_n = 2.5 X 10^4 – 5.4 X 10^4) block copolymers (PMPC-PDMS-PMPC).

Figure 5.1(d) shows the contact angle behavior of PDMS surfaces modified with bulk mixing of PDMS-b-PEO 600 in different concentrations. Initial contact angles at t=195 sec were 43º, 21º, 14º, and 9º for 1%, 2%, 3%, and 5% PDMS-b-PEO 600 modified PDMS surfaces respectively as compared to 101º for unmodified PDMS indicating a highly hydrophilic nature of the modified PDMS surfaces and surface segregation of PDMS-b-PEO 600 block copolymers from bulk PDMS. Further, when compared to PDMS surfaces modified with the swelling-deswelling method, contact angle values at t=195 sec for bulk modified PDMS were significantly lower as compared to 10:1 cross-linking density modified PDMS, i.e. 101º, 86º, 70º, and, 49º for 1%, 2%, 3%, and 5% PDMS-b-PEO 600 (Figure 5.1(b)), and more comparable to 20:1 cross-linking density modified PDMS, i.e. 38º, 8º, and 5º for 1%, 3%, and 5% PDMS-b-PEO 600 (Figure 5.1(c)). However, lower cross-linking density PDMS substrates possess

inferior mechanical properties, which often generate problems in its applications.[53] All bulk modified PDMS samples were prepared with a cross-linking density of 10:1 and it has been established in previous studies that introduction of a low amount (≤ 5% W/W) of additives in PDMS prepolymer mixes cause very limited change in mechanical properties (Young's modulus ~ 2.12 MPa for normal 10:1 PDMS as compared to ~2.05 MPa for PDMS with 5% W/W additive).[40] Further, in one control experiment poly(ethyleneglycol) methacrylate (PEGMA, MW 360) and PEG (MW 400) were used as additives at the concentration of 1% (V/W) to modify surface properties of PDMS and no change in contact angle behavior was observed as compared to unmodified PDMS (data not shown) suggesting significance of PDMS block in surface segregation of block copolymers in PDMS monoliths. Thus, bulk modification of PDMS with PDMS-b-PEO block copolymers presents a rapid, simple, and cost-effective method to fabricate PEO tethered PDMS surfaces.

Once PDMS-b-PEO 600 block copolymer was successfully incorporated in the PDMS for fabrication of hydrophilic PDMS, we investigated a range of block copolymers comprising of PDMS and PEO moieties with different molecular weights and geometries for surface modification of PDMS through the bulk mixing method. All block copolymers were incorporated at a concentration of 1% (V/W) and water contact angle results for these bulk modified PDMS substrates are summarized in Figure 5.4 (1% PDMS-b-PEO 600 results are also included for comparison with other block copolymers). Results are presented in two groups, i.e. block copolymers modified PDMS that exhibited different contact angle behavior as compared to unmodified PDMS (Figure 5.4(a)) and block copolymers modified PDMS that exhibited no difference in contact

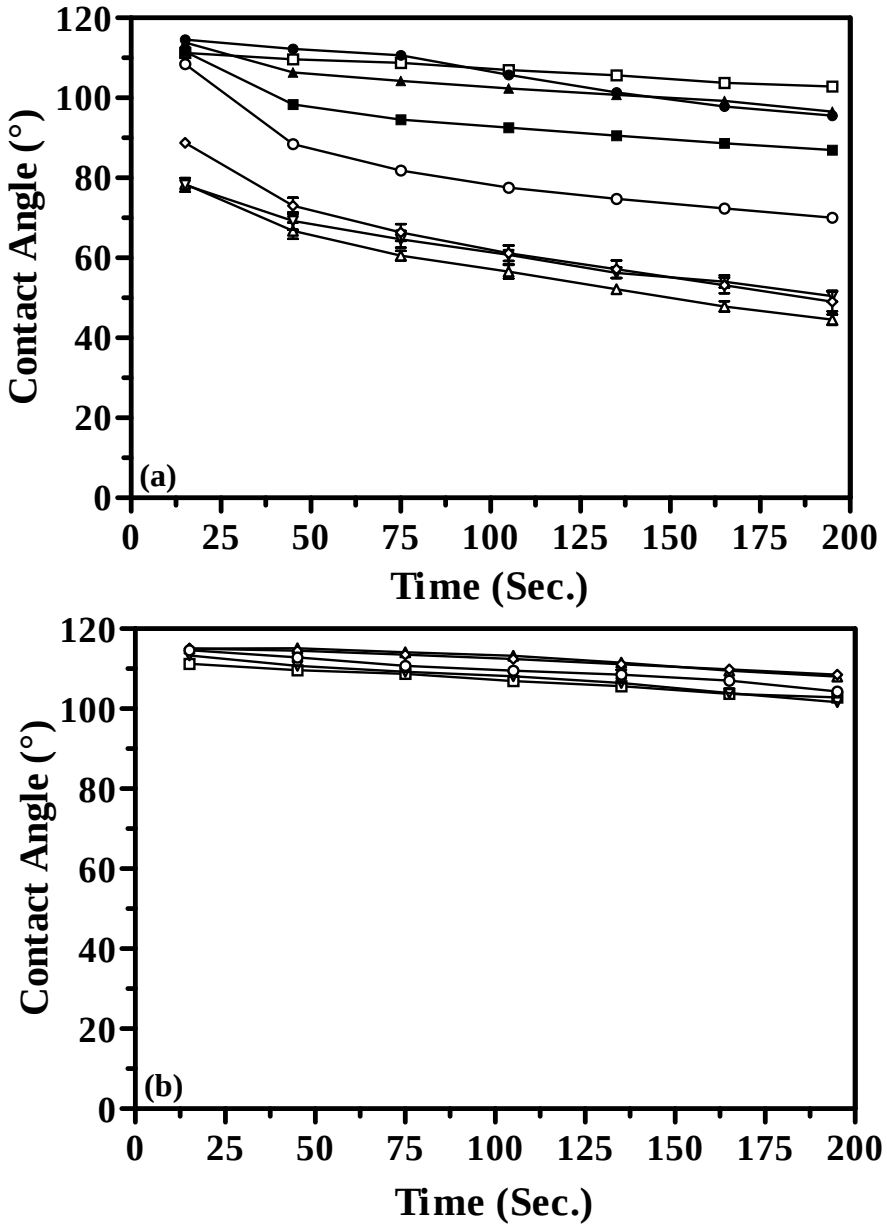

Figure 5.4. Temporal variation in water contact angle behavior on bulk modified PDMS surfaces. (a) PDMS substrates modified using 1% PDMS-b-PEO 600(–△–), 1% PDMS-b-PEO 600 (G) (–▽–), 1% PDMS-b-PEO 600 (I) (–◇–), 1% PDMS-b-PEO 1000 (–○–), 1%PEO-PDMS-PEO 1000 (–■–), 1% PDMS-PEO 1000 (–▲–), and 1% PDMS-b-PEO 3000 (G) (–●–). (b) PDMS substrates modified using 1% PDMS-b-PEO 3000(–△–), 1% PEO-PDMS-PEO 4000 (–▽–), 1% PDMS-b-PEO 5000 (–◇–), and 1% PDMS-b-PEO 10000 (–○–). Open squares (–□–) in all graphs show contact angle behavior on unmodified PDMS substrates. Error bars represent the standard error of mean (n=3).

angle behavior as compared to unmodified PDMS (Figure 5.4(b)), for clarity.

Contact angle behavior of these block copolymers clearly show molecular weight dependence, i.e. block copolymers with high molecular weight (≥ 3000) show similar contact angle behavior as unmodified PDMS (Figure 5.4 (b)). This phenomenon of molecular weight dependence can be explained through either (1) due to the higher molecular weight, block copolymer chains might be entangled with PDMS chains which consequently hinders the diffusion and surface segregation of the block copolymers in PDMS polymer network and entanglement is dependent on molecular weight of the bulk polymer expressed in terms of entanglement molecular weight (M_e)[54] or (2) due to the higher length and molecular weight of PDMS moiety in block copolymer, it is difficult for PEO chains to adsorb and reorient to the polymer/water interface.[49] The former case is anticipated because when the contact angle behavior of PDMS-b-PEO 3000, PDMS-b-PEO 3000 (G), and PDMS-b-PEO 5000 were compared, where molecular weights of PDMS segments are ~600, ~1425, and ~750 respectively, even though PDMS-b-PEO 3000 (G) has the highest molecular weight of PDMS segment, it exhibited lower contact angle, i.e. 95º (Figure 5.4(a)) as compared to PDMS-b-PEO 3000 and PDMS-b-PEO 5000, i.e. 106º and 107º, respectively (Figure 5.4(b)), at t=195 sec indicating surface segregation of PDMS-b-PEO 3000 (G).

It can also be observed that PDMS-b-PEO 1000, PEO-PDMS-PEO 1000, and PDMS-PEO 1000 with similar molecular weights but different geometry and different composition, exhibits different contact angle behavior, i.e. 67º, 85º, and 95º, respectively, at t = 195 sec (Figure 5.4(a)). Lower contact angle for PDMS-b-PEO 1000 as compared to PEO-PDMS-1000 and PDMS-PEO 1000 is attributed to longer PEO chain (~ 17-18

EO units) in PDMS-b-PEO 1000. However, PEO-PDMS-PEO 1000 and PDMS-PEO 1000 both contains 2 EO units but at different positions, i.e. PEO-PDMS-PEO 1000 is functionalized with 1 EO unit at both ends of PDMS anchor chain as compared to PDMS-PEO 1000, is functionalized with 2 EO units at one end of PDMS anchor chain, exhibits different contact angle behavior suggesting that low molecular weight block copolymers terminated with PEO on both ends are more effective in modifying surface properties PDMS as compared to block copolymers terminated with PEO on one end only.

Further, all PDMS-b-PEOs with 600 molecular weight, i.e. PDMS-b-PEO 600, PDMS-b-PEO 600 (G), and PDMS-b-PEO 600 (I), with little differences in their composition (Table 5.1) exhibited similar and very hydrophilic behavior, i.e. water contact angle values of 43º, 46º, and 48º at t=195 sec (Figure 5.4(a)), respectively. Also other block copolymers with higher molecular weight, i.e. PEO-PDMS-PEO 4000 and PDMS-b-PEO 10000, exhibited contact angle behavior similar to unmodified PDMS (Figure 5.4(b)) This behavior further supports the earlier hypothesis of molecular weight dependence, that is low molecular weight block copolymers can easily diffuse through bulk polymer network and surface segregates to fabricate hydrophilic PDMS as compared to high molecular weight block copolymers.

In summary, unusual time dependent water contact angle behavior of PEO tethered PDMS surfaces fabricated through swelling-deswelling method and bulk modification methods can be elucidated through two different molecular events as shown in Figure 5.5: (1) block copolymers containing PDMS and PEO moieties once incorporated inside PDMS substrates orient themselves in such a way so that PDMS

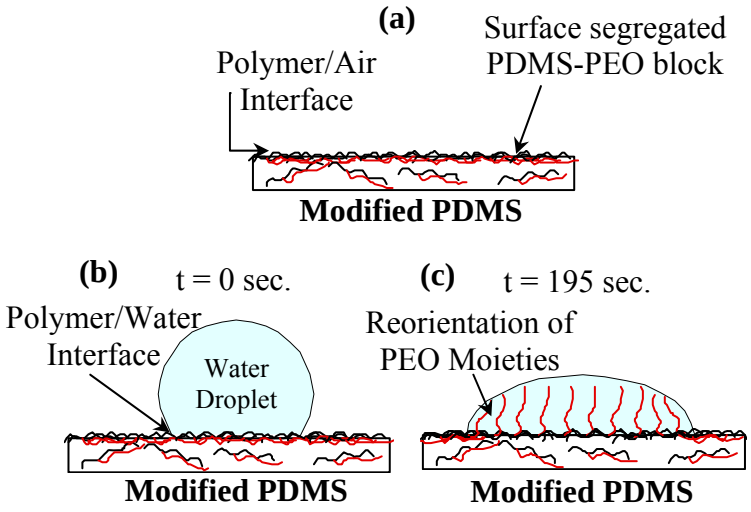

Figure 5.5. Schematic illustration of time dependent water contact angle behavior of PDMS elastomer modified with PDMS-PEO block copolymers. (a) PDMS segment of block copolymer features at the polymer/air interface to minimize the interfacial free energy. (b) Modified PDMS surface comes in contact with water and exhibit hydrophobic behavior. (c) PEO segment of block copolymer adsorb and reorient towards polymer/water interface to minimize the interfacial free energy and reduces the water contact angle over period of time.

block features at the polymer/air interface to minimize the interfacial free energy and (2) when modified PDMS surface comes in contact with water PEO moieties adsorb and reorient towards polymer/water interface to minimize the interfacial free energy.[49]

5.4.2 Optical Density at 400 nm. Optical clarity of the PDMS substrates is one of the most important properties that play a significant role in development of PDMS based microfluidic and bioassay devices. Optical density results of PDMS substrates modified by PDMS-b-PEO 600, prepared through the swelling-deswelling and bulk modification methods, are summarized in Figure 5.6. Water contact angle values at t=195 sec. for each surface are also indicated in Figure 5.6. As observed in the data as PDMS-b-PEO 600 concentration increases absorbance at 400 nm increases. Consequently optical clarity decreases for all modified PDMS substrates. This phenomenon indicates that optical clarity of the modified PDMS substrates is dependent on the PEO concentration

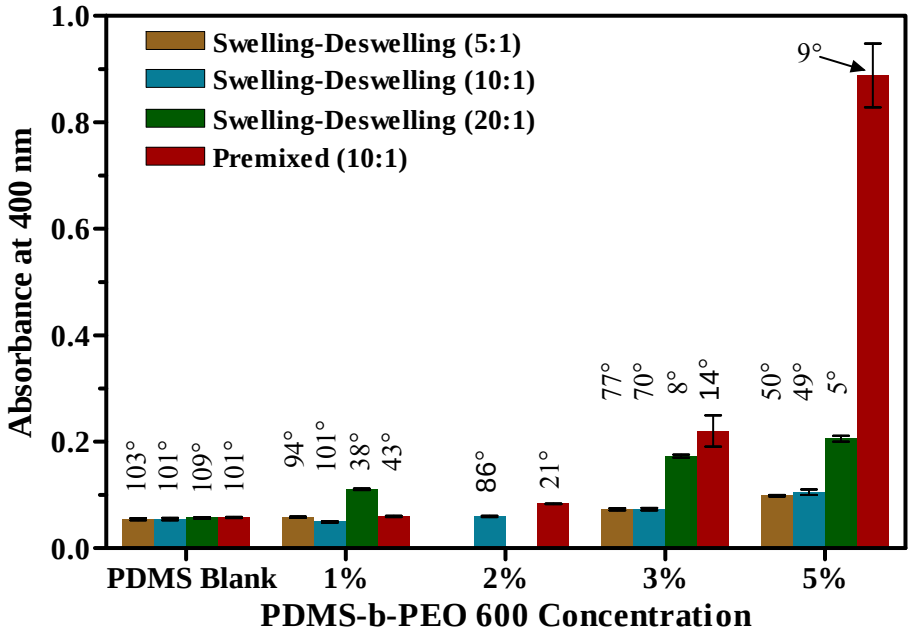

Figure 5.6. Optical density of PDMS substrates modified through swelling-deswelling and bulk mixing methods using PDMS-b-PEO 600 at specified concentration at 400 nm. Values on top of each bar represents water contact angle of respective sample at t = 195 sec. Error bars represent the standard error of mean (n=3). Paired t-test analysis suggested that PDMS substrates prepared with bulk mixing method were significantly different ($P < 0.005$) above 2% PDMS-b-PEO 600 concentration as compared to blank PDMS, while PDMS substrates prepared through swelling-deswelling method were significantly different ($P < 0.005$) above 3% PDMS-b-PEO 600 concentration as compared to blank PDMS.

and as PEO concentration increases, optical clarity of the modified PDMS substrates decreases, because PDMS itself (unmodified PDMS) produces optically very clear elastomers.

PDMS substrate modified with bulk modification method using 1% PDMS-b-PEO 600 exhibits absorbance value (0.060 ± 0.0023) almost identical to unmodified PDMS (0.058 ± 0.0023) with substantial differences in their hydrophilicity, i.e. contact angle of 43º as compared to 101º at t=195 sec. Conversely, PDMS substrates modified with the bulk modification method turn out to be very opaque above 2% PDMS-b-PEO 600 concentration, demonstrated by high absorbance values as compared to unmodified PDMS substrates. Even though these PDMS substrates exhibit very hydrophilic behavior their opaque nature hinders applicability in certain PDMS based microfluidic and bioassay devices. It has been also previously indicated by Xiao et al., where they employed bulk modification of PDMS using PLA-PEG, that above a 2% concentration of PLA-PEG transparency of PDMS microchip decreased and made it difficult to focus laser beam on the microchannels of a separation device.[46]

Optical density results of PDMS substrates modified by different block copolymers comprising of PDMS and PEO moieties prepared through the bulk modification method, are summarized in Figure 5.7 with water contact angle values at t=195 sec. Optical density of bulk modified PDMS substrates with different block copolymers indicate a strong influence of ethyleneoxide (EO) monomers present in a PEO segment of a particular block copolymer used. Optical clarity of modified PDMS substrates was directly proportional to the concentration of incorporated EO units. For example, when absorbance values of two structurally similar block copolymers PDMS-b-

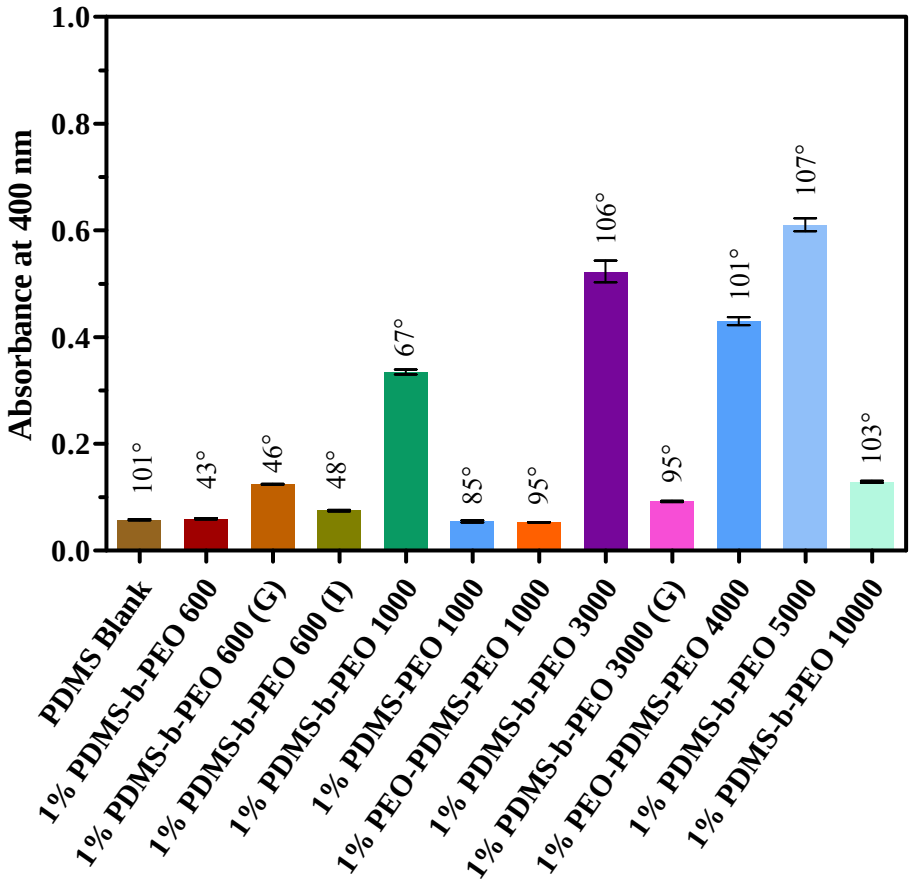

Figure 5.7. Optical density of PDMS substrates modified through bulk mixing method using specified PDMS-PEO block copolymers at 400 nm. Values on top of each bar represents water contact angle of respective sample at t = 195 sec. Error bars represent the standard error of mean (n=3). Paired t-test analysis suggested that PDMS substrates prepared using different block copolymers were significantly different ($P < 0.005$) as compared to blank PDMS except for 1% PDMS-b-PEO 600, 1% PDMS-b-PEO 600 (I), 1% PDMS-PEO 1000, and 1% PEO-PDMS-PEO 1000 ($P > 0.05$).

PEO 3000 and PDMS-b-PEO 3000 (G) were compared, where molecular weights of PEO segments are ~2400 and ~1575, respectively, PDMS-b-PEO 3000 exhibited a higher absorbance value (0.523 ± 0.0351) as compared to PDMS-b-PEO 3000 (G) (0.092 ± 0.0021). A similar type of behavior was observed for high molecular weight block copolymers, i.e. PDMS-b-PEO 5000 (PEO molecular weight ~4250) and PDMS-b-PEO 10000 (PEO molecular weight ~2500) demonstrated absorbance values of 0.610 ± 0.021 and 0.129 ± 0.003, respectively.

5.4.3 Atomic Force Microscopy. Surface topography of all modified and unmodified PDMS substrates were examined through tapping mode AFM. Mean surface roughness for all samples were determined from 25μm X 25μm images and summarized in Table 5.2 and Table 5.3. Table 5.2 lists the surface roughness values for all samples prepared through the swelling-deswelling method and exhibits similar values to the unmodified PDMS samples. However, bulk modified samples exhibit considerably greater surface roughness values as compared to unmodified PDMS substrates (Table 5.3). Further, previous AFM studies of PDMS surfaces modified with PEO have also shown increased mean surface roughness due to surface aggregation of PEO moleculaes.[55]

Surface topography images of unmodified PDMS and bulk modified PDMS with 1%, 2%, 3% and 5% PDMS-b-PEO 600 are presented in Figure 5.8 (Surface topography images of PDMS surfaces modified with swelling-deswelling method are presented in Appendix B). It is evident from these images that surface roughness of modified PDMS substrates changes dramatically at 5% PDMS-b-PEO 600 concentration (35.196 nm) as compared to at 1%, 2%, and 3% PDMS-b-PEO 600 concentration (4.532 nm, 4.414 nm,

Table 5.2. Summary of Mean Surface Roughness for PDMS Substrates Prepared Through Swelling-Deswelling Method.

Block Copolymer	Cross-linking Density	Mean Surface Roughness (Ra) (nm)
Unmodified PDMS	5:1	0.613
	10:1	0.515
	20:1	0.492
1% PDMS-b-PEO 600	5:1	0.557
	10:1	0.745
	20:1	0.685
2% PDMS-b-PEO 600	10:1	0.688
3% PDMS-b-PEO 600	5:1	0.612
	10:1	0.683
	20:1	0.855
5% PDMS-b-PEO 600	5:1	0.721
	10:1	0.838
	20:1	0.622

Table 5.3. Summary of Mean Surface Roughness for PDMS Substrates Prepared Through Bulk Mixing Method.

Block Copolymer	Mean Surface Roughness (Ra) (nm)
Unmodified PDMS	0.515
1% PDMS-b-PEO 600	4.532
2% PDMS-b-PEO 600	4.414
3% PDMS-b-PEO 600	7.006
5% PDMS-b-PEO 600	35.196
1% PDMS-b-PEO 600 (G)	6.117
1% PDMS-b-PEO 600 (I)	3.191
1% PDMS-b-PEO 1000	7.585
1% PDMS-PEO 1000	0.973
1% PEO-PDMS-PEO 1000	1.155
1% PDMS-b-PEO 3000	5.976
1% PDMS-b-PEO 3000 (G)	7.004
1% PEO-PDMS-PEO 4000	3.562
1% PDMS-b-PEO 5000	5.003
1% PDMS-b-PEO 10000	13.039

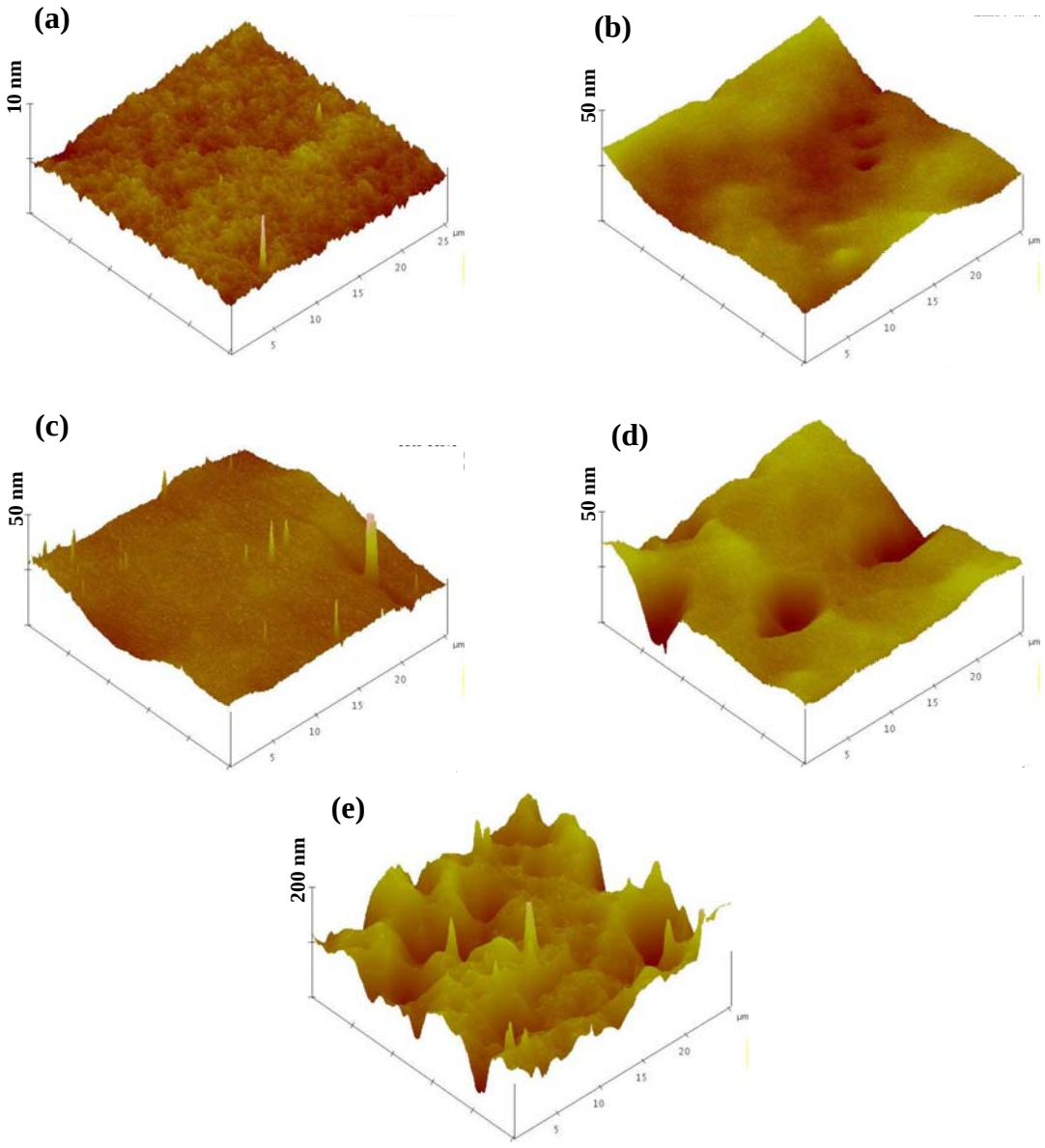

Figure 5.8. AFM images (25 X 25 μm^2) of (a) unmodified PDMS and PDMS substrates modified through bulk mixing method using (b) 1%, (c) 2%, (d) 3%, and (e) 5% PDMS-b-PEO 600. Height scale for all images was adjusted to visualize maximum surface features and is as indicated on the individual image.

and 7.006 nm, respectively) from unmodified PDMS (0.515 nm). It is believed that this increase in the surface roughness is the result of the surface segregation of block copolymers as well as the trapped air bubbles formed during the PDMS fabrication process. Further, when PDMS-b-PEO 600 was mixed in with PDMS prepolymer at 5% concentration for fabricating modified PDMS, flowability of mixture was reduced, and during the mixing process it stabilized a very large amount of air bubbles which got removed during the curing process. It is assumed that this process might have induced such a dramatic increase in surface roughness.

Surface segregation of block copolymers is further supported by the microstructure analysis of unmodified PDMS and bulk modified PDMS substrates (Figure 5.9). Figure 5.9 shows 5 µm X 5 µm topography and phase images of unmodified

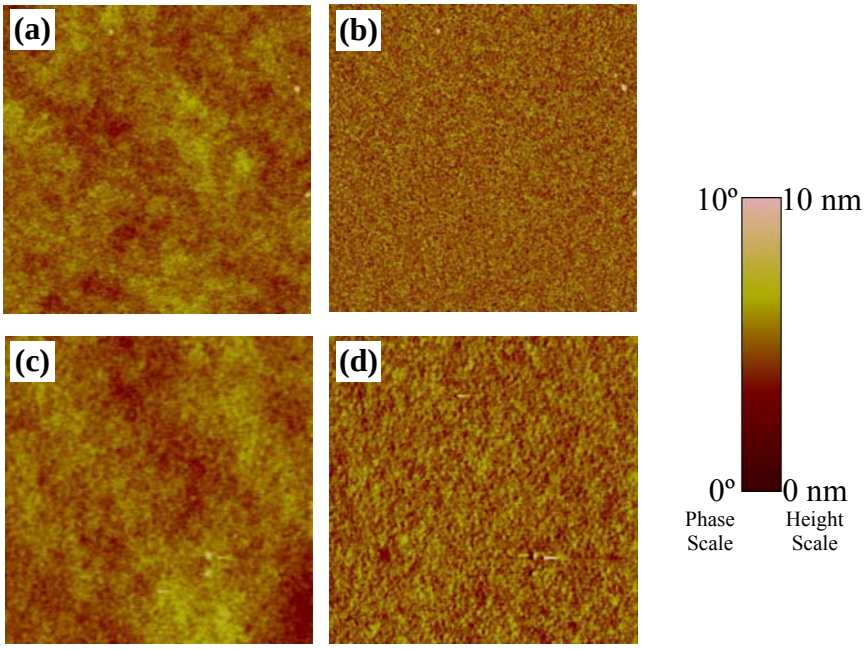

Figure 5.9. (a) Topography and (b) phase AFM images (5 X 5 μm^2) of unmodified PDMS substrates. (c) Topography and (d) phase AFM images (5 X 5 μm^2) of PDMS substrates modified with bulk mixing method using 2% PDMS-b-PEO 600.

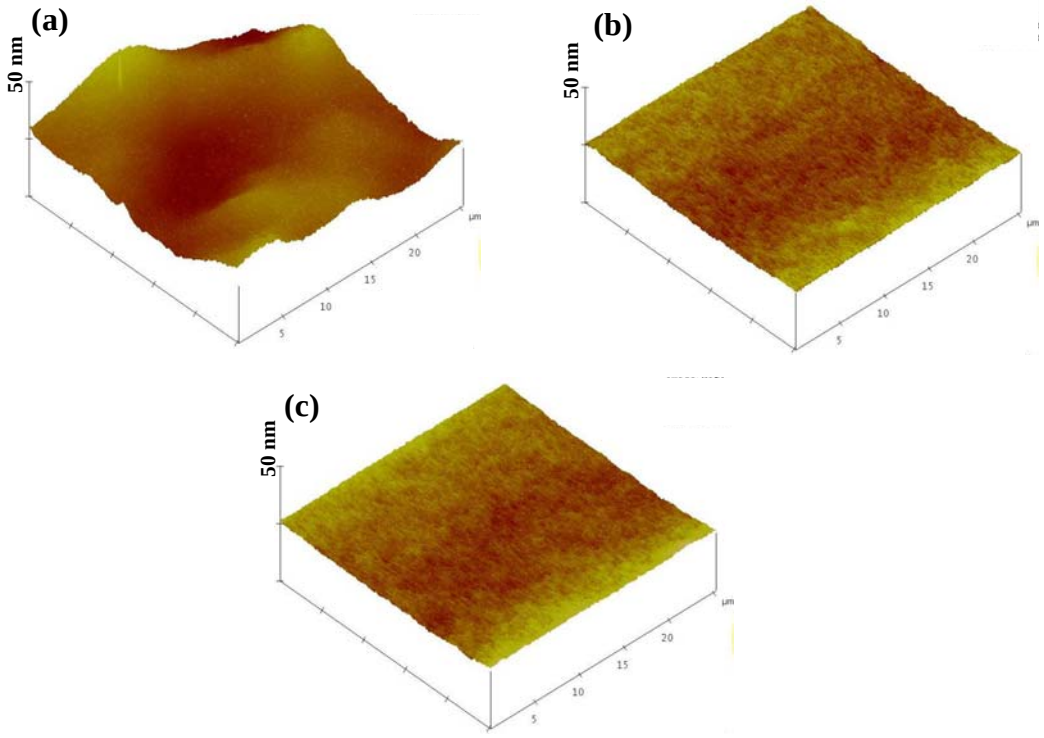

Figure 5.10. AFM images (25 X 25 μm^2) of PDMS substrates modified through bulk mixing method using (a) 1% PDMS-b-PEO 1000, (b) 1% PEO-PDMS-PEO 1000, and (c) 1% PEO-PDMS-PEO 1000.

PDMS and 2% PDMS-b-PEO 600 modified PDMS substrates. As observed in the images 2% PDMS-b-PEO modified PDMS (Figure 5.9 (c) and (d)) exhibits expanded network structure as compared to unmodified PDMS (Figure 5.9 (a) and (b)) indicating surface segregation of additive block copolymers.

Surface topography images of PDMS-b-PEO 1000, PDMS-PEO 1000, and PEO-PDMS-PEO 1000 are presented in Figure 5.10. It is evident from these images that PDMS-b-PEO 1000 exhibits considerably higher surface roughness (7.585 nm) as compared to PDMS-PEO 1000 (0.973 nm) and PEO-PDMS-PEO 1000 (1.155 nm). These differences in surface roughness with a similar molecular weight but different composition suggest that the length of PEO chains of surface segregated block copolymers play a crucial role in changing the surface roughness of modified PDMS.

5.4.4 Protein Adsorption. Surface characterization of modified PDMS substrates exhibited that PEO immobilized through PDMS-PEO block copolymers reorient toward the surface when exposed to an aqueous environment. Further, the ability of PEO tethered layers to impart protein resistance to the underlying substrate surface is well known and well studied in the literature.[56, 57] Thus, the effect of these PEO tethered PDMS surfaces on the adsorption of the plasma protein fibrinogen was investigated. Fibrinogen was selected for adsorption study due to its significance in the processes of coagulation and platelet adhesion with blood contacting biomaterials.

Fibrinogen adsorption behavior on PDMS substrates modified with PDMS-b-PEO 600 through the swelling-deswelling and bulk modification methods are summarized in Figure 5.11. From Figure 5.11 it can be observed that fibrinogen adsorption to the control PDMS surface was high (~ 1 $\mu g/cm^2$) as compared to reduced fibrinogen adsorption to all

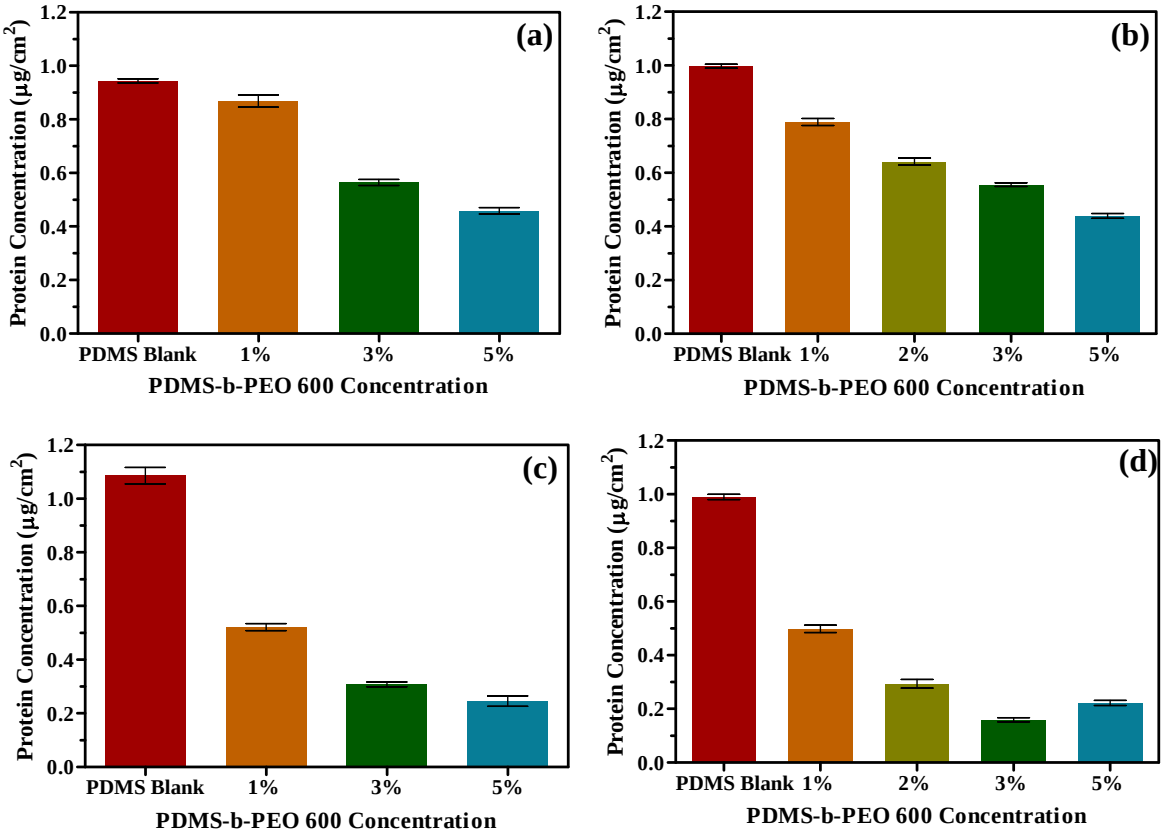

Figure 5.11. Fibrinogen adsorption from buffer on to modified PDMS surfaces. (a) 5:1 cross-linking density, (b) 10:1 cross-linking density, and (c) 20:1 cross-linking density PDMS substrates modified through swelling-deswelling method using specified concentration of PDMS-b-PEO 600. (d) PDMS substrates modified with bulk mixing method using specified concentration of PDMS-b-PEO 600. Error bars represent the standard error of mean (n=3). Paired t-test analysis suggested that protein adsorption to all modified PDMS substrates were significantly different ($P < 0.005$) as compared to blank PDMS. Further, it also revealed that PDMS substrates prepared through bulk mixing method (a) demonstrate significantly lower protein adsorption as compared to 10:1 cross-linking density PDMS substrates prepared through swelling-deswelling method (d) ($P < 0.005$).

modified PDMS substrates. Further, protein adsorption decreased with increasing concentration of PDMS-b-PEO 600 for all modified PDMS substrates, except for 5% PDMS-b-PEO 600 PDMS prepared through bulk mixing method. However, higher protein adsorption to the 5% PDMS-b-PEO modified PDMS is believed to be because of its considerably higher surface roughness (35.196 nm). This behavior of decreasing protein adsorption with increasing PDMS-b-PEO 600 concentration is mainly attributed to the increasing surface density of PEO molecules, which is also supported by contact angle analysis. Further, it has been also demonstrated previously that graft density of PEO molecules play an important role in achieving the optimal protein repellency on the surfaces.[58, 59]

Key findings from comparing the protein adsorption studied to the PDMS substrates modified with the bulk mixing and swelling-deswelling methods using PDMS-b-PEO 600 block copolymers can be summarized as: (1) Bulk modified PDMS substrates are significantly more effective in reducing protein adsorption as compared to 10:1 cross-linking density PDMS monoliths modified with the swelling-deswelling method ($P < 0.005$), i.e. ~50% reduction as compared to ~20% reduction in protein adsorption with bulk modified PDMS at a 1% PDMS-b-PEO 600 concentration level. (2) However, a similar degree of protein repellency can be achieved through the swelling-deswelling method, but through decreasing the cross-linking density of PDMS monoliths, which consequently reduce the mechanical properties of the elastomer. (3) Increasing PDMS-b-PEO 600 concentration reduces level of protein adsorption to the underlying PDMS surface indicating increasing surface density of PEO molecules.

Fibrinogen adsorption behavior on PDMS substrates modified with different

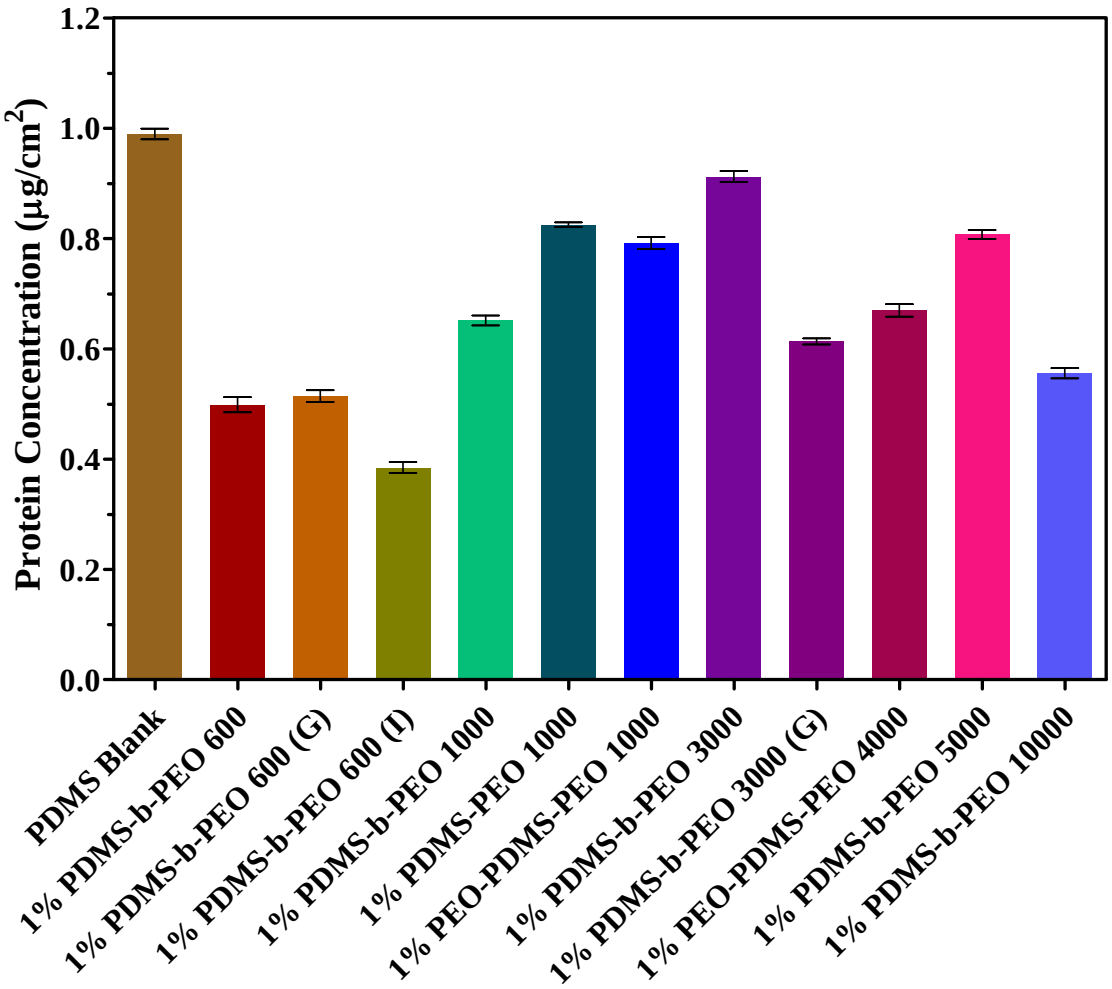

Figure 5.12. Fibrinogen adsorption from buffer on to PDMS substrates modified through bulk mixing method using specified PDMS-PEO block copolymers. Error bars represent the standard error of mean (n=3). Paired t-test analysis suggested that protein adsorption to all modified PDMS substrates were significantly different ($P < 0.005$) as compared to blank PDMS.

PDMS-PEO block copolymers through the bulk mixing method are presented in Figure 5.12. It is clear from Figure 5.12 that 1% PDMS-b-PEO 600 (I) is most effective in reducing fibrinogen adsorption to PDMS surfaces. This reduced protein adsorption as compared to 1% PDMS-b-PEO 600 and 1% PDMS-b-PEO 600 (G) can be attributed to the –OH terminated PEO moiety of the block copolymer as compared to $–CH_3$ terminated PEO moieties in other 600 M.W. block copolymer, which is in good agreement with the previous report that –OH terminated PEO molecules are more effective in repelling protein as compared to $–CH_3$ terminated PEO molecules.[60] Further, 1% PDMS-b-PEO 1000 exhibited lower protein adsorption as compared to PDMS-PEO 1000 and PEO-PDMS-PEO 1000, demonstrating the effectiveness of longer PEO chain length in repelling protein. It is well established in the literature that longer PEO chains are more effective in reducing protein adsorption.[58, 61] Moreover, all modified PDMS substrates with block copolymers of up to 3000 M.W. exhibited protein adsorption behavior in good agreement with their contact angle behavior and surface segregation hypothesis.

However, protein adsorption behaviors of PDMS substrates modified with higher molecular weight block copolymer additives, i.e. PEO-PDMS-PEO 4000, PDMS-b-PEO 5000, and PDMS-b-PEO 10000, are contradictory to their higher contact angle and surface roughness values. For example 1% PDMS-b-PEO 10000 exhibited ~40% reduction in protein adsorption, even though contact angle values (103º at t=195 sec) suggest no surface segregation or reorientation of PEO moieties to the polymer/water interface when it comes in contact with an aqueous environment. Further experimentation is going on for investigation of this unusual protein adsorption behavior exhibited by high

molecular weight block copolymers as a part of future work.

5.5 Conclusion

Hydrophilic and protein repelling PDMS monoliths were successfully prepared by incorporating a small amount of PDMS-PEO block copolymers through a simple one step bulk mixing method. Surface segregation of PDMS-PEO block copolymers was demonstrated through time dependent water contact angle analysis, which also shows the dynamic nature of the PDMS surfaces by exhibiting time dependent reorientation of PEO chains when in contact with an aqueous environment. Modification of PDMS substrates were also investigated through the swelling-deswelling procedure using PDMS-PEO block copolymers, and found to be effective in generating PEO tethered PDMS surfaces. However, the bulk mixing method was found to be more effective, simple, and rapid as compared to the swelling-deswelling method for fabrication of protein repellent hydrophilic PDMS surfaces. Further, bulk modified PDMS surfaces were found to be more stable as compared to PDMS surfaces modified with the swelling-deswelling method when stored under water for 20 days (Appendix C).

The Bulk modification method exhibited a strong reliance on the molecular weight of the block copolymer additive used, i.e. lower molecular weight block copolymers were more effective in segregating at polymer/air interface and modifying surface properties of PDMS as compared to higher molecular weight block copolymers. AFM analysis of bulk modified PDMS surfaces further confirmed the surface segregation of PDMS-PEO block copolymers by exhibiting higher surface roughness and a more expanded network structure. However, AFM analysis also suggests that at higher block

copolymer concentrations, surface roughness of PDMS surfaces increases drastically and also lead to higher protein adsorption. Further, up to ~85% reduction in fibrinogen adsorption was observed by incorporating PDMS-b-PEO 600 at 3% (V/W) concentration as compared to unmodified PDMS surfaces.

5.6 References

1. Xia, Y. N.; Whitesides, G. M. *Annu. Rev. Mater. Sci.* **1998,** 28, 153-184.

2. Xia, Y. N.; Whitesides, G. M. *Angew. Chem., Int. Ed. Engl.* **1998,** 37, (5), 551-575.

3. Quake, S. R.; Scherer, A. *Science* **2000,** 290, (5496), 1536-1540.

4. Huang, Y. G. Y.; Zhou, W. X.; Hsia, K. J.; Menard, E.; Park, J. U.; Rogers, J. A.; Alleyne, A. G. *Langmuir* **2005,** 21, (17), 8058-8068.

5. Lee, T. W.; Jeon, S.; Maria, J.; Zaumseil, J.; Hsu, J. W. P.; Rogers, J. A. *Adv. Funct. Mater.* **2005,** 15, (9), 1435-1439.

6. Lee, J. N.; Park, C.; Whitesides, G. M. *Anal. Chem.* **2003,** 75, (23), 6544-6554.

7. Makamba, H.; Kim, J. H.; Lim, K.; Park, N.; Hahn, J. H. *Electrophoresis* **2003,** 24, (21), 3607-3619.

8. Psaltis, D.; Quake, S. R.; Yang, C. H. *Nature* **2006,** 442, (7101), 381-386.

9. Whitesides, G. M. *Nature* **2006,** 442, (7101), 368-373.

10. El-Ali, J.; Sorger, P. K.; Jensen, K. F. *Nature* **2006,** 442, (7101), 403-411.

11. Huang, B.; Wu, H. K.; Bhaya, D.; Grossman, A.; Granier, S.; Kobilka, B. K.; Zare, R. N. *Science* **2007,** 315, (5808), 81-84.

12. Huang, Y. Y.; Castrataro, P.; Lee, C. C.; Quake, S. R. *Lab Chip* **2007,** 7, (1), 24-26.

13. Bartzoka, V.; McDermott, M. R.; Brook, M. A. *Adv. Mater.* **1999,** 11, (3), 257-+.

14. Abbasi, F.; Mirzadeh, H.; Katbab, A. A. *Polym. Int.* **2001,** 50, (12), 1279-1287.

15. Malpass, C. A.; Millsap, K. W.; Sidhu, H.; Gower, L. B. *J. Biomed. Mater. Res.* **2002,** 63, (6), 822-829.

16. Mata, A.; Fleischman, A. J.; Roy, S. *Biomed. Microdevices* **2005,** 7, (4), 281-293.

17. Chen, K. Y.; Kuo, J. F.; Chen, C. Y. *J. Biomater. Sci.-Polym. Ed.* **1999,** 10, (12), 1183-1205.

18. Belanger, M. C.; Marois, Y. *J. Biomed. Mater. Res.* **2001,** 58, (5), 467-477.

19. Chen, Z.; Ward, R.; Tian, Y.; Malizia, F.; Gracias, D. H.; Shen, Y. R.; Somorjai, G. A. *J. Biomed. Mater. Res.* **2002,** 62, (2), 254-264.

20. Park, J. H.; Bae, Y. H. *Biomaterials* **2002,** 23, (8), 1797-1808.

21. Unger, M. A.; Chou, H. P.; Thorsen, T.; Scherer, A.; Quake, S. R. *Science* **2000,** 288, (5463), 113-116.

22. Boxshall, K.; Wu, M. H.; Cui, Z.; Cui, Z. F.; Watts, J. F.; Baker, M. A. *Surf. Interface Anal.* **2006,** 38, (4), 198-201.

23. Lee, J.; Kim, M. J.; Lee, H. H. *Langmuir* **2006,** 22, (5), 2090-2095.

24. Ocvirk, G.; Munroe, M.; Tang, T.; Oleschuk, R.; Westra, K.; Harrison, D. J. *Electrophoresis* **2000,** 21, (1), 107-115.

25. Dou, Y. H.; Bao, N.; Xu, J. J.; Chen, H. Y. *Electrophoresis* **2002,** 23, (20), 3558-3566.

26. Decher, G.; Hong, J. D.; Schmitt, J. *Thin Solid Films* **1992,** 210, (1-2), 831-835.

27. Decher, G.; Lvov, Y.; Schmitt, J. *Thin Solid Films* **1994,** 244, (1-2), 772-777.

28. Decher, G. *Science* **1997,** 277, (5330), 1232-1237.

29. Hu, S. W.; Brittain, W. J. *Macromolecules* **2005,** 38, (15), 6592-6597.

30. Efimenko, K.; Wallace, W. E.; Genzer, J. *J. Colloid Interface Sci.* **2002,** 254, (2), 306-315.

31. Schnyder, B.; Lippert, T.; Kotz, R.; Wokaun, A.; Graubner, V. M.; Nuyken, O. *Surf. Sci.* **2003,** 532, 1067-1071.

32. Olah, A.; Hillborg, H.; Vancso, G. J. *Appl. Surf. Sci.* **2005,** 239, (3-4), 410-423.

33. Hu, S. W.; Ren, X. Q.; Bachman, M.; Sims, C. E.; Li, G. P.; Allbritton, N. *Anal. Chem.* **2002,** 74, (16), 4117-4123.

34. Hu, S. W.; Ren, X. Q.; Bachman, M.; Sims, C. E.; Li, G. P.; Allbritton, N. L. *Langmuir* **2004,** 20, (13), 5569-5574.

35. Hu, S. W.; Ren, X. Q.; Bachman, M.; Sims, C. E.; Li, G. P.; Allbritton, N. L. *Anal. Chem.* **2004,** 76, (7), 1865-1870.

36. Wang, Y. L.; Lai, H. H.; Bachman, M.; Sims, C. E.; Li, G. P.; Allbritton, N. L. *Anal. Chem.* **2005,** 77, (23), 7539-7546.

37. Patrito, N.; McCague, C.; Chiang, S.; Norton, P. R.; Petersen, N. O. *Langmuir* **2006,** 22, (8), 3453-3455.

38. He, Q. G.; Liu, Z. C.; Xiao, P. F.; Liang, R. Q.; He, N. Y.; Lu, Z. H. *Langmuir* **2003,** 19, (17), 6982-6986.

39. Barbier, V.; Tatoulian, M.; Li, H.; Arefi-Khonsari, F.; Ajdari, A.; Tabeling, P. *Langmuir* **2006,** 22, (12), 5230-5232.

40. Wu, Y. Z.; Huang, Y. Y.; Ma, H. W. *J. Am. Chem. Soc.* **2007,** 129, (23), 7226-+.

41. Yu, K.; Han, Y. C. *Soft Matter* **2006,** 2, (8), 705-709.

42. Seo, J. H.; Matsuno, R.; Konno, T.; Takai, M.; Ishihara, K. *Biomaterials* **2008,** 29, (10), 1367-1376.

43. Neys, P. E. F.; Severeyns, A.; Vankelecom, I. F. J.; Ceulemans, E.; Dehaen, W.; Jacobs, P. A. *J. Mol. Catal. A-Chem.* **1999,** 144, (2), 373-377.

44. Huang, B.; Wu, H. K.; Kim, S.; Kobilka, B. K.; Zare, R. N. *Lab Chip* **2006,** 6, (3), 369-373.

45. Luo, Y. Q.; Huang, B.; Wu, H.; Zare, R. N. *Anal. Chem.* **2006,** 78, (13), 4588-4592.

46. Xiao, Y.; Yu, X. D.; Xu, J. J.; Chen, H. Y. *Electrophoresis* **2007,** 28, (18), 3302-3307.

47. Vladkova, T. *J. Appl. Polym. Sci.* **2004,** 92, (3), 1486-1492.

48. Strom, G.; Carlsson, G. *J. Adhes. Sci. Technol.* **1992,** 6, (6), 745-761.

49. Kasemura, T.; Takahashi, S.; Okada, T.; Maegawa, T.; Oshibe, T.; Nakamura, T. *J. Adhes.* **1996,** 59, (1-4), 61-74.

50. Takahashi, S.; Kasemura, T.; Asano, K. *Polymer* **1997,** 38, (9), 2107-2111.

51. Ji, J.; Feng, L. X.; Qiu, Y. X.; Yu, X. J.; Barbosa, M. A. *J. Colloid Interface Sci.* **2000,** 224, (2), 255-260.

52. Standard Test Method for Surface Wettability and Absorbency of Sheeted Materials Using an Automated Contact Angle Tester (ASTM D5725-99). In 1999.

53. Schmid, H.; Michel, B. *Macromolecules* **2000,** 33, (8), 3042-3049.

54. Hutchings, L. R.; Narrianen, A. P.; Thompson, R. L.; Clarke, N.; Ansari, L. *Polym. Int.* **2008,** 57, (2), 163-170.

55. Chen, H.; Brook, M. A.; Sheardown, H. *Biomaterials* **2004,** 25, (12), 2273-2282.

56. Harris, J. M. ed. *Poly(Ethylene Glycol) Chemistry: Biotechnical and Biomedical Applications.* Plenum Press: New York, 1992; p 485.

57. Morra, M. *J. Biomater. Sci.-Polym. Ed.* **2000,** 11, (6), 547-569.

58. Szleifer, I. *Physica A* **1997,** 244, (1-4), 370-388.

59. Hlady, V.; Jogikalmath, G. *Colloid Surf. B-Biointerfaces* **2007,** 54, (2), 179-187.

60. Prime, K. L.; Whitesides, G. M. *J. Am. Chem. Soc.* **1993,** 115, (23), 10714-10721.

61. Halperin, A. *Langmuir* **1999,** 15, (7), 2525-2533.

CHAPTER 6

CONCLUSIONS AND FUTURE DIRECTIONS

6.1 Overview

Key findings of this dissertation work will be summarized in the first part of the chapter. The second part is the author's vision of the next research steps worthy of investigating for development of novel biosensor platforms based on the techniques that have been used in this dissertation work.

6.2 Key Findings

In this work, two different platforms were used for immobilizing protein repellent PEG/PEO molecules on surfaces for controlling non-specific adsorption of proteins. In the first approach, the Langmuir monolayer technique was investigated for fabrication of PEGylated surfaces with the help of PEG bearing lipids, while in the other approach the physical entaglement technique was investigated for immobilizing PEO molecules on PDMS— a widely used organic polymer.

In the first investigation, it was demonstrated that PEG bearing lipids (DSPE-PEG350) can be successfully introduced to neutral SME/cationic DOMA (SD) lipid mixtures at the air/water interface to reduce protein-protein interactions and define single protein binding sites on the monolayer. Here, the intrinsic inertness of the PEG brush layer in the mixed lipid monolayer reduces the nonspecific adsorption of proteins to the monolayer, while the SME and DOMA headgroups define favorable binding sites for adsorption of ferritin. Further, Atomic Force Microscopy (AFM) analysis revealed that

ferritin adsorption induces local restructuring of the fluid monolayer, resulting in the creation of protein-sized binding pockets, the dimensions of which can be fine-tuned by changing the molar ratios of the lipids.

While in the first study the Langmuir monolayer approach was investigated as a means of inducing protein-specific binding pockets or imprints in lipids monolayer with reduced non-specific protein adsorption, in the follow-up study, multi-component Langmuir monolayers comprised of protein binding lipids (SD) dispersed in a matrix of protein-repellent PEG-bearing lipids with varying PEG chain lengths were investigated for the development of a generic platform for protein patterning/detection. Fluorescence microscopy analysis revealed that mixed films of DSPE-PEG and SD lipids with similar molar ratios but different PEG chain lengths, ($PEG_{350/750/1000}$) dramatically change the phase behavior of the mixed lipid films, i.e., as PEG chain length and mole fraction increases LC domain size decreases and completely disappears for DSPE-PEG_{1000}:SD (χ_{PEG} = 0.67). Further, the protein adsorption study revealed that LC domains exhibit diminished protein adsorption while the surrounding LE regions exhibit higher protein adsorption. Thus, this self-assembly approach presents a unique technique to achieve user-defined protein adsorption patterns, and protein binding SD lipids can be replaced with specific protein binding lipids to generate specific protein patterns with reduced non-specific adsorption due to the presence of an inert PEG lipid matrix.

In the first two studies, the Langmuir monolayer technique was utilized for fabricating protein imprints as well as for generating user defined protein patterns. However, given the complication and cleanliness requirements for use of Langmuir techniques, its industrial applications have been very limited. Thus, as a final element of

this dissertation, a simple one-step method was developed for the surface modification of PDMS, a widely used medical polymer with protein repellent PEO molecules. With the help of time dependent water contact angle analysis it was demonstrated that low molecular weight block copolymers comprising of PDMS and PEO moieties can segregate on the surface if mixed in with the PDMS prepolymer before the polymerization process and generate a hydrophilic PDMS surface. Further, fibrinogen adsorption studies revealed that PEO tethered PDMS surfaces greatly reduce the non-specific adsorption of proteins as compared to controlled PDMS surfaces.

6.3 Future Directions

6.3.1 Langmuir Monolayers for Molecular Imprinting of Proteins. It was demonstrated in this dissertation that the Langmuir monolayer approach can be developed in to a powerful two-dimensional protein imprinting platform. Based on this finding our collaborators investigated formation of protein molecular imprints within Langmuir monolayers of PEG350:SME:DOMA lipid mixtures using Quartz Crystal Microbalance (QCM).[1] However, their findings suggested that only modest selectivity for protein binding to the resulting surfaces can be achieved, attributed to the lower steric barrier imparted by the smaller PEG chain length (M.W. 350 daltons). Further, it has been demonstrated in this dissertation that longer PEG chain length bearing lipids can lead to a better steric barrier, and thus, use of longer PEG chain length lipids (PEG750/PEG1000) may lead to a more effective molecular imprinting of protein with higher selectivity.

Also demonstrated is that specificity of imprint sites were highly dependent on the

size of proteins, i.e. when protein imprints generated with ferritin (M.W. ~450 kD) were challenged with bovine serum albumin (BSA) (M.W. ~ 66 kD), imprinted surfaces demonstrated a greater affinity for BSA as compared to ferritin.[1] To overcome this problem use of lipopolymers or lipids that carry specific recognition elements (analogues to functional monomer in molecular imprinting technology) will serve as a development for a more robust molecular imprinting technology through the Langmuir monolayer approach. One such example is iminodiacetate (IDA) lipids with divalent metal ions, which (Cu^{2+} or Ni^{2+}) can be used for targeting proteins with surface accessible histidine residues using metal ion coordination chemistry.[2-4] Further, based on the recent work and given the high specificity of RNA aptamers (30 to 100 nucleotide units) for proteins[5, 6] novel lipopolymers can be synthesized carrying RNA aptamer at the lipid head group end and may serve as a very robust methodology for development of Langmuir monolayer based molecular imprinting of proteins.

6.3.2 PDMS Bulk Mixing Method for Development of Protein Microarrays and Biosensors. It was demonstrated in the final part of this dissertation work that bulk mixing of low molecular weight block copolymers containing PDMS anchor chains can be successfully used for surface modification of PDMS elastomers. However, due to the physical entanglement of block copolymers alone, stability of these modified PDMS surfaces was limited under aqueous environments. Further, use of low molecular weight block copolymers with a vinyl terminated PDMS anchor chain as an additive can lead to a more stable, modified PDMS surface by taking part in the PDMS polymerization process and getting covalently attached to the PDMS network. This technique can be further applied for modification of PDMS surfaces with reactive functionalities such as –

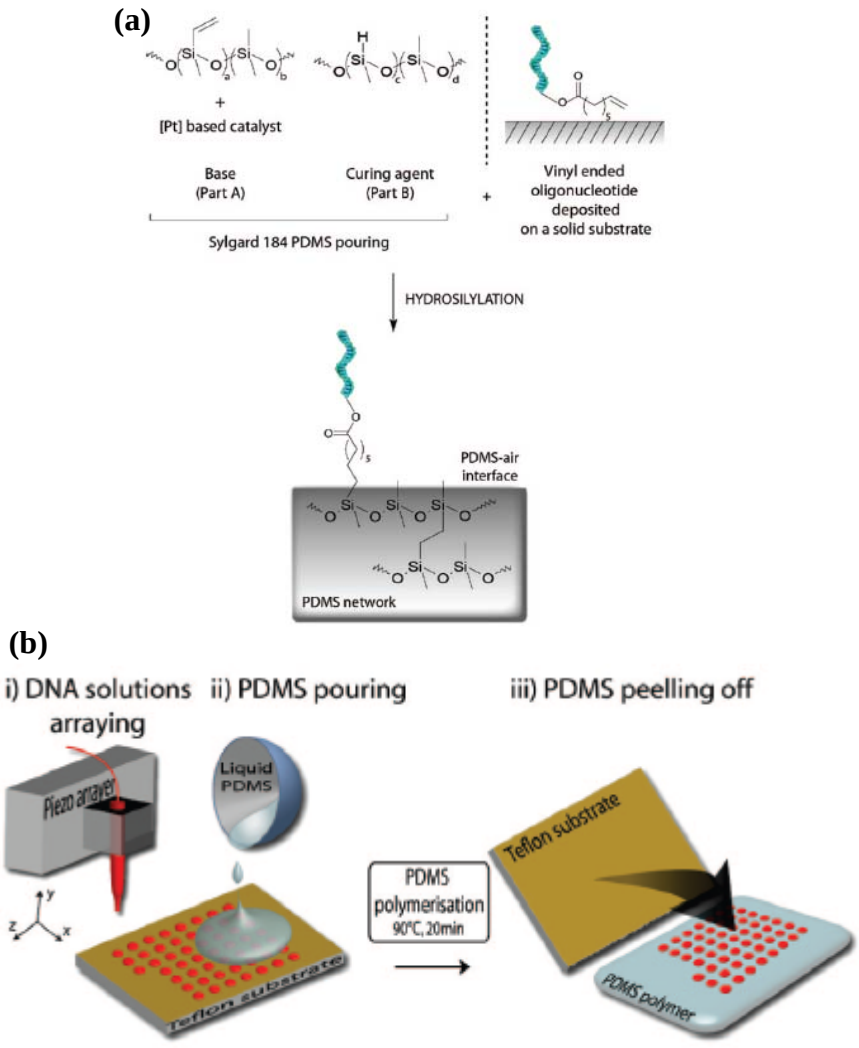

Figure 6.1. Schematic illustration of PDMS based DNA microarray chip fabrication. **(a)** Hydrosilylation reaction during PDMS Sylgard 184 polymerization and interaction with vinyl ended oligonucleotide deposited on a solid substrate. **(b)** Overview of transfer of vinyl modified DNA to the PDMS surface. Figure adapted from Ref. 7.

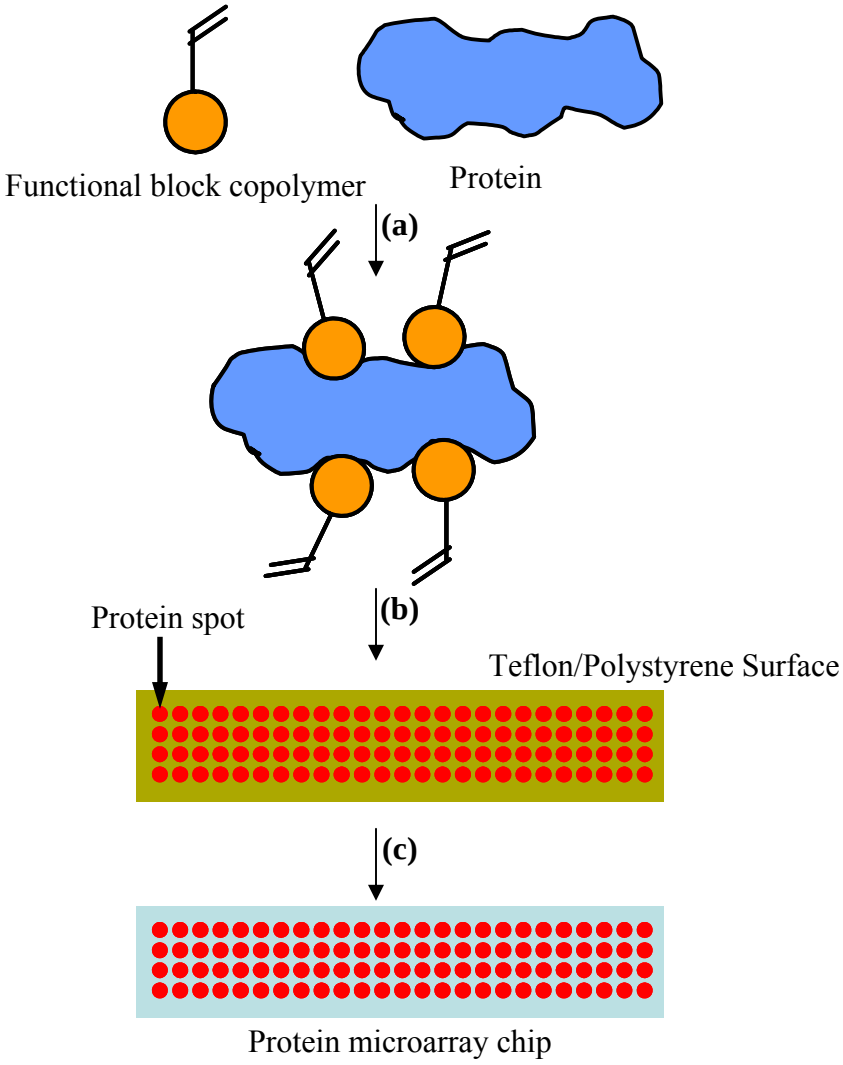

Figure 6.2. Schematic illustration of PDMS based Protein microarray chip fabrication. **(a)** Mix protein with functional block copolymer with PDMS anchor chain/functional polymer with vinyl termination. **(b)** Spot this mixture on a Teflon/polystyrene surface and allow solvent to evaporate. **(c)** Cast PDMS prepolymer and curing agent mixture on top of spotted surface and cure it in oven at elevated temperature. Once PDMS is cured on spotted surface it holds on to the functional block copolymer (imprint site) through either physical entanglement or covalent bonding through hydrosilylation reaction with vinyl terminated functional polymer. Further, protein can be eluted to generate functional microarray chip.

OH, which can be utilized for variety of different chemical coupling procedures for immobilization of specific recognition elements. Given the variety of advantageous properties of PDMS, modified PDMS surfaces can be utilized for development of robust biosensors.

In a recent investigation[7] it was demonstrated that vinyl terminated DNA can be used for the development of PDMS based DNA microarray chips as shown in Figure 6.1. Based on this finding, a novel methodology can be developed where a specific protein molecule can be mixed in with a vinyl terminated recognition element, with or without the PDMS anchor, followed by spotting of this mixture on Teflon or any other surface, which can be later polymerized on a PDMS surface through hydrosilylation reaction during the PDMS polymerization process. Thus, this technique may lead to development of a protein micro array based on a molecular imprinting technology.[8, 9] An example of this technology for development of protein microarray chip is illustrated in Figure 6.2.

Further, the unique elastomeric property of PDMS can be utilized in regenerating a surface that has been used for bio-analyte detection as shown in Figure 6.3. Briefly, once the PDMS surface has been used for detection of the target molecule/protein it can be stretched with the external force that will lead to detachment or release of analyte,

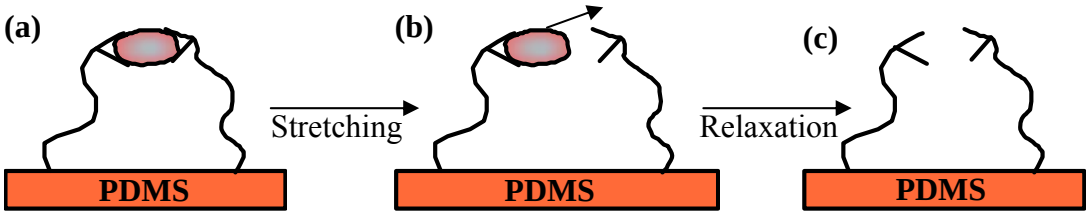

Figure 6.3. Schematic Illustration of regeneration of functionalized PDMS surface through stretching and relaxation process. **(a)** Functionalized PDMS surface with analyte. **(b)** Stretching of PDMS elastomer to release analyte. **(c)** Relaxing stretched PDMS regenerates the functionalized PDMS surface.

which can be easily washed or remove from the surface. Consequently, when the PDMS surface will be relieved from the external force, it will relax and attain its original state, regenerating the surface for use.

6.4 References

1. Turner, N. W.; Wright, B. E.; Hlady, V.; Britt, D. W. *J. Colloid Interface Sci.* **2007,** 308, (1), 71-80.

2. Pack, D. W.; Arnold, F. H. *Chem. Phys. Lipids* **1997,** 86, (2), 135-152.

3. Pack, D. W.; Chen, G. H.; Maloney, K. M.; Chen, C. T.; Arnold, F. H. *J. Am. Chem. Soc.* **1997,** 119, (10), 2479-2487.

4. Pack, D. W.; Ng, K.; Maloney, K. M.; Arnold, F. H. *Supramol. Sci.* **1997,** 4, (1-2), 3-10.

5. Tombelli, S.; Minunni, A.; Luzi, E.; Mascini, M. *Bioelectrochemistry* **2005,** 67, (2), 135-141.

6. Strehlitz, B.; Nikolaus, N.; Stoltenburg, R. *Sensors* **2008,** 8, (7), 4296-4307.

7. Heyries, K. A.; Blum, L. J.; Marquette, C. A. *Chem. Mat.* **2008,** 20, (4), 1251-1253.

8. Takeuchi, T.; Goto, D.; Shinmori, H. *Analyst* **2007,** 132, (2), 101-103.

9. Takeuchi, T.; Hishiya, T. *Org. Biomol. Chem.* **2008,** 6, (14), 2459-2467.

APPENDICES

APPENDIX A

LIPID STUCTURE AND MIXING DIAGRAM

Lipid Structure

Structures of lipids used in this work (Chapters 3 and 4) are presented in Figure A.1.

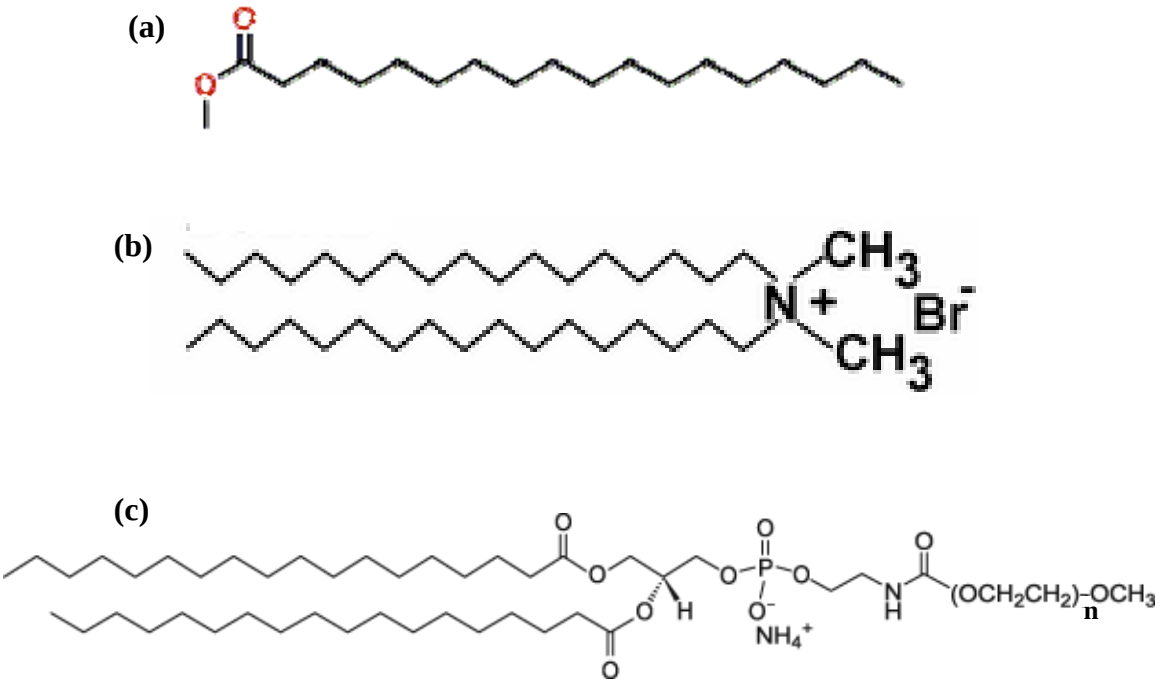

Figure A.1. Molecular structure of (a) Methyl stearate (SME), (b) Dioctadecyldimethyl-ammonium bromide (DOMA), and (c) 1,2-Diacyl-*sn*-Glycero-3-Phosphoethanolamine-N-(Methoxy(Polyethylene glycol)) (DSPE-PEG). Where for DSPE-PEG_{350} n=7, for DSPE-PEG_{750} n=16, and for DSPE-PEG_{1000} n=22.

Mixing Diagram

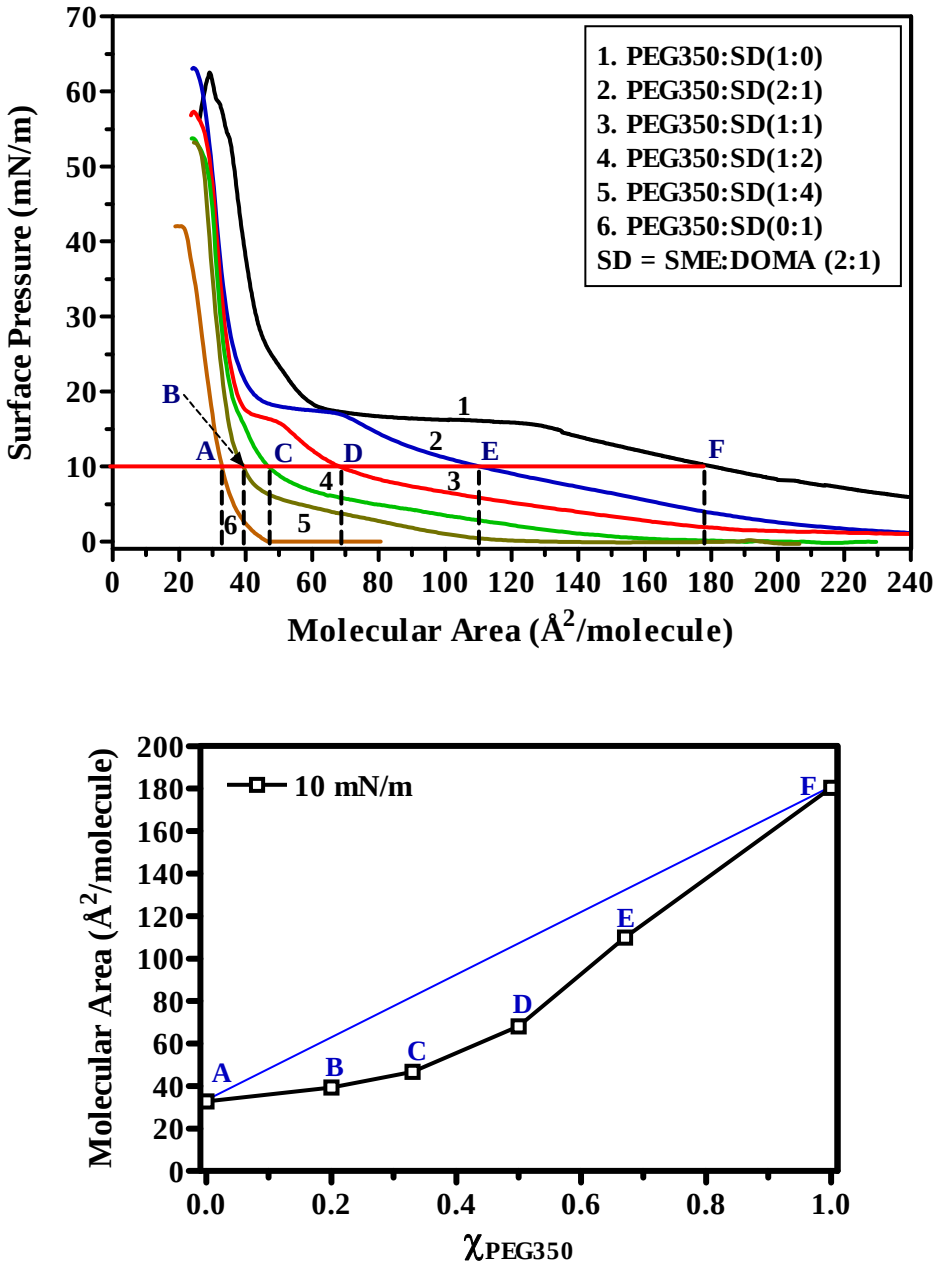

Figure A.2. (a) Surface pressure - molecular area isotherms of PEG bearing phospholipids (PEG_{350}), the binary mixture of SME:DOMA 2:1 (SD), and ternary mixture of PEG_{350}:SD prepared at the indicated molar ratios. (b) Miscibility analysis of PEG_{350}:SD monolayers at 10 mN/m surface pressures. The straight line represents additive mixing for the 10 mN/m data.

As shown in Figure A.2 the molecular area mixing diagram is constructed from surface pressure – molecular area isotherm. Where, the molecular area is occupied by a specific lipid mixture at a specific pressure plotted against the mole fraction of PEG lipid in that lipid mixture to obtain mixing diagram. Figure A.2 reveals the construction of mixing diagram for different lipid mixtures of DSPE-PEG_{350} and SD at 10 mN/m surface pressure.

APPENDIX B

ATOMIC FORCE MICROSCOPY (AFM) ANALYSIS OF MODIFIED PDMS SAMPLES

Overview

This appendix summarizes the AFM images of PDMS substrates modified with PDMS-b-PEO 600 through the swelling deswelling method (Figure B.1, B.2, and B.3), which wasn't shown in Chapter 5. Further, AFM images of PDMS samples modified with high molecular weight block copolymers (PDMS-b-PEO 3000, PDMS-b-PEO 3000 (G), PEO-PDMS-PEO 4000, PDMS-b-PEO 5000, and PDMS-b-PEO 10000) through the bulk mixing method, which were not shown in Chapter 5 are also presented here (Figure B.4).

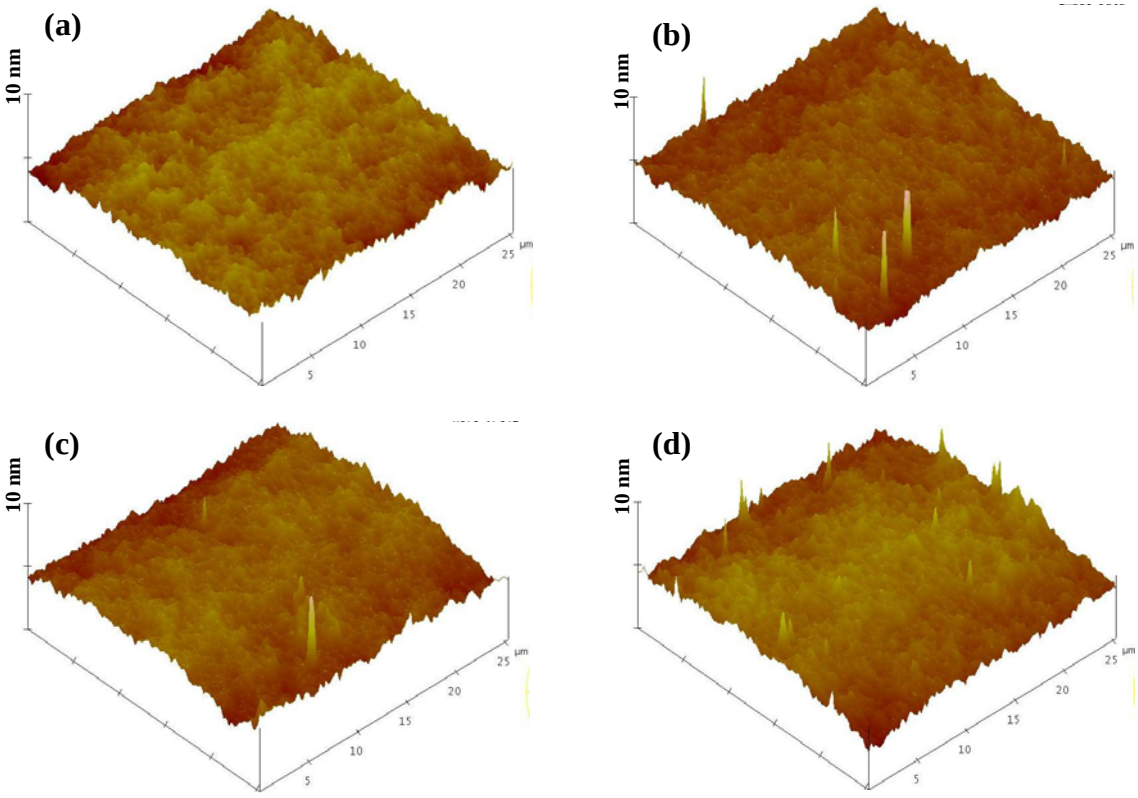

Figure B.1. AFM images (25 X 25 μm^2) of (a) unmodified PDMS (5:1) and 5:1 cross-linking density PDMS substrates modified through swelling-deswelling method using (b) 1%, (c) 3%, and (d) 5% PDMS-b-PEO 600. Height scale for all images was adjusted to visualize maximum surface features and is as indicated on the individual image.

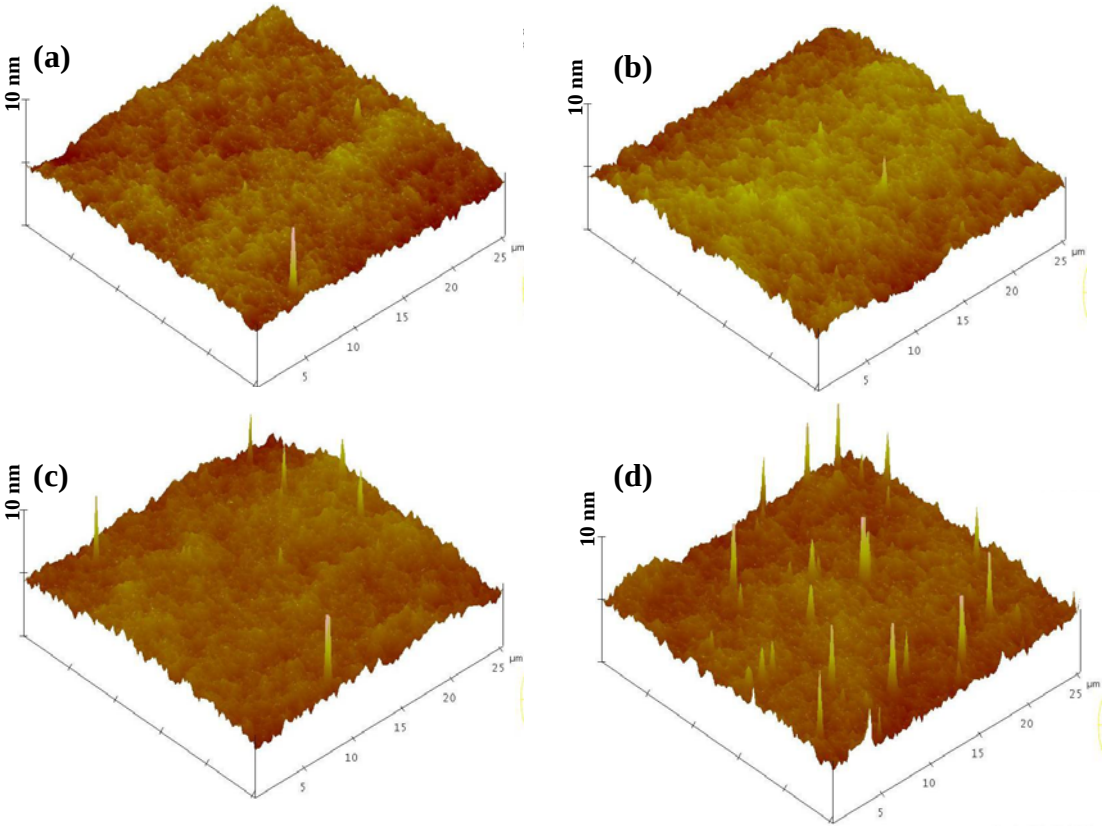

Figure B.2. AFM images (25 X 25 μm^2) of (a) unmodified PDMS (10:1) and 10:1 cross-linking density PDMS substrates modified through swelling-deswelling method using (b) 1%, (c) 3%, and (d) 5% PDMS-b-PEO 600. Height scale for all images was adjusted to visualize maximum surface features and is as indicated on the individual image.

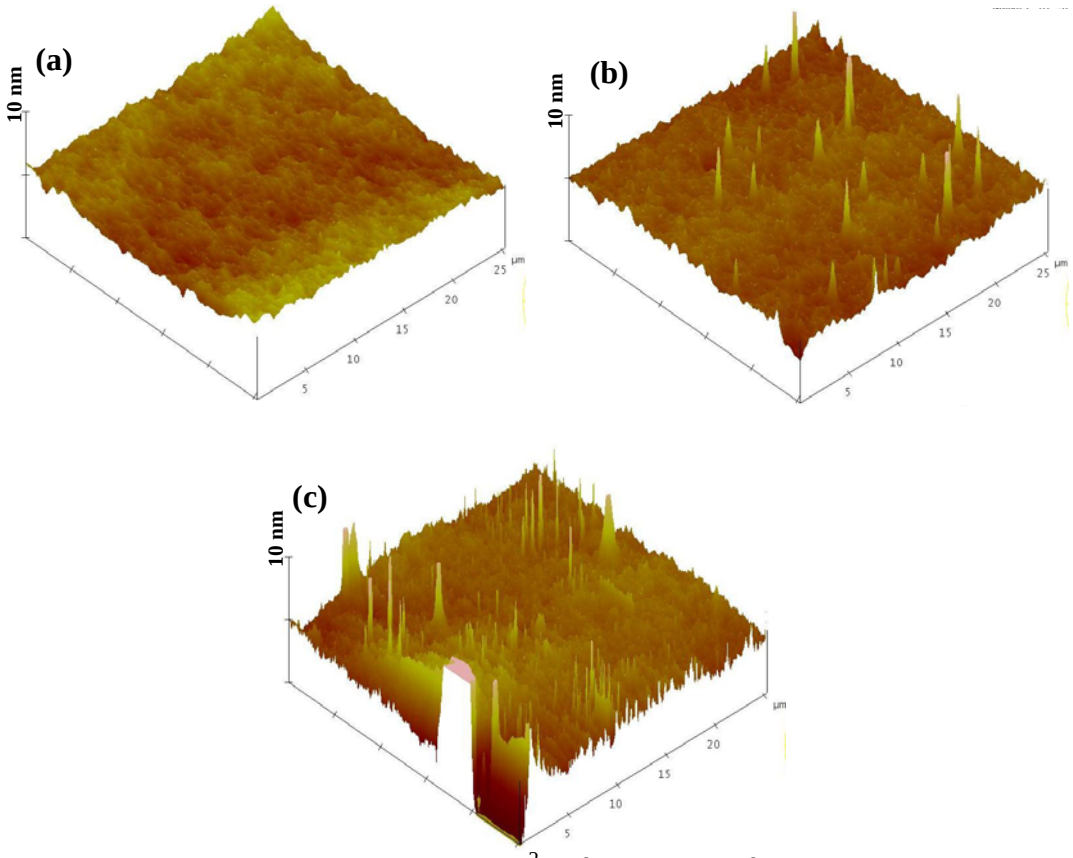

Figure B.3. AFM images (25 X 25 μm^2) of (a) unmodified PDMS (20:1) and 20:1 cross-linking density PDMS substrates modified through swelling-deswelling method using (b) 1% and (c) 3% PDMS-b-PEO 600. Height scale for all images was adjusted to visualize maximum surface features and is as indicated on the individual image.

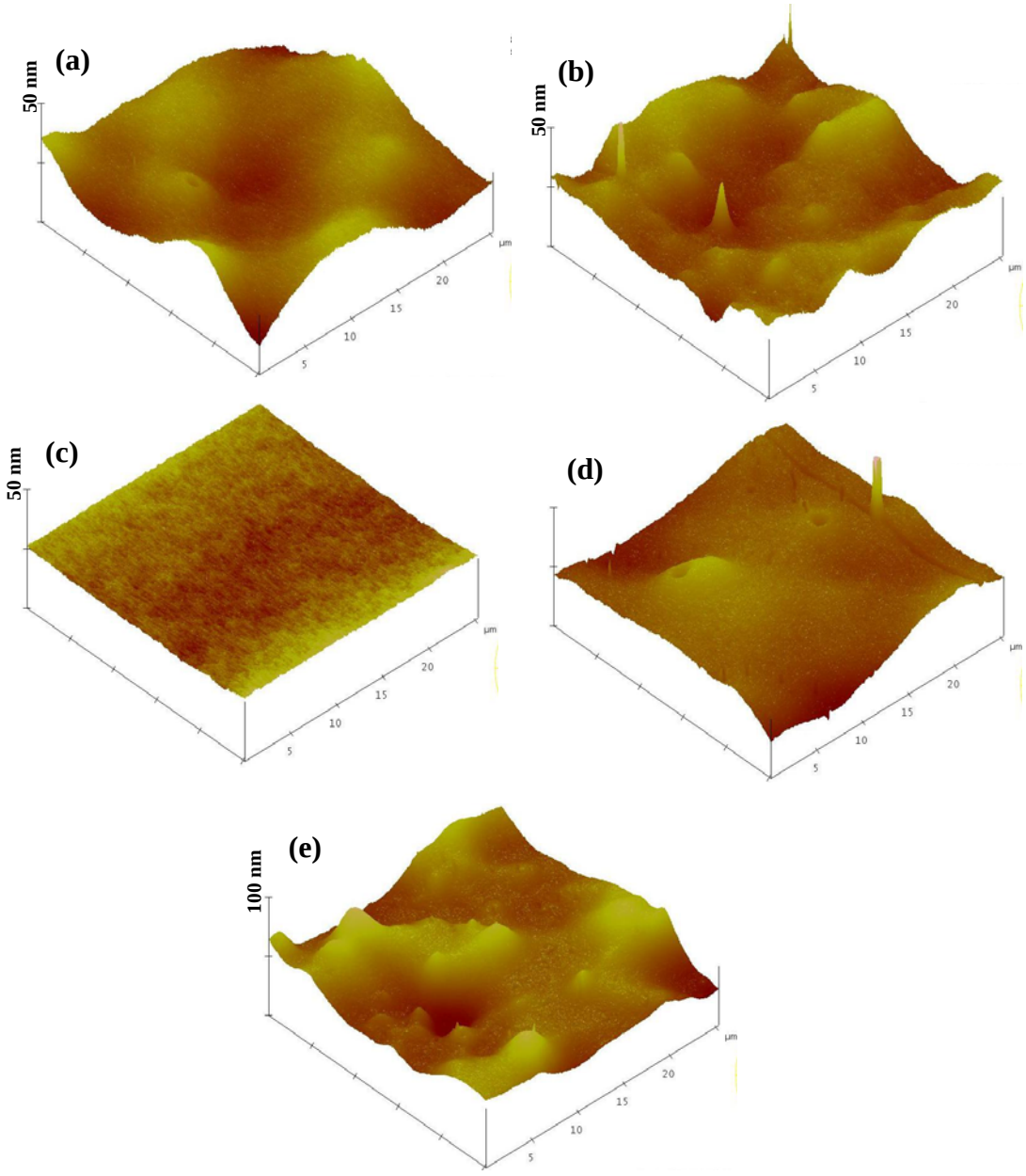

Figure B.4. AFM images (25 X 25 μm^2) of PDMS substrates modified through bulk mixing method using (a) 1% PDMS-b-PEO 3000, (b) 1% PDMS-b-PEO 3000 (G), (c) 1% PEO-PDMS-PEO 4000, (d) 1% PDMS-b-PEO 5000, and (e) 1% PDMS-b-PEO 10000. Height scale for all images was adjusted to visualize maximum surface features and is as indicated on the individual image.

APPENDIX C

STABILITY STUDY OF MODIFIED PDMS SURFACES

Introduction

It is demonstrated in Chapter 5 that modification of PDMS surfaces with PDMS-PEO block copolymers through the swelling-deswelling and bulk modification methods leads to a hydrophilic and protein repellent surface. Hydrophilicity, which also indicates the presence of PEO molecules on the PDMS surface, was determined with the help of time dependent contact angle analysis, and the data is presented in Chapter 5 (Figure 5.1, 5.2, 5.3, and 5.4). PDMS surfaces modified through both methods were found to be stable when stored in air at room temperature. However, when modified PDMS substrates were stored in an aqueous environment (water), it was found to lose its hydrophilic character over a period of time. This behavior was mainly attributed to the gradual desorption of the PDMS-PEO block copolymers in the surrounding aqueous environment, because the block copolymers were immobilized through weak physical interaction between the PDMS segment of block copolymer and PDMS monolith.

Results and Discussion

Stability of modified PDMS substrates were measured over a period of 20 days using time-dependent contact angle measurement after every five days. Figure A.1, A.2, A.3 and A.4 present stability study results for PDMS samples prepared through the swelling-deswelling and bulk mixing methods using different concentrations of PDMS-b-PEO 600. As observed in the data, all modified PDMS substrates through both methods

lose their hydrophilic character over the twenty day period. Further, PDMS substrates prepared through bulk mixing method were found to be slightly more stable as compared to samples prepared through the swelling-deswelling method.

Figure A.5 shows stability study results of the PDMS samples modified with high molecular weight PDMS-b-PEO block copolymers (PDMS-b-PEO 1000 and PDMS-b-PEO 3000 (G)) through the bulk mixing method. This suggests that even high molecular weight block copolymers gradually desorb into the surrounding aqueous environments.

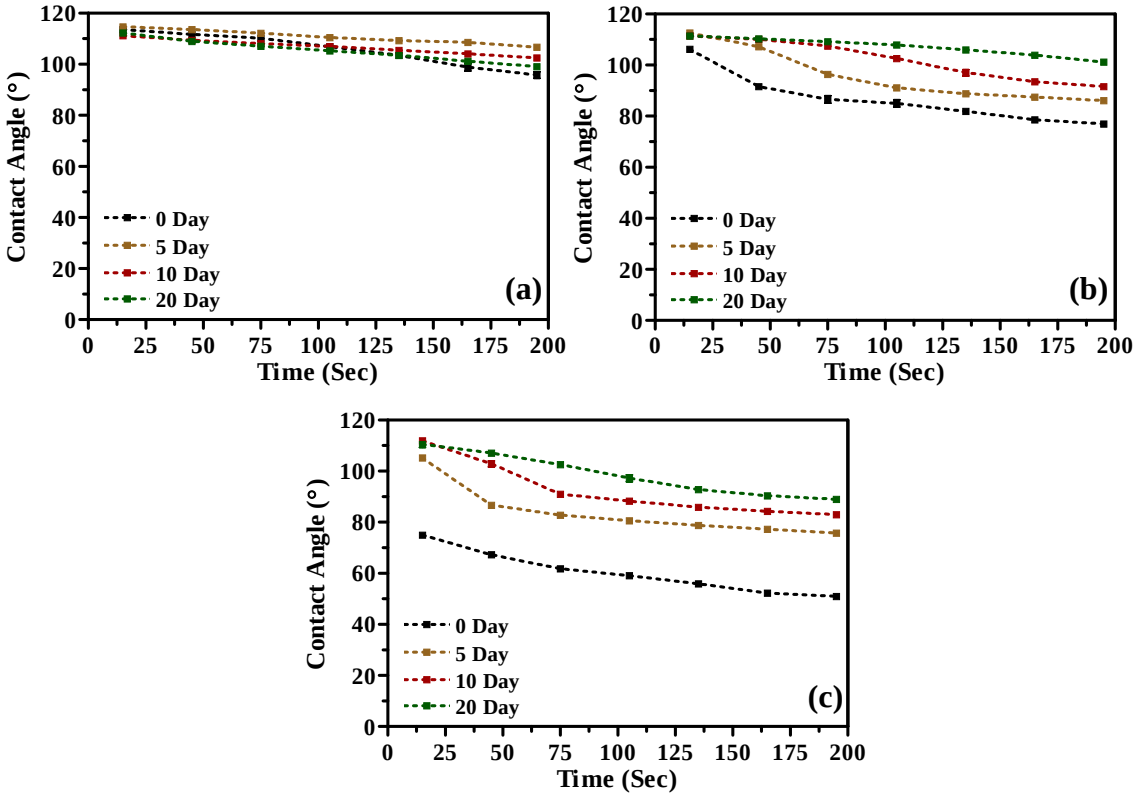

Figure C.1. Time dependent water contact angle analysis of 5:1 cross-linking density PDMS substrates modified through the swelling-deswelling method using (a) 1%, (b) 3%, and (c) 5% PDMS-b-PEO 600 over the period of 20 days when stored under dist.

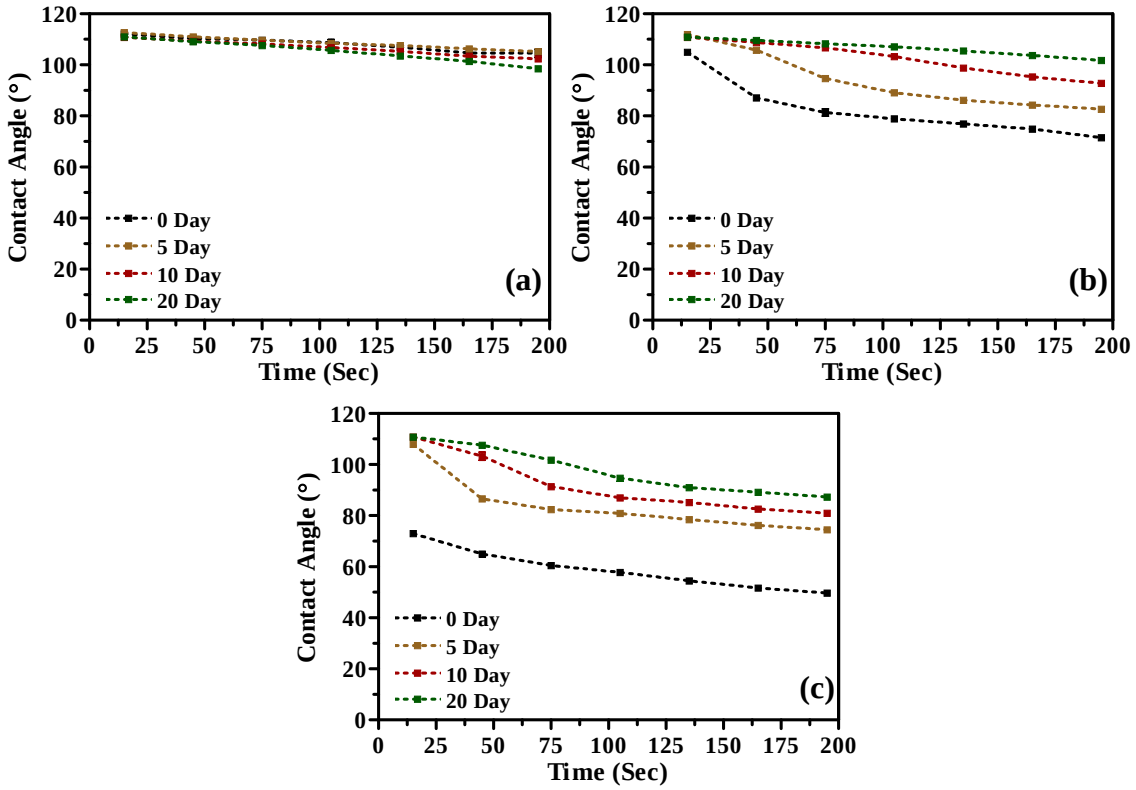

Figure C.2. Time dependent water contact angle analysis of 10:1 cross-linking density PDMS substrates modified through the swelling-deswelling method using (a) 1%, (b) 3%, and (c) 5% PDMS-b-PEO 600 over the period of 20 days when stored under dist.

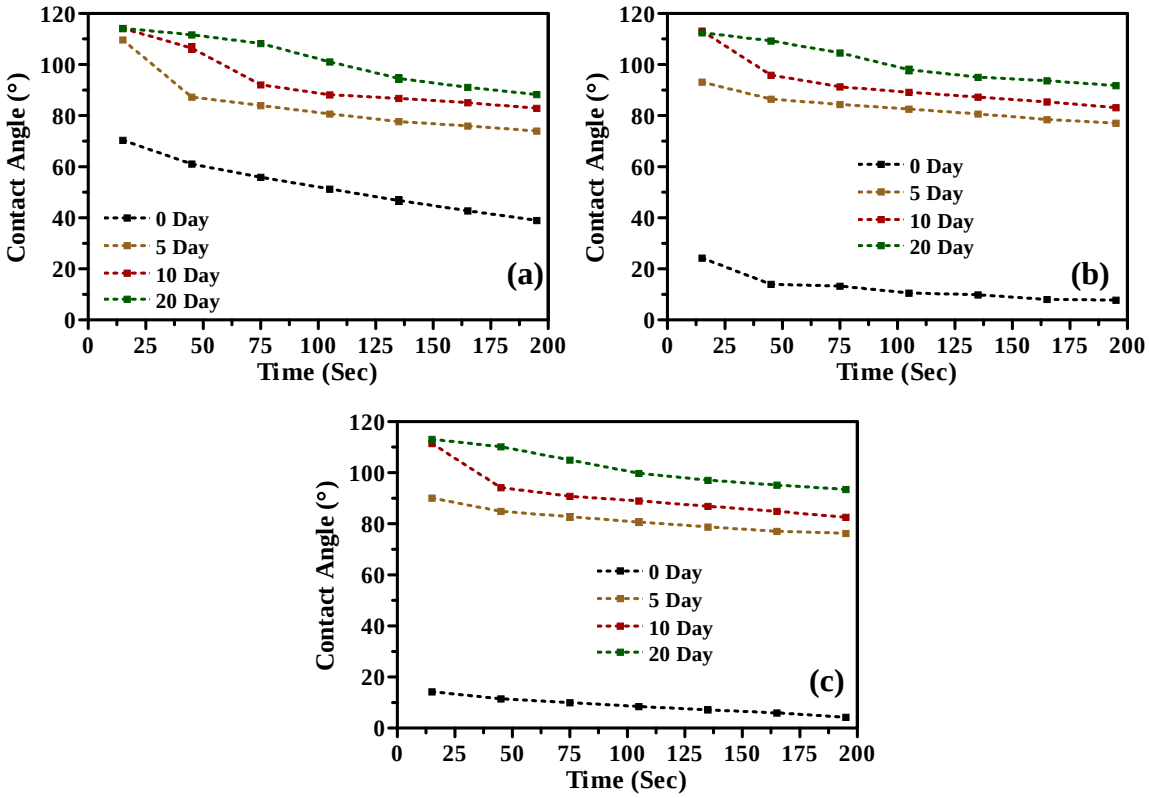

Figure C.3. Time dependent water contact angle analysis of 20:1 cross-linking density PDMS substrates modified through the swelling-deswelling method using (a) 1%, (b) 3%, and (c) 5% PDMS-b-PEO 600 over the period of 20 days when stored under dist.

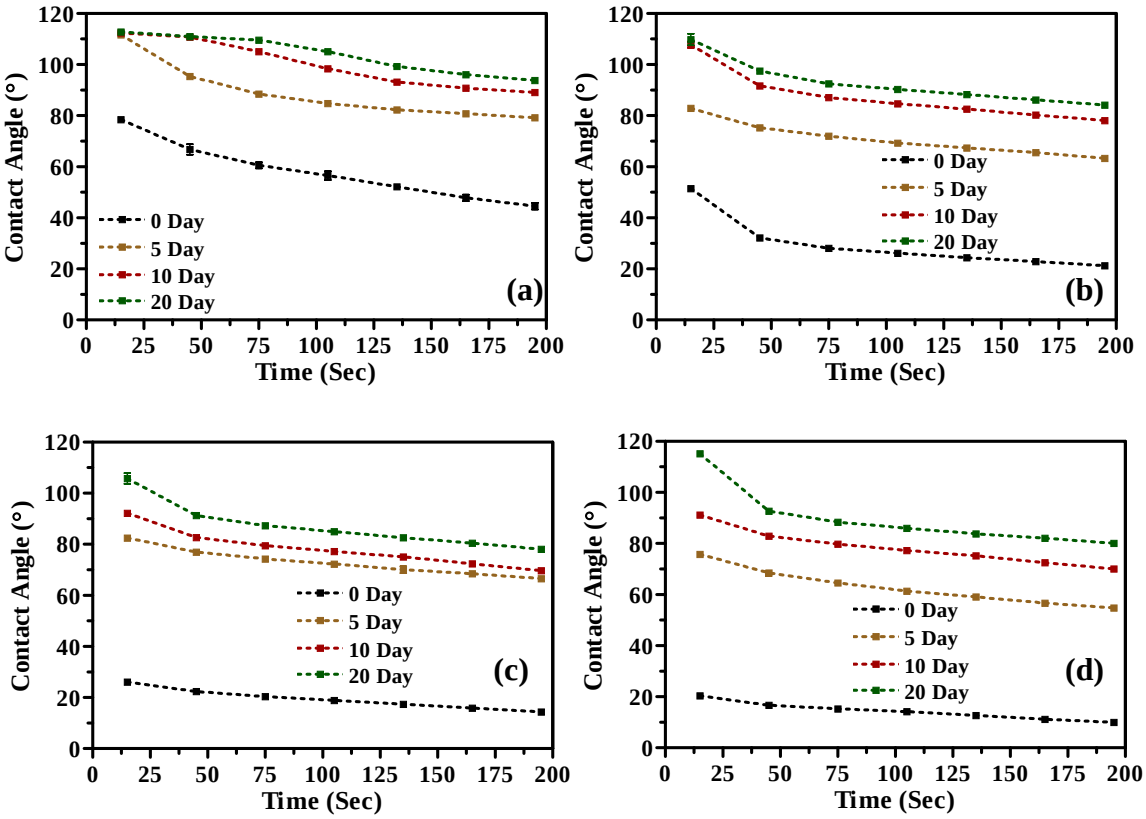

Figure C.4. Time dependent water contact angle analysis PDMS substrates modified through the bulk mixing method using (a) 1%, (b) 2%, (c) 3%, and (d) 5% PDMS-b-PEO 600 over the period of 20 days when stored under dist. water.

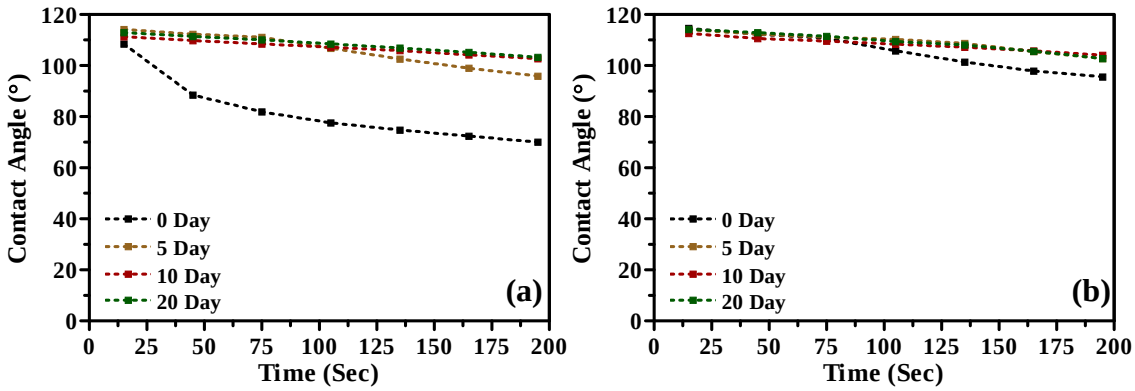

Figure C.5. Time dependent water contact angle analysis PDMS substrates modified through the bulk mixing method using (a) 1% PDMS-b-PEO 1000 and (b) 1% PDMS-b-PEO 3000 (G) over the period of 20 days when stored under dist. water.

APPENDIX D

AMERICAN CHEMICAL SOCIETY COPYRIGHT STATUS FORM

Please submit form to appropriate Editor's Office.

Name of ACS Publication: Biotechnology Progress

Author(s): David W. Britt, Mundeta A. Taveras, Revathi Pepalla, Harshil Dhruv

MS No.

Ms Title: Protein Insertion and Patterning of PEG bearing Langmuir Monolayers

Received

This manuscript will be considered with the understanding you have submitted it on an exclusive basis. You will be notified of a decision as soon as possible.

Print or Type Author's Name and Address

David W. Britt. Assistant Professor
Utah State University□Biological Engineering□4105 Old Main Hill□Logan, UT
84322-4105

[THIS FORM MAY BE REPRODUCED]

COPYRIGHT TRANSFER

The undersigned, with the consent of all authors, hereby transfers, to the extent that there is copyright to be transferred, the exclusive copyright interest in the above cited manuscript, including the published version in any format (subsequently called the "work"), to the **American Chemical Society** subject to the following (If the manuscript is not accepted by ACS or withdrawn prior to acceptance by ACS, this transfer will be null and void.):

A. The undersigned author and all coauthors retain the right to revise, adapt, prepare derivative works, present orally, or distribute or transmit to not more than 50 colleagues, their own paper, provided that copyright credit is given to the source and ACS, that recipients are informed that they may not further disseminate or copy the paper, and that all such use is for the personal noncommercial benefit of the author(s) and is consistent with any prior contractual agreement between the undersigned and/or coauthors and their employer(s). Authors/employers may post the title of the paper, abstract (no other text), tables, and figures of their own papers on their own Web sites, and include these items in their own scholarly, research papers.

B. Where a work is prepared as a "work made for hire" for an employer, the employer(s) of the author(s) retain(s) the right to revise, adapt, prepare derivative works, publish, reprint, reproduce, and distribute the work in print format, and to transmit it on an internal, secure network for use by its employees only, and additional rights under A, provided that all such use is for the promotion of its business enterprise and does not imply endorsement by ACS.

C. Whenever the American Chemical Society is approached by third parties for individual permission to use, reprint, or republish specified articles (except for classroom use, library reserve, or to reprint in a collective work) the undersigned author's or employer's permission will also be required.

D. No proprietary right other than copyright is claimed by the American Chemical Society.

E. For works prepared under U.S. Government contract or by employees of a foreign government or its instrumentalities, the American Chemical Society recognizes that government's prior nonexclusive, royalty-free license to publish, translate, reproduce, use, or dispose of the published form of the work, or allow others to do so for noncommercial government purposes. Your contract number:_____

F. ACS reserves the right to use on the publication cover all figures submitted with the manuscript.

SIGN HERE FOR COPYRIGHT TRANSFER: I hereby certify that I am authorized to sign this document either in my own right or as an agent for my employer, and have made no changes to the current valid document supplied by ACS.

David W. Britt, Assistant Professor
Print Authorized Name(s) and Title(s)

David W Britt — 5-5-2005
Original Signature(s) (in Ink) — Date

CERTIFICATION AS A WORK OF THE U.S. GOVERNMENT

I certify that **ALL** authors are or were bona fide officers or employees of the U.S. Government when the paper was prepared, and that the work is a "work of the U.S. Government" (prepared by an officer/employee of the U.S. Government as part of official duties), and, therefore, it is not subject to U.S. copyright. (This section should NOT be signed if the work was prepared under a government contract or coauthored by a non-U.S. Government employee.)

INDIVIDUAL AUTHOR **OR** AGENCY REPRESENTATIVE

Print Author's Name

Print Agency Representative's Name and Title

Original Signature of Author (in Ink) — Date — Original Signature of Agency Representative (in Ink)

☐ **WORKS SUBJECT TO CROWN COPYRIGHT:** If **ALL** authors are **bona fide** employees of the Governments of Australia, Canada, and the U.K., please check box and send to the appropriate Editor's Office for an alternative form (Blue Form).

Control#0408317A

VITA

EDUCATION

PhD, Biological Engineering *2005 - Present*
Utah State University, Logan, UT
Dissertation: Controlling nonspecific adsorption of proteins at bio-interfaces for biosensor and biomedical applications.

M.S., Biological Engineering *2003 - 2005*
Utah State University, Logan, UT
Thesis: Role of Lactose in Modifying Gel Transition Temperature and Morphology of Self-Assembled Hydrogels.

B.Tech., Dairy Technology *1998 - 2002*
Gujarat Agricultural University, Anand, Gujarat, India

SUMMARY OF RESEARCH EXPERIENCE

Utah State University, Logan, UT 2003 - Present
Graduate Research Assistant

- **Controlling non-specific adsorption of proteins at bio-interfaces for biosensor and biomedical applications (Ph.D. Dissertation)**
  - Performed protein adsorption studies on different molecular weight Poly(ethylene glycol) (PEG) bearing Langmuir monolayers.
  - Developed a detail analysis protocol to correlate phase behavior of lipopolymers (PEG bearing lipids) and lipids at the air/water interface with obtained protein adsorption patterns.
  - Successfully performed a Quartz Crystal Microbalance (QCM) study to quantify protein adsorption on molecularly imprinted PEG bearing lipid monolayers.
  - Developed and perfected a novel protocol to modify the surface of widely used elastomer Poly(Dimethylsiloxane) (PDMS) with PEG functional molecules.
- **Lactose based Self-Assembled Hydrogels (M.S. Thesis)**
  - Synthesized a novel Lactose (a low value Dairy by-product) based surfactant with fatty acid and fatty amine.
  - Performed detailed investigation of interaction between fatty acid and fatty amine with Lactose using FT-IR and NMR.
  - Investigated effect of Lactose on gel transition temperature and morphology of self-assembled hydrogels.
- **Protein Conformation Sensors**
  - Performed molecular imprinting of different protein conformations in 3-Aminophenylboronicacid (APBA) matrix.

- Standardized the QCM protocol to increase the signal to noise ratio for reliable sensor development.
- Investigated novel polymer matrices (mainly Aniline derivatives) for conformational imprinting of protein

- **Caseinate Thin Films**
  - Investigated effects of novel cross-linking agents and amphiphilic plasticizing agents on mechanical properties and water vapor permeability of caseinate (a milk protein) films.
  - Performed detail water contact angle analysis and AFM analysis on Caseinate films with different plasticizing agents.

PUBLICATIONS

- **Harshil Dhruv**, Nicholas Turner, and David W. Britt, ***"Nanoscale Prion Detection Strategies"***- *Encyclopedia of Agricultural, Food, and Biological Engineering*, **2007.** (Online Publication)
- **Harshil Dhruv**, Revathi Pepalla, Mundeta Taveras, and David W. Britt, ***"Protein Insertion and Patterning of PEG Bearing Langmuir Monolayers"***- Biotechnology Progress, **22** (1), 150 -155, **2006**.
- **Harshil D. Dhruv**, Matthew A. Draper, and David W. Britt, *"**Role of Lactose in Modifying Gel Transition Temperature and Morphology of Self-assembled Hydrogels***"- *Chemistry of Materials*, **17** (25), 6239 -6245, **2005**

CONFERENCE PRESENTATIONS

- **Harshil Dhruv**, Bradley Tuft, and David W. Britt, ***"One pot synthesis of hydrophilic protein repellent PDMS."***, Regional IBE Conference, Logan, Utah, October 18, **2008**.
- **Harshil Dhruv**, Bradley Tuft, and David W. Britt, ***"Protein repellent PDMS surfaces by non-covalent immobilization of poly(ethylene oxide): Effect of PDMS cross-linking density and PEO concentration."***, Proceedings of the 4th Annual Mountain West Biomedical Engineering Conference, Park City, Utah, September 5-6, **2008**.
- **Harshil Dhruv**, Bryon Wright, Vladimir Hlady, and David W. Britt, ***"Protein Patterning of Multicomponent PEG Bearing Langmuir Monolayers: Influence of Lipid Miscibility, Phase Behavior and PEG Chain Length"***, Proceedings of the 3rd Annual Mountain West Biomedical Engineering Conference, Park City, Utah, September 21-22, **2007**.
- Nicholas Turner, **Harshil Dhruv**, Bryon Wright, Vladimir Hlady, and David Britt, ***"Structure-Function Relationships in Protein-Imprinted Langmuir Monolayers"***, 2007 Proceeding of the Biomedical Engineering Society Annual Fall Meeting, Los Angeles, California, September 26-29, **2007**.

- **Harshil Dhruv**, and David Britt, ***"Building Protein-Specific Binding Pockets in PEG Bearing Langmuir Monolayers Through Controlled Lipid De-mixing"***, 2006 Proceedings of the Institute of Biological Engineering, Tucson, Arizona, March 10-12, **2006**.
- Nicholas Turner, Bryon Wright, **Harshil Dhruv**, Vladimir Hlady, and David Britt, ***"Protein Imprinting in Langmuir Monolayers"***, Fourth International Workshop on Molecularly imprinted Polymers, Cardiff, UK, September 10 – 14, **2006**.
- **Harshil Dhruv**, Matthew Draper, and David Britt, ***"Assembly of Mesoporous Structures as Biomolecule Detection Platforms"***, 2005 Proceedings of the Institute of Biological Engineering, Athens, Georgia, March 4-6, **2005**.
- **Harshil Dhruv**, Matthew Draper, and David Britt, ***"Self-Assembly Approaches to Organogel Construction"***, Proceedings of the Material Research Society Fall Meeting, Boston, Massachusetts, Nov 29 – Dec 3, **2004**.
- **Harshil Dhruv** and David Britt, ***"Water Contact Angle and Atomic Force Microscopy Analysis of Caseinate Thin Films"***, 2004 Proceedings of the Institute of Biological Engineering, Fayetteville, Arkansas, January 8-10, **2004**.

PATENTS

- **Harshil Dhruv**, Bradley Tuft, and David Britt, ***"Hydrophilic Surface Modification of Poly(dimethylsiloxane)"***, Provisional Patent Application, **2008**.

KEY SCIENTIFIC SKILLS

- Langmuir-Blodgett Technique
- Atomic Force Microscopy (AFM)
- Fluorescence and Phase Contrast Microscopy
- Goniometer for Contact Angle Analysis
- Plasma Chamber for Surface Modifications
- Spectrophotometer and Spectrofluorometer
- Quartz Crystal Microbalance (QCM)
- Surface Plasmon Resonance (SPR)
- Fourier Transform Infrared Spectroscopy (FT-IR)
- Differential Scanning Calorimetry (DSC)
- Scanning Electron Microscopy
- Self-Assembled Monolayers (SAMs) on Gold and Glass surfaces.
- Micro-Contact Printing and Construction of Gradient Surfaces.
- Chemical Vapor Deposition (CVD)
- Enzyme Assay
- Protein Labeling with Fluorescent Probes

AFFILIATIONS

- Material Research Society
- American Chemical Society
- Institute of Biological Engineering

HONORS

- Graduate Student Scholarship, Department of Biological and Irrigation Engineering, Utah State University, 2003.
- Outstanding Student Travel Grant Award, Utah State University, 2004.
- First prize in Student poster competition at Regional IBE Conference, 2008.